UNIVERSITÀ DEGLI STUDI DELLA TUSCIA DI VITERBO

DIPARTIMENTO DI

AGRICOLTURA, FORESTA, NATURA ED ENERGIA (DAFNE)

Corso di Dottorato di Ricerca in

BIOTECNOLOGIE VEGETALI - XXVI CICLO.

NEW BIOTECHNOLOGICAL APPROACHES FOR THE DEVELOPMENT OF A FLUORESCENCE-BASED MULTIARRAY BIOSENSOR FOR ENVIRONMENTAL AGRIFOOD MONITORING AND FOR THE PRODUCTION OF ALGAL BIOMASS

SETTORE SCIENTIFICO DISCIPLINARE
(s.s.d. BIO/13)

Tesi di dottorato di:

Dott. Silvia Silletti

Coordinatore del corso

Prof. Stefania Masci

Firma

Tutore

Dott. Maria Teresa Giardi

Firma

30 MAGGIO 2014

INDEX

PREFACE

PhD thesis is divided into two parts realized for two independent industrial projects. Thus, for data presented in this contest, confidentiality is required.

In the first part the green microalga *Chlorella minutissima* was used to produce biomass at low costs for applications in biofuel production. Algae are important resources for many beneficial bio-products. Algal cells contain pigments and other intracellular matters useful for producing antioxidants, vitamins, aquaculture nutrients, bioplastics, dyes and colorants, feedstocks, pharmaceuticals, algae fuels and especially oils for energy and health care purposes. The biomass can give biofuel by various processes of pyrolysis. In order to produce biofuel, algal cultures must produce a lot of lipids, but achieve this goal by classical methods is very expensive. For this reason in this project we produce new protocols to realize algal culture able to produce biomass and lipids at low costs, using a culture medium composed by nutrient obtained from farm and industrial wastes. During experiments, we noticed that in the algal cultures there are other microorganisms and their presence determines a greater production of biomass. The study of these organisms revealed that they are two paramecia that can live together and can establish symbiosis with *Chlorella*. Using this mutualistic relationship we show that is possible to obtain, in the same culture conditions applied for single *Chlorella* cultures a greater biomass production.

The second part of the thesis, divided in two subparts, is focused on the development of a multiarray biosensor based on fluorescence for environmental and agrifood monitoring. Biosensors are devices, which use a biological recognition element retained in direct spatial contact with a transduction system. The biosensor consists of three parts: the first element is the biomediator a biologically derived material e.g. tissue, microorganisms, organelles, cell receptors, enzymes, antibodies, nucleic acids, and biological sensitive elements created with genetic engineering, or a biomimic system e.g. aptamers, MIPs, etc. The second element is the transducer e.g. physicochemical, optical, piezoelectric, electrochemical, etc. that transforms the signal resulting from the analytes interaction with the biological element into a signal that can be measured and quantified. The third element is the associated electronics or signal processor, responsible of the visualization results in a user-friendly way.

The aim of this work is to evaluate if the symbiotic organisms of *Chlorella* can be useful for biosensor applications. This idea has been suggested by the high resistance to stress and long half-

life of the symbiotic *Chlorella* compared to the algae alone. We found that the mutualistic relationship determines changes in the culture and has positive effects on culture life. In order to discover the reasons why some organisms establish symbiosis and others do not, we study lipid content of *Chlorella* symbiotic algae and *Chlorella* non symbiotic ones. Thus, we will show the use of symbiotic cultures as biomediators to detect herbicides at low concentrations of 10^{-10}M.

In the last part of the work, using a commercial fluorometer we show the selection of optimal biomediators in order to perform analyses for quality and safety assessment of milk. Milk and its derivate products are exposed to various chemicals and microbial safety problems, such as mycotoxins, veterinary drug residues, herbicide and pesticide residues and pathogens as *Lysteria monocytogenes*. Milk contamination may be due to food fed as in the case of alfatoxin B1 which is present in maize or in farm and industrial environment. In Europe, chemical and microbial food safety is regulated by EC legislations, which set the maximum levels for various contaminants in foodstuffs. We will use biomediators in order to develop a multiarray biosensor with variuous detection cells that permit simultaneously to reveal toxic compounds and metabolites at the low concentrations required by EU legislations in milk; analyses on line, directly in cowshed, are programmed.

PART I

Process for production of algal biomass

<u>International patent:</u> WO2013088407. 14, December 2012. "Process for production of algal biomass" (Giardi M.T., Lastella L., Silletti S.)

<u>National patent</u>: Numero domanda: TO2011A001149. 2011. Titolo: "Procedimento per la produzione di biomassa algale"

FIELD OF THE INVENTION

The present description concerns a new process for production of algal biomass with a high lipid content.

Background

Algae are important resources for many beneficial bio-products. Algae cells contain pigments and other intracellular matters useful for producing antioxidants, vitamins, aquaculture nutrients, bioplastics, dyes and colorants, feedstocks, pharmaceuticals, algae fuels and especially oils for energy and health care purposes. The biomass can give biofuel by various processes of pyrolysis (Chisti 2007, Giardi et al. 2010).

Algal cultivation, similar to culturing many other microorganisms, requires both macro and micronutrients that can be obtained from either organic or inorganic sources. Typical commercial algal growth methods, however, rely on the use of exogenously added pure chemicals and micronutrients needed to sustain the algal cultures. Many examples of algal cultivation exist in the art. The cultivation of algae occurs in proper photobioreactors which can be closed or open systems. Examples of closed photobioreactors for algal cultures are provided in U.S. Pat. Nos. 2,732,663; 4,473,970; 4,233,958; 4,868,123; and 6,827,036. Examples of open air photobioreactor systems used for cultivation of algae are disclosed, for example, in U.S. Pat. Nos. 3,650,068; 3,468,057; 3,955,318; and 4,217,728.

These methods are nevertheless expensive.

Moreover, it is known in the literature that nitrogen, salt, heavy metal stresses in algae are used to induce algal lipid production.

The application of these kinds of stress is, nevertheless, generally limited to non-continuous batch processes in closed systems bioreactors where algae are initially grown in rich chemical medium to provide a large algal biomass followed by imposing nitrogen deprivation or other types of stresses by rapid exhaustion and/or adjustment of nutrients in the medium.

In those conditions, stress pushes the algal biosynthesis towards overproduction of lipids.

However, the disadvantage deriving from the application of different kinds of stress to the algal culture is a decrease in the yield of the overall biomass obtained from the process.

The biomass produced generally ranges from 0.1 till a maximum of 2 g/l in autotrophic conditions; higher yields can be obtained in cases of mixotrophic conditions and only under optimal (non-commercially sustainable) growth conditions (pure salts, right levels of illumination, small volumes of culture).

Moreover, algal scale up in big volumes is difficult due to several factors: i) difficulty in obtaining a correct mass movement, ii) selection of right levels of light inside the mass.

For photosynthesis to work, light must reach the algae. If a layer of algae is more than a few centimeters thick, organisms on the surface shade those underneath, blocking the sunlight. An alternative is to spread horizontally the algae.

However, algae would need to cover an area of about 9 million hectares to produce enough biodiesel to cover Europe's annual transport requirement of 370 billion liters.

Imposing light inside the biomass by various lamp sources can be also dangerous: it is known that high levels of light, instead of promoting photosynthesis, can cause an inhibition called photoinhibition at the level of the activity of photosystem II apparatus (Barber & Andersson 1992; Mattoo et al. 1999).

In conclusion, the growth of algal biomass, particularly for biofuel production on an industrial scale, is considered still economically difficult and object of intense research (Gouveia & Oliveira 2009; Savage, 2011).

Mutualistic symbioses are important ecological relationships that are generally defined as two or more species living together and providing benefit to each other. Several microalgal endosymbioses, for example involving flatworms and various protists contribute globally to the primary productivity of aquatic ecosystems (Fujishima 2009).

An example of a symbiotic cultivation for industrial production of an algal biomass is reported in US-A-2011/0045564. This document discloses a co-cultivation of at least one algal species with at least one aerobic bacterial species and at least one diazotroph under continuous sustainable symbiotic conditions.

Such a cultivation process requires a minimal addition of exogenous nutrients but it is nevertheless affected by some drawbacks. This process, for example, requires a cultivation medium suitable to induce at least one nitrogen stress response in the cultured algal cells to obtain a high lipid production.

Nevertheless, as already emphasized stresses applied to the algal culture can reduce the content of overall biomass production.

There is, therefore, from both environmental and economic perspectives a pronounced need for novel methods able to i) provide high algal biomass growth with a minimal reliance on exogenous added fertilizers and chemicals to sustain the algal cultures (e.g. using surface water and/or groundwater as the primary culture medium) and ii) avoid the necessity of imposing stresses on the algal biomass for higher lipid production.

Summary of the invention

Considering these premises, the need is felt for better, more efficacious solutions able to provide an algal biomass producing process industrially sustainable.

According to the present description, the above said object is obtained by means of the solution specifically recalled in the attached claims, which constitutes an integral part of the present description.

In one embodiment, the present description concerns a process for producing an algal biomass comprising:

i) inoculating in an aqueous cultivation medium at least a first algal species and at least a first protozoan species obtaining a symbiont co-culture, the at least first protozoan species being suitable to generate symbiosis with the at least first algal species;

ii) cultivating the symbiont co-culture obtaining an algal biomass;

iii) harvesting at least a portion of the algal biomass.

A preferred embodiment of the production process described herein concerns use of a symbiosis deriving from a protozoan, preferably a ciliate and/or a flagellate protozoan, containing symbiotic algal organisms inside its cytoplasm.

In one embodiment, the process herein described allows to produce algal biomass by minimal addition of exogenous nutrients (like waste organic substances and technical salts), thus maintaining production at low costs and environmentally friendly.

A further embodiment of the present description concerns further inoculating in the cultivation medium algae and/or cyanobacteria as preys which, providing nutrients deriving from their metabolic products, contribute to increase the yield of biomass production.

The production process disclosed in the present application is characterized by a continuous symbiotic co-cultivation system which provides several advantages in terms of high levels of biomass and lipid production.

Moreover, such a production process enables algal growth with an enhanced bioproduct yield (e.g., on a per-algal cell basis) with an easy scale up process.

The total biomass is increased also due to the high reproduction speed of the protozoan. In addition, both the alga and the protozoan have the ability to accumulate large amounts of lipids, which can be used as a feedstock for biofuel/bioliquid production without the need of generating any additional stress to the cultivating system.

Another advantage of the production process herein disclosed is that it is broadly applicable to different algae photosymbionts and can be practiced with a broad range of suitable symbiotic protozoa.

The algal biomass obtained according to the instant description is useful for bioproduction. The obtained algal biomass can be employed for production of (but not limited to) bioliquids, biofuel, biodiesel, bioethanol, biogasoline, biocrude, biogas, and also pharmaceuticals, therapeutics, antioxidants, nutraceuticals, cosmetics, cosmeceuticals, food, feedstock, dyes, colorants and bioplastic.

DETAILED DESCRIPTION

In the following description different embodiments will be described in detail, by way of non-limiting example, with reference to a process for producing an algal biomass.

It is clear that while the experimental data provided below refer to use of a symbiosis between specific algal and protozoan species, the process herein described is broadly applicable to many types of algal species able to create a symbiotic system with protozoan species able to infect the algal organism in a permanent or transient manner.

In the description that follows, numerous specific details are presented to provide a thorough understanding of the embodiment. The embodiments can be practiced without one or more of the specific details, or with other methods, components, materials, etc. In other instances, well-known structures, materials, or operations are not shown or described in detail to avoid obscuring aspects of the embodiments.

Reference throughout this specification to "one embodiment" or "an embodiment" means that a particular feature, structure or characteristic described in connection with the embodiment is included in at least one embodiment. Thus, the appearances of the phrases "in one embodiment" or "in a certain embodiment" in various places throughout this specification are not necessarily all referring to the same embodiment.

Furthermore, the particular features, structures or characteristics may be combined in any suitable manner in one or more embodiments.

The headings provided herein are for convenience only and do not interpret the scope or meaning of the embodiments.

An embodiment of the present description concerns a process for producing an algal biomass comprising:

i) inoculating in an aqueous cultivation medium at least a first algal species and at least a first protozoan species obtaining a symbiont co-culture, the at least first protozoan species being suitable to generate symbiosis with the at least first algal species;

ii) cultivating the symbiont co-culture obtaining an algal biomass; and

iii) harvesting at least a portion of the algal biomass.

The process object of present description provides commercially adequate algal biomass yield with a high lipid content which, unlike stressed algae grown alone in culture without any other symbiont organism, can be sustained on a continuous symbiotic basis in both open and closed systems.

Moreover, the instant description provides a process for a sustainable continuous cultivation of algae-bearing protozoa with minimal addition of exogenous nutrients.

In the process herein described, a significant proportion of the macronutrients, necessary for the symbiotic culture, derives from the photosymbiont products continuously produced during symbiotic cultivation.

The source of a significant proportion of carbon, CO2, magnesium, potassium, calcium, oxygen and other macronutrients for the living organisms of the symbiotic culture come, in fact, from metabolic

cellular products deriving from the co-cultivation itself. More specifically, a portion of CO2 and oxygen present in the cultivation medium is endogenously derived from the aerobic metabolism of the protozoan component. On the other hand, the algae can supply the host paramecium with photosynthetic products, mainly maltose and sugars. Inside the host cell, the algae show a higher rate of photosynthetic oxygen production than in the isolated condition, thereby guaranteeing an oxygen supply for their host. The paramecium can supplythe algae with nitrogen components and CO_2.

Algae species suitable for the co-culture described in the present application include but are not limited to marine, brackish water and freshwater algae and include species that are derived from acidic or basic water. The algae species include micro and macro algal species like eukaryotic algae such as diatoms, green, red and brown algae and cyanobacteria.

Different algal species may require for their metabolic activity different cultivation conditions (temperature in the range from 21 to 35 °C, cultivation medium containing different salt concentrations, pH ranging from 6 to 8).

The lipid content of the algal biomass obtained by means of the process herein described is significantly higher than that obtained through stressed algae grown alone in culture without any other symbiont organism.

The increased content of lipids ranges from 57-90% of the dried weight biomass, for the specific case of *Chlorella minutissima* infected by a *Paramecium sp*., compared to the range of 30-50% obtained with the algae alone.

A particularly preferred embodiment of the present description concerns the cultivation of symbiotic

systems comprising a *Paramecium spp.* (a ciliate protozoan) with *Chlorella spp.*

In a most preferred embodiment, the process for production of an algal biomass provided very good results in terms of algal biomass yield using as the first algal species *Chlorella minutissima* and two different protozoa species able to generate symbiosis with *Chlorella minutissima*, namely *Tetrahymena pyriformis* and *Chilomonas paramecium*.

According to an embodiment, the algal species and the protozoan species can be present in the cultivation medium in a ratio comprised between 500:0.1 and 50:5, preferably about 100:1.

According to a further embodiment, the inoculum in the cultivation medium of a second algal species and/or cyanobacteria as source of nutrients is provided. Such an addition increases the algal biomass yield in a long term cultivation. Such suitable algal species and/or cyanobacteria are not able to generate symbiosis with the protozoa species.

According to a still further embodiment, the algal biomass yield can be increased by harvesting a portion of algal biomass, optionally followed by adding new cultivation medium or water, wherein said operations may be performed repeatedly during a long term period.

The harvested portion of the algal biomass may comprise algal and paramecium biomass, as well as part of the cultivation medium.

In table 1 a list of protozoa species which can infect algal species suitable to create a symbiotic system efficiently usable in the process object of the instant application is provided (first and second columns, respectively). The third column provides a list of algae and cyanobacteria that can be used as exogenous nutrient of the symbiotic system.

Table 1.

Protozoa for symbiotic association	Algae for symbiotic association	Algae and Cyanobacteria as nutrient
Chilomonas paramecium	***Chlorella sorokiniana***	***C. ellipsoidea***
Tetrahymena pyriformis	***Chlorella vulgaris***	***C. mirabilis***
Colpoda steinii	***Chlorella minutissima***	***C. saccharophila***
Paramecium bursaria	***Chlorella variabilis***	***C. zofingiensis***
Paramecium aurelia	***Parachorella kessleri***	***C. protothecoides***
Paramecium caudatum	***Choricystis parasitica***	***Botrycoccus braunii***
Climacostomum virens	***Chlorella sp.***	***Chroomonas salina***
Euplotes daidaleos		***Cyclotella* spp.**
***Vorticella* spp.**		***Euglena gracilis***
Paramecium sp.		***Haematococcus pluvialis***

According to the instant description, the expression “algal biomass” means the biomass obtained by the symbiont culture of the algal species and the protozoan species. Therefore, the algal biomass contains both the algal cells and the protozoan cells, as well as part of the aqueous cultivation medium.

According to the instant description, the expression “exogenous nutrients” means nutrient compounds that are added by the operator during the cultivation phase of the symbiont co-culture. Exogenous nutrients useful in the process herein described comprise, i.a. technical salts, glycerol, molasses, hormones (preferably vegetal natural hormones like for example cytokines or indolaceutic acid), aminoacids (for example glutammic acid, asparagine, alanine, lysine), vitamins

(for example A, B, C, PP, K vitamins), microelements (like boron, iron, manganese, molybdenum, zinc, copper, cobalt), humic substances like humic and fulvic acids, agro-industrial waste materials and plant detritus.

Symbioses, in general, are defined as two or more species living together in beneficial coexistence. This type of mutualistic interaction plays an important role in maintaining populations living under precarious environmental conditions.

In particular, algal-bearing protozoa are ubiquitous and abundant components in oceanic and freshwater systems of different trophic interactions.

The mixotrophic nutrition mode of algal-bearing ciliates, combining both phagotrophy and phototrophy, is considered to be an adaptation allowing exploitation of oligotrophic environments.

In symbiotic processes, phototrophic endosymbionts are ingested by the host, but are able to escape digestion and to utilize the waste products of the metabolism of their host. Mixotrophic organisms combine the advantages of a heterotrophic nutrition mode with autotrophic energy gain, through algal symbionts.

An example of a stable symbiosis is the mutualistic relationship between the ciliate *Paramecium bursaria* (Hymenostomatia) and unicellular green alga *Chlorella* (Trebouxiophyceae). This symbiosis represents a permanent association with hereditary

symbionts, where each algal cell is enclosed in an individual perialgal vacuole derived from the host digestive vacuole to protect from lysosomal fusion. The exclusive mutualistic relationship of *P. bursaria* with 'zoochlorellae' in natural conditions has long been considered as a fact, but aposymbiotic *P. bursaria* natural populations have been recently reported (Fujishima, 2009; Summerer, 2008).

Different *Chlorella* species (like for example, *C. vulgaris*, *P. kessleri*, *C. variabilis*, *C. sorokiniana* and *C. minutissima*) have been found to have distinct suitability for the establishment of stable symbioses in *P. bursaria* and infection rates have been shown to be affected by specificity of host and potential symbiont, such as recognition of surface antigens or by physiological conditions of the partners involved.

Actually, it is known that *C. ellipsoidea*, *C. saccharophila*, *C. luteoviridis*, *C. zofingiensis*, *C. mirabilis* and several other algal species are incapable to establish a symbiosis with *Paramecium bursaria.*

However it is possible to adapt some *Chlorella spp.* to the host (Summerer, 2007).

The presence of glucosamine in the rigid wall of the alga cells is a prerequisite for the realization of

symbiotic association between *P. bursaria* and *Chlorella* species. On the contrary, the presence of glucose and mannose in the rigid wall of algal cells characterizes "infection-incapable" algal species.

Many ciliates acquire photosynthesis capacity through stealing plastids or harboring intact endosymbiotic algae in not stable association. Both phenomena are a form of mixotrophy and are widespread among ciliates and flagellate.

Mixotrophic ciliates and flagellates are abundant in freshwater and marine ecosystems, sometimes making substantial contributions toward community primary productivity.

Unique adaptations may also be found in certain algal endosymbionts, facilitating establishment of symbiosis and nutritional interactions, while reducing their fitness for survival as free-living cells.

Certain strains of *M. rubrum* may have a stable association with their cryptophytic organelles, while others need to acquire a cryptophytic nucleus through feeding.

Very large numbers (3466 ml-1) of ciliated protozoa were found living beneath the oxic-anoxic boundary in a stratified freshwater pond. Most ciliates (96%) contained symbiotic algae (*Chlorella* spp.). Peak abundance was in anoxic water with almost 1mol free CO2 m^{-3} and a midday irradiation of 6μmol/$m^{-2}s^{-1}$. Photosynthetic rate measurements of metalimnetic water indicated a light compensation point of 1.7μmol/$m^{-2}s^{-1}$ which represents 0.6% of sub-surface light. It has been calculated that photosynthetic evolution of O_2 by symbionts is sufficient to meet the demand of the host ciliates for 13 to 14 hours each day. Each 'photosynthetic ciliate' may therefore become an aerobic island surrounded by anoxic water (Finlay et al., 1996).

As previously reported, some ciliates (e.g. *Paramecium bursaria)* form symbiotic relationship preferably with algae of *Chlorella* genus. Paramecium cells may harbor several hundreds of symbiotic *Chlorella* cells in their cytoplasm. Each symbiotic alga is enclosed in a special membrane called Perialgal Vacuole (PV), derived from the host Digestive Vacuole (DV) membrane of the protozoan. The Perialgal Vacuole is able to protect algal cells preventing the fusion to the host lysosoms.

By a biological point of view the symbiosis between the protozoan and the alga species takes place as follows:

- in the first stage, after mixing the two organisms, the alga appears in the cytoplasm by budding of the digestive vacuole membrane of the protozoan.
- in the second stage, after the algal appearance in the cytoplasm, the vacuole enclosing a single green alga differentiates into the perialgal vacuole from the digestive vacuole.

- in the third stage, the alga localizes beneath the host cell cortex. At about 24 h after mixing, the alga increases by cell division and establishes endosymbiosis.
- the final fourth stage is characterized by the presence of the condensed vacuolar membrane of *Paramecium* and by the brown color of digested algae which become small in diameter.

Various benefits are induced in both the host *Paramecium* and the algae by algal infection.

Alga-bearing paramecium cells can divide better than the alga-free cells. Alga-bearing paramecium cells show a higher survival rate than the alga-free cells under various stressful conditions, like for example administration to the culture of 0.5mM nickel chloride ($NiCl_2$) or 150mM hydrogen peroxide or exposing the culture to high temperatures (40°C).

Moreover, the host paramecia can receive protection against UV damage by their symbiotic algae which contain protecting substances which confers their capability to thrive in sunlit UV-exposed waters.

Furthermore, because the timing of the cell division of both algae and the host paramecia is well coordinated, the symbiotic algae can be distributed to the daughter cells.

The relationship between some species of *Paramecium* and *Chlorella* spp. is a mutualism and, therefore, the alga-free paramecium cells and the symbiotic algae are still keeping the ability to grow without a partner (Fujishima, 2009).

Alga-free paramecium cells can be produced easily from alga-bearing cells using one of the following methods: rapid cell division; cultivation under the constant dark condition, X-ray irradiation, treatment with 3-(3,4-dichlorophenyl)-1,1-dimethylurea (DCMU – a blocker of electron flow in photosystem II), treatment with the herbicide paraquat or treatment with cycloheximide (an eukaryotic protein synthesis inhibitor).

On the other hand, symbiotic algae can be isolated from alga-bearing paramecium cells by sonication, homogenization or treatment with some detergents.

Furthermore, by mixing the alga-free paramecium and the isolated symbiotic algae, endosymbiosis can be easily established again.

Moreover, paramecium species need simple cultivation conditions to get mass culture.

Applicants have unexpectedly discovered that symbiosis between an algal species and a protozoan species is very effective in terms of production of algal biomass. The presence of the protozoan in the co-cultures provides for adequate and sustained algal growth and preserves the capability of high rate lipid production without needing application of any stress conditions to the culture.

Tetrahymena pyriformis is a teardrop-shaped, unicellular, ciliated freshwater protozoan about 50μm

long. *Tetrahymena* species are very common in aquatic habitats and are non-pathogenic, have a short generation time of about 2h and can grow to high cell density in inexpensive media. *Tetrahymena pyriformis* structure is characteristic since it exhibits striking nuclear dimorphism: two types of cell nuclei, a large somatic macronucleus and a small germline micronucleus, exist in a single cell at the same time and carry out different functions with distinct cytological and biochemical properties. In addition, *Tetrahymena* possesses hundreds of cilia and microtubules in its cytoskeleton. These cylindrical polymers of tubulin can grow as long as 25 micrometers and are highly dynamic.

Microtubules are important for maintaining cell structure, providing platforms for intracellular transport. Tetrahymena genus includes several species and the most common are: *T. pyriformis, T. thegewischi, T. hyperangulari, T. malaccensis, T. pigmentosa, T. thermophila and T. vorax.* Recently, the whole macronuclear genome has been sequenced for *Tetrahymena thermophila.*

Chilomonas paramecium (19-30μm) occurs in 8 species, recently ascribed to *Cryptomonad* flagellatae.

It is a colorless organism which contains a leucoplast. *Chilomonas paramecium* shows a peculiar swaying swimming behavior, caused by a stereospecific asymmetry in cell shape with clearly definable dorso-ventral/right-left sides, and are easy to recognize due to a unique set of characters. It can be grown in relatively simple solutes even only with inorganic salts, it divides at a fairly uniform rate and it lives and thrives in a temperature range extending over twenty degrees.

Chilomonas paramecium, when grown in a favorable environment, contains a large quantity of stored food material in the form of starch granules and neutral fats. Mast and Pace (1933) demonstrated that it produces starch, fats and proteins in a wholly inorganic medium, with one part of CO_2 added to 5 parts of air at atmospheric pressure. Starch and fat are byproducts of metabolism which can be utilized as food materials under adverse conditions of nutrition.

In the following some no limiting examples of the process for producing an algal biomass according to the instant description are provided.

Different physical states for the mixed culture of microorganisms were identified:

· Motile in which the paramecia move quickly and prey algae;

· Motile in which paramecia show intact algae inside their bodies and increase greatly their size, *Tetrahymena* from 50μm increases till 150μm and *Chilomonas* from 20μm increases till 100μm or more;

· The two paramecia can coexist in the same culture or one type, mainly *Tetrahymena*, can be preponderant;

· Non motile, with algae inside: in this state, called cyst, the paramecium suspends animation and cell metabolic activities are slowed down.

Unfavorable environmental conditions - such as lack of nutrients or oxygen, extreme temperatures, lack of moisture, presence of toxic chemicals, which are not conducive for the growth of the microbe - trigger the formation of a cyst;

· Algae that initially are single and have small dimension of 10μm, after infection greatly increased till 3 times;

· Algae join together in big aggregations mainly over the cysts;

· The macro culture shows green, yellow and brown biomass with a state similar to glue, mostly precipitated and in part floated;

· Inside the culture it is possible to observe formation of microtubuline filaments;

· With culture refresh, encysted microorganisms reach an environment favorable to growth and survival, the cyst wall breaks down by a process known as encystation and the forms become again motile;

· After refreshment, culture color pass through different colors: green, yellow and brown; for a high biomass production it is useful/advisable to maintain the co-culture in the above green or yellow stage since brown stage corresponds to partially digested alga, by means of repetitive dilutions of the culture medium. These repetitive dilutions cause an increased division of the alga-bearing paramecium and the reestablishment of the green color of the co-culture followed again by the various colored phases.

· *Chlorella* algae result highly protected in this endosymbiotic process. *Chlorella* alone culture, using waste material as nutrient, does not survive over 7 and occasionally 30days while, when infection with protozoa occurs, it can survive up to several months. Moreover, when the culture is not infected with the identified paramecia, it becomes prey of several other types of predators that do not establish endosymbiosis (e.g. rotifers). Generally, culture of *Chlorella* alone rapidly decrease with a consequent high viscosity due to the release of microtubules in association with glycerol.

Weight of algal biomass was determined by harvesting 20% of the culture at the base of the bioreactor. 5 samples of 100ml of algal biomass were taken, under strong aeration for homogenization, and subsequently dried at 90°C for at least 10 days till a weight constancy and production of a fine powder.

Therefore, as already stated, the algal biomass contains both the algal cells and the protozoan cells, as well as part of the aqueous cultivation medium.

Weight of algal biomass produced by the above described co-culture symbiotic system was compared to the weight of algal biomass obtained by a culture of algae without protozoa.

RESULTS

Example 1

Biomass yields produced by a minimal exogenous nutrition of technical degree of the above described co-culture symbiotic system and of the culture of the alga grown alone are reported in table 2.

Table 2.

days of culture	***Chlorella minutissima***	***Chlorella minutissima*-bearing paramecium sp.**
Biomass produced in g/l		
1	**1**	**1**
2	**0.85**	**1.15**
3	**1.51**	**1.82**
4	**1.44**	**2.37**
5	**1.77**	**5.82**
6	**2.25**	**5.05**
7	**2.43**	**6.88**
8	**2.76**	**7.38**
9	**2.93**	**7.96**
10	**3.42**	**7.04**

11	**3.64**	**7.32**
scale up: cultivation medium volume was doubled with water		
12	**2.08**	**3.49**
13	**2.58**	**8.64**
14	**2.89**	**10.52**
15	**3.03**	**12.51**

The relative standard deviation, calculated on n=6 sampling of one typical pattern of growth, was less than 10%.

The results of table 2 show a higher yield of biomass (till 2-3 times) produced by the co-culture system after some days than that obtained by the culture of the alga grown alone. Particularly, the doubling of the culture medium volume leads to an increase of the yields of more than 4 times of *Chlorella*-bearing paramecium compared to *Chlorella* grown alone.

Moreover, the experiment demonstrates that the scale up of algal symbiont is suitable more than for algae alone leading to an increase in yield of biomass.

Example 2 – Evaluation of infection specificity of different algal species

In order to define specificity of infection, Ps culture was mixed with other algae belonging to the genus *Chlorella* and comparison between different associations was performed by relative weight of the same quantity of all cultures. This test was performed using the TAP and KOB media, exposed to red light at 10μmol/m^2s, in continuous low agitation and harvested at the same day. The results are provided in table 3.

Table 3.

Algae	Medium	Alga alone	Algae infected with Ps culture 100:1
Chlorella minutissima	**TAP**	+	+++
Chlorella sorokiniana H1957		+	++
Chlorella sorokiniana H1986		+	+++
Chlorella vulgaris		++	+++
Choricystis parasitica		+	++
Chlorella minutissima	**KOB**	+	+
Chlorella sorokiniana H1957		+	++
Chlorella sorokiniana H1986		+	++
Auxenochlorella protothecoides		+	+
Choricystis parasitica		+	+

We observed that in presence of protozoa, algae were aggregated and under microscope they were larger than those in single culture. In this experiment, we found that in TAP medium, the aggregation is more evident in presence of *Chlorella minutissima* and *Chlorella sorokiniana* H1986, while in KOB medium formation of endosymbiosis seems to be inhibited.

Example 3 – Evaluation of further inocula of algae-bearing paramecium(a) on overall algal biomass yield

The symbiotic culture was obtained as described in Example 1, in two months culturing. The only difference is that further inocula of algae-bearing paramecium in TAP medium were performed to the culture medium at different time intervals.

Relative amounts of algal cells/paramecium at the beginning were maintained in a ratio of about 100:1 and addition of algae-bearing paramecium (in the same ratio of 100:1 for the algal cell/paramecium symbiont) was repeated every 3 days. The algae-bearing paramecium were freshly prepared and added in the second stage of infection.

The repetitive addition of symbiotic organisms provided a higher biomass yield, as shown in table 4, wherein the biomass production after addition of fresh algae-bearing paramecium is provided. The table represents a typical pattern of growth.

Table 4.

Day	Day Dried weight (g/l) Symbiont
1	**0.9**
2	**4.9**
3 - addition	**6.2**
4	**8.9**
5	**10.7**
6 - addition	**19.2**
7	**22.3**
8	**29.4**
9 - addition	**20.2**
10	**18.0**
11	**19.6**
12 - addition	**20.5**
13	**20.3**

The relative standard deviation, calculated on n=6 sampling of one typical pattern of growth, was less than 10%.

Example 4 – Evaluation of repetitive harvesting of algal biomass during the production process on overall algal biomass yield

The alga-bearing paramecium was obtained as in Example 1, in two months culturing. The culture was grown in a vessel of 15l for 6 months adding quantity of glycerol 12.5g/l and 100µl/l of vigor ultra per day; a process of harvesting 20-50-70% of the algal biomass and water re-addition to the initial volume was regularly applied on alternate days or on consecutive days.

Table 5 shows that higher biomass yields were obtained one day after harvesting the algal biomass and cultivation medium re-addition to initial volume, that was accompanied by the typical cycle of color steps: green-faintly, yellow-brown. The process could be repeated without any production interruption.

Results reported in table 5 (representing a typical pattern of growth) show that during a 20 days production, harvesting alternatively 20-50% of the biomass, and re-addition of water in the co-culture on alternative days lead to high yield of algal biomass till about 10 g/l.

On the contrary, daily repetition of harvesting and re-addition of water leads to poorer yields of about 2g/l.

Table 5.

Day	**-**	**Dried weight (g/l)** **Symbiont**
1	**harvesting/water re-addition**	**5.59**
2	**-**	**2.71**
3	**harvesting/water re-addition**	**14.57**
4	**-**	**2.01**
5	**harvesting/water re-addition**	**8.51**
6	**-**	**2.02**
7	**harvesting/water re-addition**	**4.33**
8	**-**	**4.83**
9	**harvesting/water re-addition**	**5.40**

10	**harvesting/water re-addition**	**2.32**
11	**harvesting/water re-addition**	**1.62**
12	**harvesting/water re-addition**	**2.24**
13	**harvesting/water re-addition**	**2.45**
14	**-**	**2.74**
15	**-**	**4.01**
16	**harvesting/water re-addition**	**3.23**
17	**-**	**6.06**
18	**harvesting/water re-addition**	**8.54**
19	**-**	**3.45**
20	**harvesting/water re-addition**	**10.02**

The relative standard deviation, calculated on n=6 sampling of one typical pattern of growth, was less than 10%.

Interestingly, culture realized according to the process herein described can be maintained for months.

As usual for biological material, seasonal differences in the yields of accumulated biomass are observed from a minimum of 1-2 g/l and occasionally till a maximum of 20-30 g/l.

Example 5 – Evaluation of inoculum(a) of algae/cyanobacteria in the culture medium during the production process on overall algal biomass yield

Symbiotic culture was obtained as described in Example 1, in two months culturing. The only differences are that glycerol was reduced to 1 g/l and *Chlamydomonas reinhardtii* cells were added to the co-culture as additional exogenous nutrient.

This example illustrates that the addition of a second alga species (in TAP or Chalkley's medium) to the co-culture is useful to reduce content of organic nutrient (in the specific case glycerol).

The results reported in table 6 (representing a typical pattern of growth) show that addition of such digested algae to the co-culture leads to higher yield of algal biomass production compared to the biomass obtained by a culture of algae grown alone (see for comparison table 2 second column).

Table 6.

Day	**Biomass dried weight (g/l) Symbiont + nutrition with alga *Chlamydomonas***
1	**0.9**
2	**4.0**
3	**6.1**
4	**6.2**
5	**8.8**
6	**12.1**
7	**11.0**
8	**12.3**
9	**11.5**
10	**10.1**
11	**15.3**
12	**18.7**
13	**19.0**

The relative standard deviation, calculated on n=6 sampling of one typical pattern of growth, was less than 15%.

Example 6 – Evaluation of different paramecia/algae combinations on overall algal biomass yield

In the present example, we have tested different paramecia/algae combinations, in order to determine if biomass production increased and if symbiosis occurs with other paramecia.

We used as microalgae *C. minutissima* (CM) and *C. sorokiniana* H1986 (CS) and as protozoa *P. bursaria, P. caudatum* and Ps cultures.

Table 7.

Name	Biomass - dry weight on 3th day (g/l)	Biomass - dry weight on last day (g/l)
CM+Ps	**1.5**	**2.2**
CM+*P. bursaria*	**4.8**	**1.0**
CM+*P. caudatum*	**3.5**	**1.0**
CS+Ps	**1.6**	**2.0**
CS+*P. Bursaria*	**1.3**	**2.5**
CS+*P. caudatum*	**1.4**	**2.0**

The relative standard deviation, calculated on n=4 sampling of one typical pattern of growth, was less than 16%.

These data indicate that at the beginning of the experiment, associations between CM/*P. bursaria* and CM/*P. caudatum* are more productive than association with Ps, but at the end, productivity of these two cultures is reduced. CM+Ps culture instead is more productive towards the end of the experiment, indicating that the presence of these protozoa, determines an adaptation to endosymbiosis in a longer term.

In the case of the alga *C. sorokiniana*, the production of the three different cultures gives almost the same biomass.

Example 7 – Evaluation of Chlamydomonas reinhardtii as infected alga on overall algal biomass yield

In order to demonstrate Chlorella symbiosis specificity, we have co-cultivated the same paramecia indicated above with *Chlamydomonas reinhardtii* (CR).

This experiment was carried out for 20 days and results are reported in table 8.

Table 8.

Name	Biomass - dry weight on 7°day (g/l)	Biomass - dry weight on last day (g/l)
CR	**0.9**	**0.8**
CR+ *P. bursaria*	**1.3**	**0.9**
CR+ P. caudatum	**0.8**	**0.2**
CR+Ps	**1.8**	**0.9**

The relative standard deviation, calculated on n=4 sampling of one typical pattern of growth, was less than 16%.

The yield obtained in this experiment are poor compared to previous ones, especially at the end of the experiment, indicating that the presence of paramecia do not result in an increase of the productivity of the *Chamydomonas reinhardtii* culture and that this alga species is not able to establish symbiosis with the tested protozoa.

Example 8 – Characterization of algal biomass composition

Symbiotic cultures were obtained according to Example 3. The particular composition of the biomass was found to comprise cells, lipids, starch, microtubules, and soluble sugars such as glycogen, explaining that it appears as a "glue". The biomass was mostly present as precipitate in big aggregations, in part floating and in part in solution in a ratio depending on the age of the culture. In conditions of daily nutrition of 2.5g/l glycerol and 100µl/l vigor ultra, with scale up to 200L, the content of lipids is preponderant and increases with the age of the culture (table 10).

The age of the culture was calculated as days of culture starting from the first infection day, after mixing the two microorganisms, and when symbiosis was established, co-culture and algal culture were compared for the content of total lipids.

Table 10 provides the average lipid content per dried biomass in percent determined by the gravimetric method of Logan 2008.

Table 10 shows that the lipid content greatly increased in the co-cultivation system compared to the culture of the alga grown alone from 47 till 90% of lipid per dried biomass after infection of algae with paramecium for a long time indicating that lipid content increases with the age of the culture after the infection.

Table 9.

days of culturing	% of lipids per dried biomass	
	alga alone (CM)	Symbiont (Ps+CM)
7	47	57
30	40	87
90	n.d.	90
120	n.d.	91

The relative standard deviation, calculated on n=6 sampling of one typical pattern of growth, was less than 10%. *n.d.* not determined since the culture of alga alone did not resist 90-120 days in culture. Most of the cultures with algae alone and waste material die after only 7 days and occasionally lasted till 30 days.

For the characterization of the samples, analysis by gas chromatography of the single lipid components was performed by lyophilizing the culture samples.

In table 11 the quantities of fatty acids contained in the biomass treated samples are expressed in percentage to obtain a whole vision of the categories of produced fatty acids. It is clear that there is a slight different distribution of the various lipid classes.

In the tested conditions of temperature, nutrition and selected extraction method, the first sample (Ps+CM) is richer on PUFA (about 35%) than the CM sample (about 26%). In details, the sample PS+CM has a slightly major production of arachidonic acid omega-6 (about 29% against 20% for CM) and similar production of DHA omega-3 (about 6%). *CM+caudatum* lipid distribution is more similar to CM+Ps production than *CM+bursaria*.

Table 10.

Fatty acids	Ps+CM	Bursaria+CM	Caudatum+CM	CM
14:0	**10.16**	**1.20**	**7.81**	**12.27**
16:0	**24.88**	**30.73**	**25.52**	**23.69**
9c-16:1	**1.45**	**1.58**	**2.01**	**2.19**
17:0	**1.13**	**3.41**	**1.49**	**2.02**
18:0	**6.26**	**7.89**	**5.32**	**6.42**
9c-18:1	**8.93**	**14.21**	**12.35**	**13.29**
11c-18:1	**4.99**	**6.42**	**4.99**	**6.99**
18:2 omega-6	**17.87**	**11.85**	**19.36**	**13.91**
18:3 omega-6	**2.84**	**1.09**	**1.66**	**1.60**
18:3 omega-3	**3.28**	**4.56**	**4.38**	**2.62**
18:4 omega-3	**0.95**	**0.48**	**0.72**	**0.57**
20:3 omega-6	**1.51**	**2.91**	**1.33**	**2.05**

In **Table 10** the yield of FAME obtained by three methods of extraction are reported for CM+Ps. We performed a comparison of lipid production using 5different extractions and esterification methods:

- Method A1: extraction with methanol-chloroform 1:2 and esterification by NaOH in methanol;
- Method A2: extraction with methanol-chloroform 1:1 and esterification by NaOH in methanol;
- Method A3:extraction with methanol-chloroform 1:1 and esterification by NaOH in methanol/benzene.

Between the two extractive methods A2 and A3 we obtained major components with more alcoholic functions (mono-glycerids and diglycerids) compared to the method 15A1 that is for apolar and phospholipidic components.

The total lipid amount extracted with method A1 and method A2 is similar while, fatty acid composition changes after the esterification procedure due to the different composition of lipids.

The third column on 20the right shows how the quantity of fatty acids varies using the second method of esterification that allows to transform efficiently the cholesterol components.

The method A1 has allowed to derivative phospholipid components and triglycerides, while the method A3 has 25allowed to derivative well the components of cholesterol.

Table 11.

Fatty acids	Ps+CM	Bursaria+CM	Caudatum+CM	CM
20:4 omega-6	**6.61**	**0.75**	**5.32**	**2.77**
20:5 omega-3	**0.79**	**2.65**	**0.75**	**0.23**
22:0	**2.43**	**6.07**	**2.50**	**4.20**
22:6 omega-3	**0.89**	**2,05**	**1.14**	**2.21**
24:0	**5.04**	**2.16**	**3.35**	**2.96**
SFA	**49.89**	**51.46**	**46.00**	**51.57**
MUFA	**15.36**	**22.21**	**19.35**	**22.48**
OMEGA-6	**28.83**	**16.60**	**27.67**	**20.33**
OMEGA-3	**5.92**	**9.74**	**6.98**	**5.63**
PUFA	**34.75**	**26.34**	**34.65**	**25.96**

In addition, to screening microalgae for elevated biomass productivity and intrinsic cellular lipid content, the fatty acid profile of microalgae is an important characteristic as it ultimately affects the quality of biodiesel production. The length of carbon chain of saturated and unsaturated fatty acids affects biodiesel properties such as cetane number, oxidative stability and cold-flow properties. Generally, high proportion of saturated fatty acids (SFA) and monounsaturated fatty acids (MUFA) are preferred for increased energy yield, superior oxidative stability, and higher cetane numbers. However, oils dominated by these fatty acids are prone to solidify at low temperature. While oils rich in polyunsaturated fatty acids (PUFAs) have very good cold-flow properties, they are, on the other hand, more susceptible to oxidation.

Results in tables 10 and 11 show that the majority of fatty acids presents in isolated cultures were C16:0 (about 23-25%), 16:1 (about 10-12%) and omega-3 and 6 which comprised 35-40% of the

total FAME. SFA and MUFA were predominant at >60% of the total lipid content which is favorable for high cetane number. However, also PUFAs in range of 35-45% exceeded the requirements in the International biodiesel Standard for Vehicles (EN14214). PUFA are high-value fatty acids for nutrition, food additives and aquaculture nutrients. In order to comply with biodiesel standard on the PUFA ratio, these components can be hydrogenated or extracted before the rest of oil is converted into biodiesel. That makes the oils derived biodiesel less susceptible to oxidation in storage and takes full advantage of algae-paramecium symbiotic culture.

Naturally, details of implementation and the embodiments may vary widely with respect to what is described and illustrated without thereby departing from the scope of protection of the present invention, as defined in the annexed claims.

REFERENCES

Yusuf Chisti. Biodiesel from microalgae. *Biotechnology Advances* 25 (2007) 294–306.

Bio-Farms for Nutraceuticals. Functional Food and Safety Control by Biosensors series: A*dvances in Experimental Medicine and Biology*, Vol. 698, Giardi, Maria Teresa; Rea, Giuseppina; Berra, Bruno (Eds.) 1st Edition., 2010, XXVIII, 332 p. 65 illus.

M Fujishima. Endosymbionts in *Paramecium. Microbiology Monographs*, Volume 12, (2009) Ed. M. Fujishima Series Ed., A Steinbuchel, Publisher Springer-Verlag Berlin Heidelberg.

J Barber and Andersson B. (1992). Too much of a good thing: light can be bad for photosynthesis. *Trends Biochem Sci.* 17(2), 61-6.

AK Mattoo, MT Giardi, A Raskind, M Edelman. (1999). Dynamic metabolism of photosystem II reaction center proteins and pigments. *Physiologia Plantarum*. 107(4), pages 454–461.

N Savage. *(2011).* The scum solution: The green slime that covers ponds is an efficient factory for turning sunlight into fuel, but growing it on an industrial scale will take ingenuity. *NATURE,* 474, 15- 16.

L Gouveia and AC Oliveira. (2009). Microalgae as a raw material for biofuels production. *J Ind Microbiol Biotechnol* 36, 269–274.

M Summerer, B Sonntag and R Sommaruga. (2007). An experimental test of the symbiosis specificity between the ciliate *Paramecium bursaria* and strains of the unicellular green alga *Chlorella. Environmental Microbiology 9(8), 2117–2122.*

M Summerer, B Sonntag, and R Sommaruga (2008). Ciliate-Symbiont specifity of freshwater endosymbiotic *Chlorella. J. Phycol.* 44, 77–84.

ES Kaneshim. Lipids of *Paramecium. (1987). Journal of Lipid Research.* 28, 1241-1258. Blackwell Publishing Ltd

JM Logan, TD Jardine, TJ Miller, SE Bunn, RA Cunjak, and MoE Lutcavage. (2008). Lipid corrections in carbon and nitrogen stable isotope analyses: comparison of chemical extraction and modelling methods. *Journal of Animal Ecology. 77, 838–846.*

EH Harris. (1989). *The Chlamydomonas sourcebook*: a comprehensive guide to biology and laboratory use. San Diego, Academic Press.

M Kobayashi, T Kakizono, S Nagai. (1991). Astaxanthin production by a green alga, Haematococcus pluvialis accompanied with morphological changes in acetate media. *J of Fermentation and Bioengineering* 71(5), 335-339.

Finlay B.J**.,** Maberly S.C., and Estaban G.F. (1996). Spectacular abundance of ciliates in anoxic pond water: contribution of symbiont photosynthesis.

Nakajima T, Sano A, Matsuoka H. (2009). Auto/eterotrophic endosymbiosis evolves in a mature stage of ecosystem development in a microcosm composed of an alga, a bacterium and a ciliate. BioSystems 96. 127-135.

ATTEMPT OF MOLECULAR ANALYSIS

To confirm organism identification, PCR analyses were performed. Total DNA was extracted from the culture of *Thetraymena pyriformis* and *Chilomonas paramecium* isolated from our cultures, obtained by Sciento and from *Chlorella minutissima* single culture.

MATERIALS AND METHODS

For these analyses we followed the indication of literature (Mullis K.B., 1983).

Attempt of PCR analyses, *nad10* gene for *Tetrahymena pyriformis* and 18S gene for *Chilomonas paramecium* were chosen. On the website www.ncbi.nlm.nih.gov we found sequences of these two genes. All sequences of the same gene found in GeneBank are aligned by BLAST program and identical gene fraction for all strains was selected and used to draw primers.

Primer sequences used in this work and drown using Primer3 http://primer3.ut.ee/ are shown in **Table 1**.

Organism	Primer name	5'-3' sequence	Tm	Fragment length amplified (bp)
Chilomonas paramecium	**PF1**	**AAGCAGGCTGTTGCTTGAAT**	**55.3**	**172**
	PR1	**TGCTTTCGCACAAGTTCATC**	**55.3**	
	PF2	**AGGGCCAAACGGTCTTCTTAT**	**57.9**	**180**
	PR2	**CCAGAGGCTGACAGTTCACA**	**59.4**	
Tetrahymena pyriformis	**PF1tet**	**GCTCCGGGCTTAAGAAGATT**	**57.3**	**180**
	PR1tet	**TAAAGCCTCTGCTGTTGGTG**	**57.3**	
	PF2tet	**TTTTGGTTTGGCTTGTTGTG**	**53.2**	**215**
	PR2tet	**TTGCGCAGCTACCCATAGAT**	**53.2**	

Table 1. List of the primers used in this work. For each primer the name, the sequence, the melting temperature (Tm) and the length of the DNA fragment amplified were indicated.

Total DNA extraction.

For DNA extraction DNeasy plant mini Kit (Qiagen) was used, as suggested by Hoef-Emden, 2005.

DNA extraction was performed on lyophilized samples of *Chilomonas paramecium, Tetrahymena pyriformis* isolated in our laboratories, *Chilomonas paramecium* and *Tetrahymena pyriformis* obtained by Sciento http://www.sciento.co.uk/ and *Chlorella minutissima*.

Samples were obtained lyophilizing overnight the pellet collected centrifuging 100ml of each culture for 15min at 5000rpm.

Lyophilized samples were treated for DNA extraction performed by DNeasy plant mini kit (Qiagen), as suggested by Hoef-Emden, 2005. Below, the kit protocol is reported.

Grind tissue under liquid nitrogen to a fine powder using a mortar and pestle. Transfer the tissue powder and liquid nitrogen to an appropriately sized tube and allow the liquid nitrogen to evaporate. Do not allow the sample to thaw. Add 400µl of Buffer AP1 and 4µl of RNase stock solution (100mg/ml) to a maximum of 100 mg of ground (wet weight) or 20mg (dried) plant or fungal tissue and vortex vigorously. Incubate the mixture for 10min at 65°C. Mix 2–3 times during incubation by inverting tube. Add 130µl of Buffer AP2 to the lysate, mix, and incubate for 5min on ice and Centrifuge the lysate for 5min at full speed. Apply the lysate to the QIAshredder spin column sitting in a 2ml collection tube and centrifuge for 2min at maximum speed. QIAshredder removes most precipitates and cell debris. Transfer flow-through fraction from step 5 to a new tube (not supplied) without disturbing the cell-debris pellet. Add 1.5volumes of Buffer AP3/E to the cleared lysate and mix by pipetting. Apply 650µl of the mixture from step 7, including any precipitate, which may have formed, to the DNeasy mini spin column sitting in a 2ml collection tube. Centrifuge for 1min at ≥6000xg and discard flow-through. Repeat step 8 with remaining sample. Discard flow-through and collection tube. Place DNeasy column in a new 2 ml collection tube, add 500µl Buffer AW to the DNeasy column and centrifuge for 1min at ≥ 6000xg (≥ 8000rpm). Discard flow-through. Add 500µl Buffer AW to the DNeasy column and centrifuge for 2min at maximum speed to dry the membrane. Transfer the DNeasy column to a 1.5ml or 2ml microcentrifuge tube and pipet 100µl of preheated (65°C) Buffer AE directly onto the DNeasy membrane. Incubate for 5min at room temperature and then centrifuge for 1min at ≥6000xg (≥8000rpm) to elute. Repeat elution (step 12) once as described.

DNA quantification was performed by nanodrop at 260nm using 2µl of each sample. The results are reported below.

Using 1% agarose gel, DNA quality was determined.

For PCR analysis, reaction mix was prepared as follow:

Components	**Volume µl**
DNA 50ng	**X**
Buffer 1X	**5**
$MgCl_2$	**1.5**
P1+P2 20µM	**2.5**
dNTPs 10mM	**1**
Taq polymerase	**0.25**
ddH_2O	**X**
Total volume	**50**

Table 2. List of PCR mix components.

The amplification cycle used was: First denaturation at 94°C for 3min, denaturation 94°C for 45sec, annealing for variable temperature depending on primer Tm for 30sec, Elongation at 72°C for 1min and 30sec, Final elongation at 72°C for 10min. Amplification steps were repeated for 30cycles.

PCR products were analyzed by electrophoresis on 1% agarose gel with 1X TAE buffer and using 1Kb DNA ladder as marker.

RESULTS AND DISCUSSION

After few days from the inoculum of *Chlorella minutissima* in liquid culture medium (TAP) observations of the cultures under optical microscope revealed the presence of other organisms. We decided to study the phenomenon by microscope observations, in order to identify microorganisms. Comparing photos of our organisms with on line information, we identified them as paramecia, that are ubiquitous freshwater organisms found in almost all kind of freshwater habitats (Sommaruga & Sonntag, 2009; Landis, 1988). After, according to similarity with our organisms, we have ordered from Sciento http://www.sciento.co.uk/ various organisms and for comparison between our organisms and the other ones, we have identified isolated paramecia as *Chilomonas paramecium* and *Tetrahymena pyriformis*.

To confirm organism identification, PCR analyses were performed. In the first part of this study, we analyzed *in silico* on the NCBI website www.ncbi.nlm.nih.gov the sequences of those two organisms in order to draw specific primers: however, we have seen that there are no complete genome sequences for those two organisms, but also pieces of sequences of various genes.

Our research in GeneBank has highlighted that for *Tetrahymena pyriformis* many strains have been previously identified and that for each gene sequence the specific sequence for each strain are reported. We did not know what strain is present in our cultures. For the identification of our paramecium the sequence of the *nad10* gene was chosen. By comparison of *nad10* sequence gene between *Tetrahymena* strains present in GeneBank, a piece of 490bp conserved from all the strains

was identified. Subsequently, on these sequence using a website Primer3 (www.primer3.ut.ee) two pairs of primers were obtained. For *Chilomonas paramecium* the sequence of *18S* gene was selected and two pairs of primers were drown.

In order to identify our organisms, total DNA using the DNeasy Plant mini kit was extracted from the culture reported in **Figure 1**.

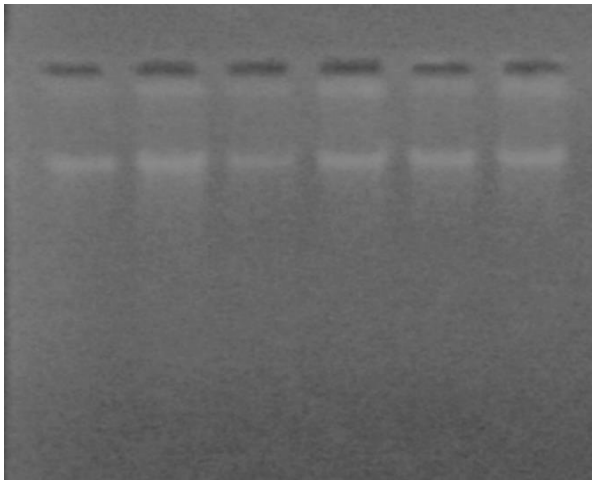

λ CM tetra chilo tetra1 chilo1

Figure 1. Electrophoresis gel. From left to right λ DNA, *C. minutissima*; *Tetrahymena pyriformis* isolated; *Chilomonas paramecium* isolated; *Tetrahymena pyriformis* (1) by Sciento and *Chilomonas paramecium* (1) by culture collection total DNAs are shown.

From this photo is possible to see that DNA quality of each sample was good although the quantity was not much. Various tests were performed in order to obtain DNA amplification, modifying melting temperatures, annealing times and DNA template quantity but none case of amplification was obtained. This negative result is due to the chosen gene sequences and to the designed primers, probably because the identified sequences were not adapted for our organisms. A genomic analysis may be necessary in the future.

More detailed analyses were performed that are not presented for confidentiality reasons.

PART II

Biosensors for agrifood monitoring

INTRODUCTION

What is a biosensor?

Biosensors are devices, which use a biological recognition element retained in direct spatial contact with a transduction system (IUPAC definition) (Thevenot et al., 1999). The biosensor consists of three parts: the first element is the biomediator a biologically derived material e.g. tissue, microorganisms, organelles, cell receptors, enzymes, antibodies, nucleic acids, and biological sensitive elements created with genetic engineering, or a biomimic system e.g. aptamers, MIPs, etc. The second element is the transducer e.g. physicochemical, optical, piezoelectric, electrochemical, etc. that transforms the signal resulting from the analytes interaction with the biological element into a signal that can be measured and quantified. The third element is the associated electronics or signal processor, responsible of the visualization results in a user-friendly way (Cavalcanti et al., 2008). These devices can be grouped according to their biological element or their transduction system. In the following figure a biosensor scheme is presented.

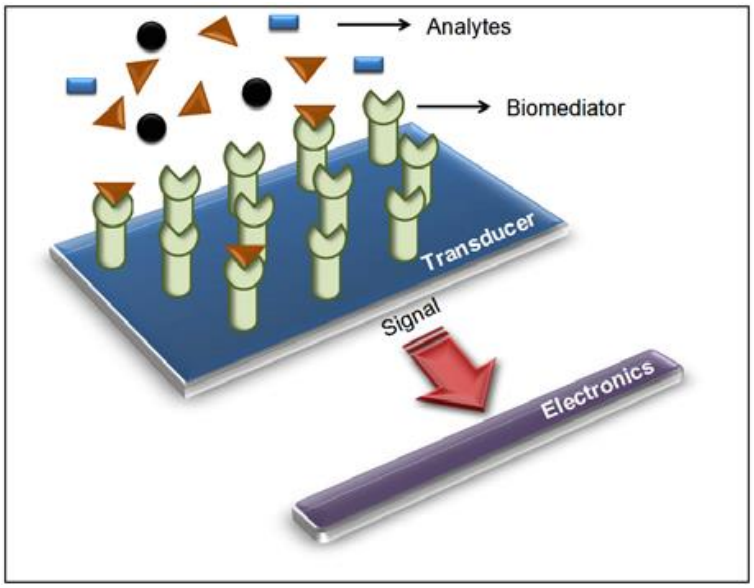

Figure 1. Schematic representation of a biosensor.

The exploitation of the selectivity of the biological element is the "driving force" of the biosensor (Mascini, 2005).

Looking at the past it is clear that the concept of biosensor has evolved. The first example of biosensor was illustrated by entrapping the enzyme glucose oxidase in a dialysis membrane over an oxygen probe. Since the beginning of the‘80s, several authors started to prove the concept of biosensor as a system in which an enzyme is coupled to electrochemical-optical sensors (Scognamiglio et al., 2013; Scognamiglio et al., 2012; Mascini, 2005).

Then, enzymes, organelles, bacteria, specialized biological tissues containing specific enzymes were coupled to potentiometric, amperometric, optical, thermometric or piezoelectric devices, etc. Recently, the concept evolved again in the attempt to replace or mimic the biological material with synthetic chemical compounds, such as MIPs (Molecular Imprinted Polymers) .

Thus, enzymes and biological elements based on enzymes or mimetic material represent the "catalytic elements" class. The second important class is represented by the "affinity elements" composed by antibodies, lectins, nucleic acids (DNA and RNA) and recently also synthetic ligands.

Catalytic events or affinity events have not the same scheme of transduction. If the biological recognition element present in the sensing layer is an enzyme or generally a biocatalyst, the reaction takes place in the presence of the specific target analyte and an increasing amount of co-reactant or product is consumed or formed in a short time depending on the turnover.

Using a biological system catalytic or affinity two main problems can be occur: the associated fragility and the operational activity. Most proteins have an optimal pH range in which their activity is maximal and this pH range should be compatible with the transducer. Moreover, most of the biological systems have a narrow range of operating temperature (15÷40°C). The most important problem and main drawback for industrial exploitation is the short lifetime associated with the biological elements. Lifetime of at least months or few years is the prerequisite for a suitable market and the fragility of the assembled systems has always limited the diffusion of biosensors into the market (Giardi et al., 2006; Rouillon, 2005).

However, the biosensor advantages are simplicity, small size, robustness, low cost, ability to generate reliable and continuous information, high selectivity and sensitivity, depending on the biomediator type and immobilization methods. This innovative technology represents a valid support to other efficient analytical methods (HPLC, or GC-MS etc.), and finds for instance useful applications in pre-screening analyses.

Biosensors have various application fields as reported in the following list: medical applications e.g. glucose monitoring in diabetes patients (Newman & Turner, 2005) and other medical health related targets (Vo-Dinh, & Cullum, 2000); environmental applications, e.g. detection of pesticides in water contaminants (Touloupakis et al., 2005); remote sensing of airborne bacteria, e.g. in counter-

bioterrorist activities (Hofstadler et al., 2005); detection of pathogens (Pohanka et al., 2007); determination of toxic levels of substances before and after bioremediation; detection of drug residues, such as antibiotics and growth promoters (Ravindra et al., 2007); analysis of food quality (e.g. content of phenols in wine, tea and oil) (Johanneke et al., 2006).

Trasducer systems

As reported above, biosensors can be classified for their trasducer system in electrochemical, potenziometric, piezoelectric and optical et al. These biosensors will be briefly described in the following.

Conductimetric biosensors. The conductimetric principle of measurement is widely applicable to chemical systems, because many chemical reactions produce or consume ionic species and thereby alter the overall electrical conductivity of the solution its resistance being determined by migration of all ions that are present in a solution. The principle of a conductimetric biosensor involves the application of an electric field across a pair of microelectrodes surrounded by an electrolyte or a buffered solution containing an immobilized enzyme on a sensor and the species to be detected. An electric field is generated by a sinusoidal voltage waveform across the electrode to minimize or to eliminate the undesirable electric process and to overcome the problems related to the temperature variation in the single cell device. An example of conductimetric biosensor is the "urea biosensor", where the urease enzyme is immobilized on a chip to detect urea. The enzyme catalyzes the decomposition of urea which produces bicarbonate ions increasing the conductivity of the tested solution (Watson et al., 1987/88).

Potenziometric biosensors. Potentiometric biosensors use an Ion-selective electrode (ISE) to transduce a biological reaction into an electrical signal.

In particular, the reactions involve the release or absorption of ions. An immobilized enzyme layer catalyzes the biological reaction which generates or absorbs ions, when the reaction involves H^+ ions, a pHmeter is the ISE used.

These sensors are mainly based on field effect transistors (FETs) and were first proposed by Peter Bergveld in 1970 as the ion sensitive field-effect transistor (ISFET). Enzyme-sensitive field-effect transistors (ENFETs) can be fabricated from ISFETs by applying a thin overlayer of enzyme-loaded gel on the ion-selective membrane (Bergveld, 2003). Three types of potenziometric

biosensors are the most widely used: glass electrodes for cations (which normally is a pH electrode), pH electrode with a gas permeable membrane and solid state electrodes. Different example of potenziometric biosensors have been developed, for example to detect urea, penicillin or glucose (Eggins, 2002).

The potential developed across an ion-selective membrane separating two solutions is measured at virtually zero current, meaning high impedance and no interference to the reaction (Blum, & Coulet, 1991). A biorecognition element is immobilized on the outer surface or captured inside the membrane. The Nernst potential of the pH glass electrode is described by the Nicolsky-Eisenman equation (Buerk, 1993).

Potentiometric measurements involve exactly non-faradaic electrode processes with no net current flow and operate on the principle of the charge density accumulation at an electrode surface, resulting in the development of a significant potential at that electrode. This potential is proportional to the logarithm of the analyte activity present in the sample and is measured relative to an inert reference electrode that is in contact with the sample.

Amperometric biosensors. The signal in these biosensors is generated by the electron exchange between the biological system (in the bioreceptor layer) and one electrode. In general, using the amperometric biosensors, the analyte is involved or undergoes a redox reaction that can be followed measuring the current in an electrochemical cell.

The analytes, or the species involved through a (bio)chemical reaction, change the state of oxidation at an electrode. The electron flow is proportional to the amount of species electrochemically converted at the electrode (Belluzo et al., 2008).

The most common biosensors are based on chronoamperometric experiments, where the current is monitored as function of time. Usually, for one experiment a single potential step is used. The analysis of chronoamperometry data is based on the Cottrell equation, which defines the current-time dependence for linear diffusion control (Pinalysa et al., 2005). Amperometric biosensors can work in two- or three-electrode configurations. The first case consists of reference and working (containing immobilized biorecognition component) electrodes. The main disadvantage of the two-electrode configuration is the limited control of the potential on the working electrode surface at the highest currents. Because of this problem the linear range could be shortened. To solve this problem a third auxiliary electrode is employed. In this case the voltage is applied between the reference and the working electrodes, and current flows between the working and the auxiliary electrodes. An example of three electrode sensors is given in **Figure 2** (Pohanka & Skládal, 2008).

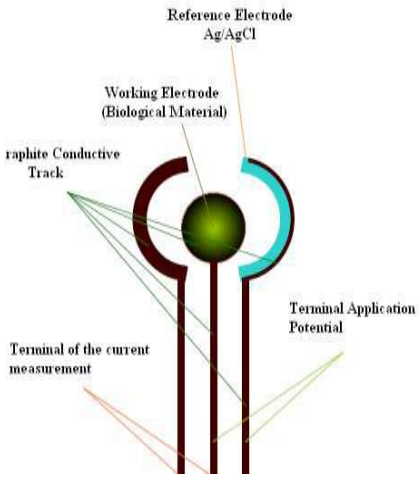

Figure 2. The principal features of the Screen Printed Electrode (SPE).

The amperometric biosensors are among the most common biosensors studied both in the past and today. This type of biosensors permit to use different types of biological material e.g. enzymes, cells, tissues, proteins, antibodies, nucleic acids and various analytes for numerous applications such as: clinical use (e.g. detection of infection-marker antibodies, acetylcholine); biological oxygen demand; Detection of simple molecules such as glutathione, L-alanine, pyruvate, lactate, and cholesterol (Belluzo et al., 2009); food analysis such as lactate, citrate, glutamate, ethanol, etc. (Prodromidis & Karayannis, 2002); environmental analysis to detect toxic compounds such as pesticides, various phenol types, surfactants, antibiotics, toxins etc. (Mozas et al., 2004; Buonasera et al., 2010).

An important tool used for development of amperometric biosensors is the voltammetric analysis, used to investigate electrolysis mechanisms. In this technique several voltages are applied vs. time to the electrode and the corresponding current that flows is monitored to identify the specific potential of the electrochemical reaction. In the typical cyclic voltammetry, a solution component is electrolyzed (oxidized or reduced) by placing the solution in contact with the electrode surface making this surface sufficiently positive or negative in voltage to force electron transfer. In general, the reaction on the surface is started with a particular voltage with respect to a half-cell reference (such as calomel or Ag/AgCl); at a linear rate the electrode voltage is changed to a higher or lower one and finally at the same linear rate, the voltage to the original value is changed back. When the surface becomes sufficiently negative or positive a solution species can receive electrons from the surface or transfer electrons to the surface. Those result on a measurable current in the electrode circuitry that can be detected. When the voltage cycle is reversed generally also the electron transfer

between electrode and the chemical species is reversed leading to an "inverse" current peak (Kissinger & Heineman 1983; Van Benschoten et al., 1983).

Piezo-electric biosensors are principally based on the measurement of the change in resonant frequency of a piezo-electric crystal due to mass changes on its surface. These changes are caused by the interaction between the tested species and the biospecific agents immobilized on the crystal surface. This interaction determines resonant frequency changes due to molecules adsorbed or desorbed from the surface of the crystal. The frequency of vibration of the oscillating crystal normally decreases when the analyte binds to the receptor coating the surface. Such sensors operate by the propagation of acoustoelectric waves either along the surface of the crystal or through a combination of bulk and surface and are commonly referred to as surface acoustic (SAW) wave devices (Rajinder, 1994). Most common piezoelectric biosensors include microgravimetric immunoassays, microbial assays, DNA hybridization, enzyme based detections and gas phase biosensors (Ngeh-Ngwainbi et al., 1990).

Optical biosensors are mainly composed of a light source, an optical transmission medium (fiber, waveguide, etc.), an immobilized biological recognition element (enzymes, antibodies, protein, microbes, cells, etc.) and an optical detection system. The optical biosensors are classified according to the transduction method (fluorescence, luminescence, etc.), geometry (Surface Plasmon Resonance, Fiber Grating Based Sensors) and Evanescent Wave Fiber Optic Biosensors.

Some of the advantages offered by an optical biosensor are selectivity and specificity, remote sensing, isolation from electromagnetic interference, fast, real-time measurements, multiple channels/multi parameters detection, compact design, minimally invasive for in vivo measurements, choice of optical components for biocompatibility, detailed chemical information on analytes.
Optical biosensors can use chemiluminescence, luminescence or fluorescence: chemiluminescence occurs by exciting molecules with a chemical reaction whereas luminescence occurs by exciting molecules with a light and consequent re-emission of light at a longer wavelength (Patel et al., 2010).
In the most commonly form of an optical biosensor the transduction process induces a change in the phase, amplitude, polarization, or frequency of the input light in response to physical or chemical changes produced by the biorecognition process.

Optical devices may have fiber optic probes on the tip of that enzymes and dyes (often fluorescent) have been immobilized. These probes consist of at least two fibers. One is connected to a light source of a given wavelength range that produces the excitation wave. The other connected to a photodiode detecting the change in optical density at the appropriate wavelength (Nunes & Marty, 2006).

Surface Plasmon Resonance transducers measures changes in the refractive index at and near the surface of the sensing element. SPR measurement is based on the detection of the attenuated total reflection of light in a prism with one side coated with a metal (e.g. gold). When a p-polarized incident light passes through the prism and strikes the metal at an adequate angle it induces a resonant charge wave at the metal/dielectric interface that propagates a few microns. The total reflection is measured with a photodetector as a function of the incident angle (Tao et al., 1999). For example, when an antigen binds to an antibody that is immobilized on the exposed surface of the metal the measured reflectivity increases. This increase in reflectivity can then be correlated to the concentration of antigen.

Sensing elements

Functional biorecognition material is a key component of biosensors. Generally they have high affinity (low detection limit), high specificity (low interference), wide dynamic range, fast response time and long shelf life. The antibodies are the most frequently used biorecognition molecules in the optical biosensor community. However, enzymes were the first recognition elements used in the biosensors. Other recognition elements are nucleic acids such as aptamer and DNAzyme for the monitoring of environmental pollutants, photosynthetic organelles and photosynthetic organisms such as microalgae. An in-depth description of each class of sensing elements is shown below (Jose´, 2003).

Antibodies are selective proteins produced by B-lymphocytes in response to antigenic structures. Molecules larger than about 10kDa can stimulate an immune response. Antibodies are produced as monoclonal and polyclonal varieties, with monoclonal antibodies binding to a single epitope and polyclonal antibodies being capable of binding to multiple epitopes. Many antibodies are commercially available and commonly used in immunoassays. Antibodies are usually immobilized on the surface of the transducer by covalent attachment by conjugation of amino, carboxyl,

aldehyde, or sulfhydryl groups. Furthermore, binding may not be reversible and regeneration of the surface may require drastic changes in conditions like low pH, high ionic strength, detergents, etc. Therefore, efforts are being made to produce low cost single use sensors. Immunosensors usually employ optical or acoustic transducers. The main advantage of immunosensors over other immnunological methods (e.g., ELISA formats) is the better regeneration and binding properties of the sensing surface, which is critical for the successful reuse of the same sensor surface and the accuracy of detection results; this makes immunosensor potentially suitable for in-field measurements. In environmental analysis targets of interest are usually pesticides, persistent organic pollutants (POPs), endocrine disrupting chemicals (EDCs), small molecule substances (molecular weight <1kDa. Antibody immobilization is always utilized in preparing sensor surface of immunosensors (Mahleret al., 2009). However, the control over the number of antibodies and their orientation and relative position to the sensor surface is difficult (Mahler et al., 2009a). This type of biomediators can be reused using a regeneration process. The cycles of regeneration are usually no more than fifteen since in each cycle antibody activity decreases leading to inaccurate detection results. Recently, hapten-carrier-protein conjugates as bio-recognition molecules were immobilized onto the surface of immunosensor in order to obtain the stable reusable sensor (Hermanson, 1996).
Immunosensors based on specific antigen-antibody interactions have become the gold-standard technique in clinical diagnostics and environmental monitoring (Jose´, 2003).

Aptamers are single-stranded oligonucleotides that fold into complex three-dimensional structure and bind strongly and selectively to one certain kind of target or one class of targets (Borisov & Wolfbeis, 2008). Aptamers offer a useful alternative to antibodies as sensing molecules and have opened a new era in development of affinity biosensing due to their unique characterizations. In vitro selected aptamers could be produced for any target such as proteins, peptides, amino acids, nucleotides, drugs, heavy metal ions, and other small organic and inorganic compounds. Aptamers could be chemically synthesized without the complicated and expensive purification steps by eliminating the batch-to-batch variation found when using antibodies (Ronkainen et al., 2010).
Furthermore, modifications in the aptamer through chemical synthesis can be introduced enhancing the stability, affinity and specificity of the molecules. In addition, aptamers are more stable than antibodies and thus are more resistant to denaturation and degradation. Often the affinity parameters of aptamer-target complex can be changed for higher affinity or specificity. In addition, aptamers have a higher temperature stability and can recover their native active conformation after denaturation whereas antibodies are large temperature-sensitive proteins that can undergo

irreversible denaturation. Recently, several DNA/RNA aptamers have been selected for POPs, EDCs, organophosphorus pesticides, antibiotics, biotoxins, and pathogenic microorganisms. Aptamers have become increasingly important molecular tools for environmental bioassay, for example in the detection of EDCs in water (Mehta & Rouah-Martin, 2011). Through the "signal-on" mode or the "signal-off" mode, reflecting the extent of the binding process thereby allowing for quantitative measurement of target concentration, several DNA aptamer fluorescence-based sensors have been developed for the detection of Hg2+, Pb2+ and other trace pollutants. Although a variety of aptamers has been successfully selected for environmental contaminants the detection of the real water samples is still in the cradle (Zhang et al., 2005).

DNAzymes are small single-stranded nucleic acids that fold into a well-defined three-dimensional structure with high specificity to various ligands such as low-molecular-weight organic or inorganic substrates, macromolecules or metal ion (Zhang et al., 2011). DNAzymes have a promising capacity to selectively identify charged organic and inorganic compounds at ultratrace levels in environmental samples or biological systems. Furthermore, DNAzymes can perform chemical modifications on nucleic acids while aptamers can bind a broad range of molecules (Hollenstein et al., 2008). A combination of these two molecules has generated a new class of functional nucleic acids known as allosteric DNAzymes or aptazymes. Combining the specificity of nano-biological recognition probes and the sensitivity of laser-based optical detection DNAzymes are capable of provide unambiguous identification and accurate quantification of environmental pollutants, ranging from small ions to large molecules. RNA-cleaving DNAzymes are the most widely used due to their simple reaction conditions fast turnover rates and significant modifications of their substrate lengths. Using the selection *in vitro* of specific DNAzymes, several fluorescence biosensors have extensively been developed for the detection of various heavy metal ions, such as Pb^{2+}, Cu^{2+}, Mg^{2+}, Ca2+, Zn2+, Co2+, Mn2+, $UO2^{2+}$, Hg2+ and Ag+, etc (Zhang et al., 2011; Hollenstein et al., 2008).

Moreover, DNAzymes and aptazymes have already found many applications in almost every aspect of DNA nanotechnology, which result to new materials and devices that may penetrate into many other fields for practical applications, including environmental monitoring.

Enzymes are historically the first molecular recognition elements included in biosensors and continue to be the basis for a significant number of publications reported for biosensors in general as well as for environmental applications (Guibault, 1976). Enzymes are biological molecules that

catalyze (i.e., increase the rates of) chemical reactions and are usually very specific. Enzyme biosensors have several advantages such as stable source of material, the possibility of modifying the catalytic properties or substrate specificity by means of genetic engineering and catalytic amplification of the biosensor response by modulation of the enzyme activity with respect to the target analyte (Cosnier & Innocent, 1993). Their commercial availability at high purity levels makes them very attractive for mass production of enzyme sensors. Their main limitations are that pH, ionic strength, chemical inhibitor and temperature affect their activity, in fact, most enzymes lose their activity when exposed to temperatures above 60°C. Moreover enzyme biosensors have some limitations for the detection of environmental pollutants which include the limited number of substrates for which enzymes have been evolved, the limited interaction between environmental pollutants and specific enzymes and the lack of specificity in differentiating among compounds of similar classes (Jose´, 2010). However, artificial or synthetic enzymes could be a useful alternative to natural ones for the development of new biosensors which are more robust, available, chemically malleable and cheap in comparison with their natural analogues. Most of the enzymes used in biosensor fabrication are oxidases: that consume dissolved oxygen and produce hydrogen peroxide. Enzymes have been immobilized at the surface of the transducer by adsorption, covalent attachment and entrapment in a gel or an electrochemically generated polymer, in bilipid membranes or in solution behind a selective membrane (Jose´, 2010). Enzymes are commonly coupled to electrochemical and fiber optic transducers.

Microorganisms such as bacteria and fungi can be used as biological elements as indicators of toxicity or for the measurement of specific substances. For example, cell metabolism (e.g., growth inhibition, cell viability, substrate uptake), cell respiration or bacterial bioluminescence have been used to evaluate the effects of toxic heavy metals. Many cell organelles can be isolated and used as bioreceptors. Since cell organelles are essentially closed systems, they can be used over long periods of time (Karube, 1987). Whole mammalian tissue slices or *in vitro* cultured mammalian cells are used as biosensing elements in bioreceptors (Jose´, 2010). Microbial cells have the advantage of being cheaper than enzymes or antibodies, can be more stable and can carry out several complex reactions involving enzymes and cofactors. Conversely, they are less selective than the enzymes, have longer response and recovery times and may require more frequent calibration. Microorganisms have been immobilized for example, in nylon nets (Karube, 1987), cellulose nitrate membranes (Watanabe & Tanaka, 1991) or acetyl cellulose (Karube et al., 1991).

Another class of sensing elements or biomediators is constituted *by photosynthetic organisms* and *photosynthetic organelles*. In general, their use is associated to the environmental monitoring and in particular to pesticides and herbicides (Brayner et al., 2011; Rawson et al., 1987).
It is know that photosynthesis in green microalgae and higher plants occurs into chloroplasts that are cellular organelles which contain membrane-made closed structures (thylakoids) tightly leant one to the other to form piles, named grana as shown in **Figure 3**.

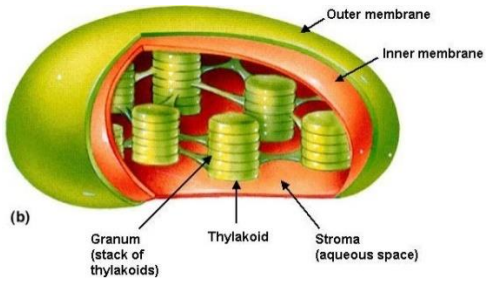

Figure 3. Schematic representation of a chloroplast. It is composed by two membranes, thylakoids packed to form grana. Grana are present in the fluid space within chloroplasts, named stroma.

Within thylakoid membranes the chlorophyll is associated in complexes containing up to 250 molecules among which only a few number are directly involved in the photochemical reactions producing ATP all the other ones are used as light-harvesting antennae. The antennae have the function to collect and convey the light to the producing molecules of the ATP (Nagyvary & Bechert, 1999; Stryer, 1995). The Photosynthetic apparatus (**Figure 4**) is composed of two photosystems named Photosystem I (PSI) and II, present in the thylakoids.

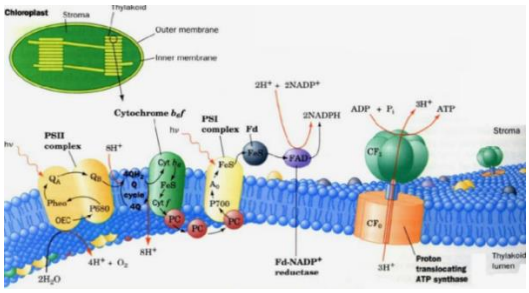

Figure 4. The Photosynthetic apparatus is arranged in the Photosystem I (PSI) and II (PSII) present in the thylakoids.

As shown in the figure, PSI and PSII are constituted by the ensemble of several proteins and pigment protein complexes that work in concert in order to build up functional units of metabolic importance. These interactions lead to the generation of a transmembrane proton gradient necessary

to ATP synthesis and to the production of the reducing power necessary to NADPH biosynthesis (Rawn, 1988; Stryer, 1995). The chlorophylls of the light-harvesting complex of PSII absorb the light radiation and transfer it to the pigment P680 (primary electron donor of PSII). This pigment is constituted by a group of pigments that are excitonically coupled, in fact when they absorb a photon tact as a single molecule. P680 is the strongest biological oxidizing agent known at present (Stryer, 1995).

When the light arrived to PSII is absorbed by chlorophyll-protein harvesting complexes then it is funneled to the photochemically active reaction center composed by the subunits D1, D2 and Oxygen Evolving Complex (OEC). Here photoexcitation converts P680 into the oxidized form $P680^{+}$ thus triggering a single electron transfer first to a pheophytin cofactor then to a plastoquinone molecule Qa located in D2 and finally to a second plastoquinone Qb in the D1 protein as shown in the **Figure 5**.

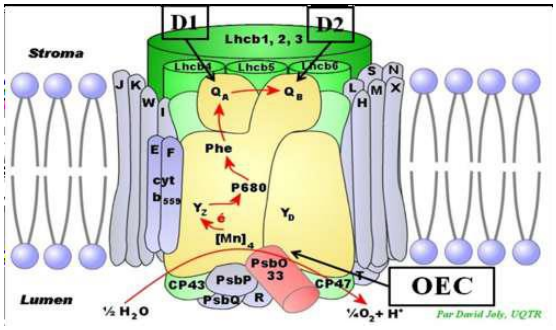

Figure 5. PSII scheme composed by D1 and D2 proteins and Oxygen Evolving Complex (OEC), Qa and Qb binding site.

After, the photooxided P680 dimer is reduced by the electrons recovered from the oxidation of water to molecular oxygen operated by a Mn-containing complex bound to the reaction center (**Figure 5**). The global reaction catalyzed by PSII is the light induced electron transfer from water with the concomitant release of O_2 to the second plastoquinone, together with the production of a transmembrane proton gradient.

As mentioned above, using photosynthetic organisms and organelles it is possible to detect herbicides presence in waters, environment or agrifood products because herbicides act directly on the photosynthetic system inhibiting the photosynthetic process. About 30% of herbicides including phenylurea, triazine and phenolic herbicides inhibit photosynthetic electron flow by blocking the PSII quinone-binding site and thus modifying chlorophyll fluorescence (Ackerman, 2007). Various

amperometric and some optical biosensors are developed to detect various kind of herbicides. (Rodriguez-Mozaz et al., 2006).

In our laboratories amperometric biosensors and biosensors based on fluorescence using photosynthetic microorganisms such as green microalgae (*Chlamydomonas reinhardtii*) and thylakoids of spinach were previously realized in order to monitoring pollutant presence in water, environment and agrifood products (Scognamiglio et al., 2013; Buonasera et al., 2010; Tibuzzi et al., 2007).

Particularly important for our present work is the phenomenon of autofluorescence in photosynthetic organisms. The capture of light energy for photosynthesis is enhanced by networks of pigments in the chloroplasts arranged in aggregates on the thylakoids. These aggregates are called antennae complexes. Evidence for this kind of picture came from research by Robert Emerson and William Arnold in 1932 when they measured the oxygen released in response to extremely bright flashes of light. They found that some 2500 molecules of chlorophyll was required to produce one molecule of oxygen, and that a minimum of eight photons of light must be absorbed in the process.

The model that emerges is that of some 300 chlorophyll molecules and 40 or so beta carotenes and other accessory pigments acting as a light harvesting antenna surrounding one chlorophyll a molecule that is a part of an action center. A photon is absorbed by one of the pigment molecules and transfers that energy by successive fluorescence events to neighboring molecules until it reaches the action center where the energy is used to transfer an energetic electron to an electron acceptor.

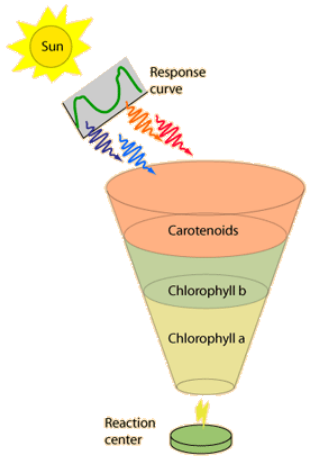

Figure 6. Fluorescence model.

The fluorescence model would suggest that each transferred photon has a longer wavelength and lower quantum energy with some energy being lost to heat.

When a photon reaches the chlorophyll a in the reaction center, that chlorophyll can receive the energy because it absorbs photons of longer wavelengths than the other pigments. Two types of chlorophyll centers have been identified, and are associated with two protein complexes identified as Photosystem II and PhotosystemI (**Figure 7**).

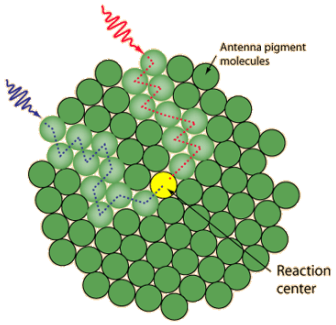

Figure 7. Representation of the photosystem.

Part IIa

Biosensors based on symbiotic forms of *Chlorellae* for herbicides analyses

Results from the European project Bravoo, call FP7 Ocean of tomorrow.

INTRODUCTION

In the last decades, among biosensors based on photosynthetic organisms, those based on green microalgae have assumed a lot of importance. Their importance is due to the simplicity of application respect to other photosynthetic materials, such as thylakoids. Microalgae are now widely used as relevant biological indicators in the field of environmental impact studies. Owing to their ubiquity, short life cycles, easiness of culture and high sensitivity to a number of pollutants, these organisms are frequently utilized in ecotoxicological screening of contaminated freshwater (Husu et al., 2013; Sanchez-Ferandin et al., 2013), environment and agrifoods (Lavecchia et al., 2013).

In addition, using whole photosynthetic microorganisms there is the possibility to explore whole biochemical processes operated by complex macromolecular assemblies (e.g. respiration, photosynthesis, etc.) (Husu et al. 2013; Shitanda et al., 2005; Vedrine et al., 2003). Furthermore, microorganisms are suitable of reliable genetic engineering procedures, so paving the way to the fine-tuning of selectivity and sensitivity proprieties of the biosensing element (Husu et al. 2013; Buchinger & Reifferscheid, 2012) Between photosynthetic microorganisms, *Chlamydomonas reinhardtii* is commonly used as sensing element for the development of optical and amperometric biosensors. *C. reinhardtii* is a well-known unicellular alga, whose genome, proteome and metabolism have been extensively investigated. Since 1980s, this alga has been widely employed as a model system for genetic manipulations and for the study of photosynthesis and PSII (Husu et al., 2013; Giardi et al., 2013; Rea et al., 2011; Harris, 2009; Merchant et al., 2007).

Several computational and molecular biology studies have been carried out on *C. reinhardtii* strains for the design and realization of sensitive and real time PSII-based biosensing devices (Rea et al., 2009; Wilski et al., 2006; Oettmeier et al., 1991).

For biosensoristic purpose a very small quantity of algae of some micrograms of chlorophyll is necessary.

In particular for biosensoristic analyses it is important to consider the modification in the fluorescence curve of the photosynthetic organisms due to the presence of the analyte. This modification is evaluate by Kautsky effect (Kautsky, 1931). The parameters important in this work are:

- F0: initial fluorescence. It is related to the activity of the PSII light harvesting structure. The F0 level is reached after some nanoseconds from the start of light excitation.
- FM: maximum fluorescence is the maximum intensity of the fluorescence transient, normally reached after hundreds of milliseconds to several seconds from light excitation. The Fm level increases with higher excitation light intensities. This is true for not saturating excitation light intensities, after a given intensity the light becomes saturating and there is not further dependence on the Fm level.
- Fj: fluorescence at the J region of the curve at about 2ms.
- Fv: variable fluorescence (FM – F0).
- Fv/FM: useful on plant vitality analysis.
- Vj: Vj= (Fj−F0)/(Fm−F0). Useful to detect pesticides acting on QA pocket binding site.
- Area above the curve and between F0 and FM is also used on pesticide detection.

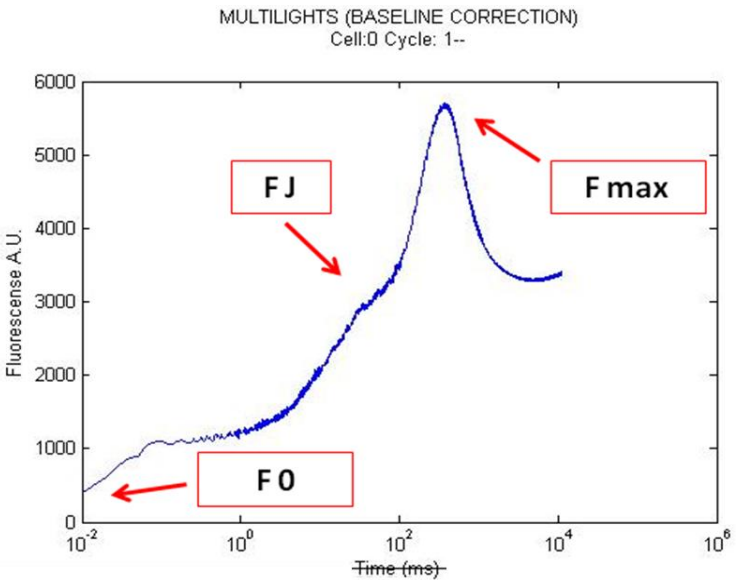

Figure 8. Example of fluorescence curve of *Chlamydomonas reinhardtii* at photosystem II level.

AIM OF THE WORK

The aim of this work was to evaluate if the symbiotic organisms of *Chlorella* can be useful for biosensor applications. This idea has been suggested by the high resistance to stress and long half-life of the symbiotic *Chlorella* compared to the alga alone; however, another possibility should be analyzed: whether the symbiosis could determine resistance to herbicides suggested by the PV membrane enveloping the algae cells (see paragraph in the following).

MATERIALS AND METHODS

Microorganisms cultures

*Chlorella minutissima UT*EX2341 was grown in liquid Kobayashi medium (KOB), according to Kobayashi et al. 1991. Liquid culture was incubated for three days at 26°C under 50μmol/m^2s light intensity and 120rpm stirring.
After three days, 10ml of this culture were inoculated in 100ml of TAP (Gormant & Levine, 1965).

The paramecia were grown in liquid Chalkley's medium as reported by Sciento http://www.sciento.co.uk/.

Lipid analyses

Lipid analyses were performed on lyophilized samples of *Chlorella minutissima*, *Chlorella sorokiniana* H1986, *Chlorella prototecoides* and *Chlorella mirabilis* cultures. In particular, 200ml of each culture were centrifuged for 15min at 5000rpm and pellets were lyophilized overnight.
For total lipid extraction, samples were grinded in chloroform/methanol 1:1. The organic phase composed by neutral lipids, cholesterylesters and phospholipids, was evaporated under vacuum to obtain extracted lipids. In turn, the extracts were subject to the transesterification process by

NaOH/MeOH/benzene for 15min. Lipids with esterified fatty acids were converted into their corresponding methylesters (FAME) (Liu, 1994).

In order to quantify fatty acids present in our samples, after calibration with fatty acid standards, gas chromatography was performed in collaboration with CNR, LIPINUTRAGEN (www.lipinutragen.it). GC method consisted by different steps: split injection (50:1) of the FAME solution on GC Agilent 6850 equipped by column 60m x 0.25mm x 0.25µm of (50%-cyanopropyl)-methylpolysiloxane (DB23, Agilent) using as detection system flame ionization. Injector temperature was 230°C. Conditions used in this protocol were: start temperature 195°C for 26min, increase of 10°C/min until 205°C maintained for 13min and following by a second increase of 30°C/min until 240°C maintained for 10min. This protocol was performed at constant pressure of 29psi with hydrogen as carrier gas.

Pesticide detection

For biosensoristic approaches *Chlorella minutissima* and *Chlorella minutissima+Tetrahymena pyriformis* cultures were used.

In order to compare the life of the single algal culture and of the symbiotic culture, we try to cultivated them of a long period in TAP medium, at 26°C under 50µmol/m^2s light intensity and 120rpm stirring. The protocol of cultivation provided a refresh with fresh medium of half of the total culture volume every one month. For both the cultures, every 15days, vitality of the cells was evaluated by Hansatech measuring the value of Fv/Fm fluorescence parameter, after 10min of dark.

For these tests diuron was used as pesticide model. A stock concentration of 10^{-3}M diuron was prepared in MeOH. From this concentration, dilutions in distillated H_2O were obtained.

The protocol used for these tests is in the following:

Algal and mixed cultures obtained as described above, with 1.5 O.D. at 682nm were used.

First measurements were performed using TAP in order to obtain the baseline setting instrument at 127arbitrary units.

After, for initial fluorescence curve determination, sample was analyzed using standard instrument procedure:10min of dark, 11sec of light at 127arbitrary units.

Measurements with diuron were performed added pesticide to the algal culture with subsequent exposition to light at 50µmol/m^2s for 10min. After this exposition, measurements were performed as described below. Diuron concentrations tested were between $2x10^{-10}$ and $2x10^{-8}$M.

Biosensoristic analyses were performed by the optical "Multilight sensor".

RESULTS

Cultures and preliminary studies on the symbiotic mechanism

In our laboratories, symbiosis between *Chlorella minutissima* and *Tetrahymena pyriformis* was studied for industrial purposes that are not reported in this work for confidentiality reasons of the results.

However, symbiotic process has been previously reported and deeply studied in the years 1940-60' (Brown & Nielsen, 1974; Karakashian, et al., 1968). It is known that some green algae from *Chlorella* genus are able to establish symbiosis with protists like paramecia and bacteria, some flatworms and cnidaria (Sommaruga et al., 2008; Landis, 1988).

In order to study, for our biosensoristic purposes the phenomenon that occurred in the culture of *Chlorella minutissima* we analyzed step by step the culture evolution by macroscopic and microscopic observations.

At the macroscopic level we noticed different phases. When *Chlorella* grows alone the culture appeared homogeneous, instead about a week after the inoculum with the paramecium, the culture presented green clumps: the size of these clumps was relative to the culture volume. After about another week, clumps from green became yellow and after brown, due to the presence of digested algae. Refreshing the culture after some weeks for an half of its total volume, it was possible to observe the evolution of the culture again.

At the same time, we analyzed culture at microscopic level using an optical microscope with focus 40X. In these observations, it was clear the difference between the various phases of the culture. *Chlorella* cultures appeared composed by single cells while after a week from inoculum with *Tetrahymena* the cultures showed green clumps. During the second week, *Tetrahymena* cells appeared more numerous and green with green algal cells in their bodies clearly visible. In the second week, it was possible to notice clumps composed by green, yellow and brown cells and big round cells with cilia. In this phase, motile paramecia disappeared and the algae appeared of higher size than culture alone (of the order of 2-6 times), surrounded by thick membranes (called PV);

after refresh green algal cells and motile paramecia reappeared. This behavior has been reported for co-cultures of these paramecia in the literature (Sommaruga & Sonntag, 2009). After these observations it was clear that an endosymbiosis was establish after about a week of mixed culture and that time was selected for our biosensoristic analyses.

Preliminary analyses for the comprehension of the symbiosis mechanism

It is known that not all algae of the Chlorella genus are able to establish symbiosis. Until today, the reason of this phenomenon is unknown, though various hypotheses have been formulated, but not substantiated. Preliminary results obtained for lipid analyses indicated that there was a difference in the total lipid content between algae able to perform symbiosis and non-symbiotic ones. This result, led us to think that the process of symbiosis can be influenced by the lipid content of the different Chlorellae. In order to confute our hypothesis, we analyzed for lipid content two algae able to perform symbiosis and two non-symbiotic ones. As symbiotic algae, *C. minutissima* and *C. sorokimiana* H1986 were tested and *C. prototecoides* and *C. mirabilis* as non-symbiotic.

The lyophilized samples were treated with chloroform : methanol in a ratio 1:1 in order to separate the organic phase, constituted from neutral lipid, cholesterylesters and phospholipids. Organic phase was evaporated to obtain the lipid extracts reported in **Table 1**.

Sample	Lyophilized quantity (mg)	Extracted lipid quantity (mg)	% Yield of the lipid extract
***Chlorella minutissima* (symbiotic)**	**5.9**	**4.7**	**79.7**
***Chlorella sorokiniana* (symbiotic)**	**7.8**	**5.8**	**74.4**
***Chlorella prototecoides* (non-symbiotic)**	**5.6**	**3.3**	**58.9**
***Chlorella mirabilis* (non-symbiotic)**	**6.1**	**3.6**	**59.0**

Table 1. Lipid analyses of symbiotic algae, *C. minutissima* and *C. sorokimiana* H1986 and of non-symbiotic *C. prototecoides* and *C. mirabilis*.

After, these extracts were subjected to transesterification and the lipids containing esterified fatty acids were transformed in the correspondent metilesters. In order to identify the composition in the various fatty acids of the four samples, a GC analysis was carried out and the data obtained are shown in the **Table 2**. In **Table 3** the lipid extract quantity and the % yield of the single lipids for all analyzed samples are reported.

Fatty acids µg/ml	*C. minutissima*	*C. sorokiniana H1986*	*C. prototecoides*	*C. mirabilis*
14:0	**0.01**	**0.03**	**0.08**	**0.04**
16:0	**0.53**	**1.97**	**2.01**	**0.93**
9c 16:1	**0.02**	**0.11**	**0.04**	**0.03**
17:0	**traces**	**traces**	**traces**	**traces**
18:0	**0.09**	**0.17**	**0.25**	**0.25**
9c 18:1	**0.16**	**0.37**	**0.70**	**0.29**
11c 18:1	**0.02**	**0.13**	**0.70**	**0.09**
18:2 ω6	**0.28**	**2.20**	**4.31**	**0.46**
18:3 ω6	**0.10**	**0.09**	**0.15**	**0.28**
18:3 ω3	**0.77**	**7.69**	**2.61**	**1.62**
18:4 ω3	**traces**	**traces**	**traces**	**traces**
20:3 ω6	**traces**	**traces**	**traces**	**traces**
20:4 ω6	**traces**	**traces**	**traces**	**traces**
20:5 ω3	**0.13**	**0.18**	**0.33**	**0.33**
22:0	**0.04**	**0.06**	**0.09**	**0.10**
22:6 ω3	**0.01**	**0.15**	**0.01**	**0.01**
24:0	**traces**	**traces**	**traces**	**traces**
SFA	**0.67**	**2.24**	**2.44**	**1.33**
MUFA	**0.22**	**0.62**	**1.45**	**0.41**
ω6	**0.38**	**2.29**	**4.46**	**0.75**
ω3	**0.91**	**8.03**	**2.96**	**1.97**
PUFA	**1.29**	**10.32**	**7.42**	**2.72**

Table 2. List of fatty acids composition (expressed as µg/ml) of the four sample analyzed obtained by gas chromatography.

In the **Table 3** the same results are reported as % of the single components over the total content.

Fatty acids %	*C. minutissima*	*C. sorokiniana H1986*	*C. prototecoides*	*C. mirabilis*
14:0	**0.57**	**0.33**	**0.97**	**1.45**
16:0	**29.33**	**18.84**	**21.56**	**26.26**
9c 16:1	**1.07**	**0.85**	**0.39**	**0.65**
17:0	**traces**	**traces**	**traces**	**Traces**
18:0	**4.65**	**1.46**	**2.42**	**4.62**
9c 18:1	**9.25**	**3.49**	**7.40**	**8.11**
11c 18:1	**1.38**	**1.21**	**7.07**	**2.38**
18:2 ω6	**12.00**	**15.95**	**35.08**	**10.00**
18:3 ω6	**1.55**	**0.24**	**0.46**	**2.29**
18:3 ω3	**31.79**	**54.62**	**20.78**	**34.02**
18:4 ω3	**traces**	**traces**	**traces**	**Traces**
20:3 ω6	**traces**	**traces**	**traces**	**Traces**
20:4 ω6	**traces**	**traces**	**traces**	**Traces**
20:5 ω3	**6.08**	**1.44**	**2.89**	**7.68**
22:0	**1.86**	**0.45**	**0.78**	**2.29**
22:6 ω3	**0.42**	**1.06**	**0.14**	**0.20**
24:0	**traces**	**traces**	**traces**	**Traces**
SFA	**36.44**	**21.12**	**25.75**	**34.64**
MUFA	**11.72**	**5.56**	**14.89**	**11.16**
ω6	**13.54**	**16.20**	**35.54**	**12.29**
ω3	**38.30**	**57.12**	**23.82**	**41.91**
PUFA	**51.84**	**73.32**	**59.36**	**54.20**

Table 3. Representation of the data obtained by GC as % of the single component over total components.

From these results it is possible to see that there is a different distribution of the lipid classes and a different ratio between SFA and MUFA among the analyzed samples.

Use of symbiotic cultures as biomediators

The mixed cultures were used as biomediators for pesticide detection in a biosensor based on fluorescence analysis.

Before tests with the pesticide, we measured vitality of our cultures, in order to determine if there was a difference between the two cultures. We refreshed the culture and every two weeks we measured the Fv/Fm fluorescent parameter used to evaluate cell vitality.

The data obtained in this experiment are shown in **Table 4**.

Days from inoculum	***Chlorella minutissima* in TAP**	***Chlorella minutissima* + *Tetrahymena pyriformis* in TAP**
	Fv/Fm	
7	**0.60+/-0.02**	**0.78+/-0.01**
15	**0.73 +/-0.02**	**0.78+/-0.01**
30	**0.50 +/-0.02 refresh half- volume in TAP**	**0.78+/-0.02**
45	**0.35 +/-0.02**	**0.75+/-0.03**
60	**n.d.**	**0.75+/-0.03**
75	**-**	**0.61+/-0.03**
90	**-**	**0.50+/-0.04**
105	**-**	**0.78+/-0.02 refresh half-vol in TAP**
120	**-**	**0.72+/-0.02**
135	**-**	**0.70+/-0.03**
150	**-**	**0.78+/-0.02**
165	**-**	**0.68+/-0.03**
180	**-**	**0.65+/-0.02**
195	**-**	**0.62+/-0.04**
210	**-**	**0.60+/-0.04**
225	**-**	**0.64 +/-0.01 refresh half-vol in TAP every month**
365	**-**	**0.75+/-0.02**

Table 4. Analysis in a long-term of fluorescence activity (Fv/Fm ratio) of the culture *Chlorella minutissima* and *Chlorella minutissima +Tetrahymena pyriformis*.

In biosensoristic tests diuron [(1,1-dimethyl, 3-(3',4'-dichlorophenyl) urea)] a broad-spectrum residual herbicide was used. This compound acts blocking the electron transfer on the PSII with the consequent photosynthesis inhibition. The experiments were performed comparing *Chlorella minutissima* response to symbiotic culture response. The results obtained were shown in the **Table 5**.

Diuron concentration (M)	**Fluorescence parameter 1-Vj *C. minutissima***	**Fluorescence parameter 1-Vj *C.minutissima*+ *T. pyriformis***
0	**0.37±0.02**	**0.58±0.04**
$2x10^{-10}$	**0.34±0.07**	**0.54±0.01**
$2x10^{-9}$	**0.21±0.06**	**0.43±0.02**
$2x10^{-8}$	**0.05±0.01**	**0.06±0.01**

Table 5. Comparison parameter 1-Vj between *C. minutissima* and *C.minutissima+T. pyriformis* (from the Sciento collection) cultures at various diuron concentrations. The data are shown as average of 1-Vj obtained by measurements performed on 5cells of the instrument. For each value standard error is reported.

DISCUSSION

In this work we studied for the first time an endosymbiosis mechanism that involve green alga *Chlorella minutissima* and protozoa for its possible application for biosensoristic purposes. In general, symbiosis is defined as two or more species living together and providing benefit to each other (Margulis & Fester, 1992; Caron & Swanberg, 1990; Landis, 1988). This mutualistic interaction plays an important role in maintaining populations living under precarious environmental conditions (Landis, 1988). Symbiosis can be facultative or obligate, depending on whether the organisms can live an independent existence (Sommaruga & Sonntag, 2009). The most famous symbiosis is that between the ciliate *Paramecium bursaria* and the unicellular green alga *Chlorella vulgaris* (Sommaruga & Sonntag, 2009).

Tetrahymena pyriformis is a free-living ciliate paramecium with cell size between 40 and 60µm and an elongated form. As other ciliated protozoan *Tetrahymena* presents two types of cell nuclei: one bigger non-germline macronucleus and one small germline micronucleus in each cell at the same time and they both carry out different functions with distinct cytological and biological properties (Roberts et al., 1981).

In the experiments performed we discovered that the establishment of symbiosis determines changes both at macroscopic and microscopic level and different phases were observed. In **Figure 9** the macroscopic culture evolutions are reported.

A

B

C

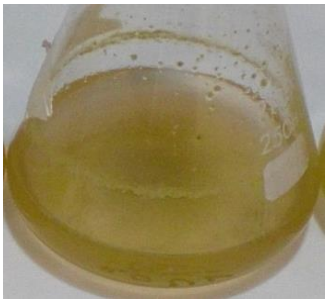

D

Figure 9. Principal steps in symbiosis culture evolution. A) Culture of *Chlorella minutissima* 3 days after inoculum from Petri disks. B) Culture of *Chlorella minutissima* 2 days after addition of *Tetrahymena* culture. C) Mix culture 2 weeks after culture start. D) Mix culture 3 weeks after start.

We observed that after three weeks by a refresh of the 50% of the culture with fresh medium it is possible to re-obtain a green culture.

At microscopic level differences can be seen, as shown in **Figure 10**.

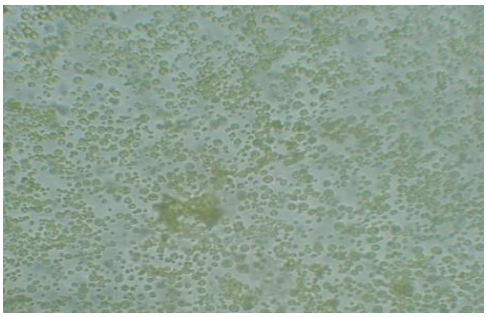

A

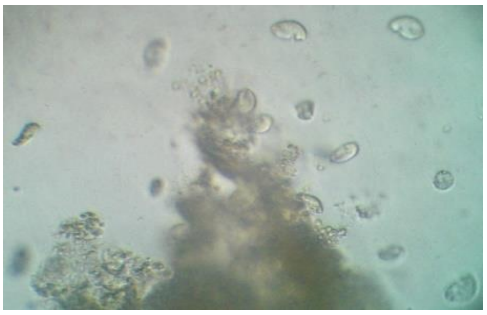

B

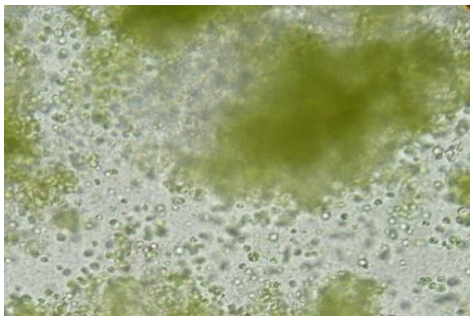

C

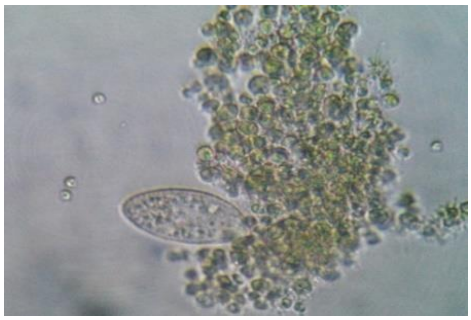

D

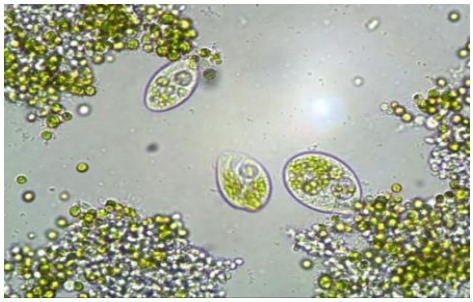

E

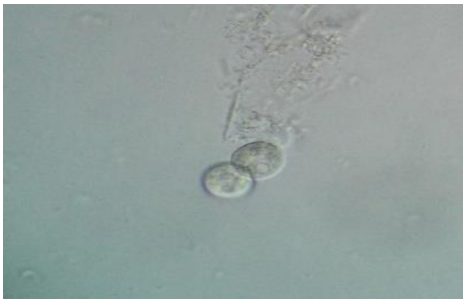

F

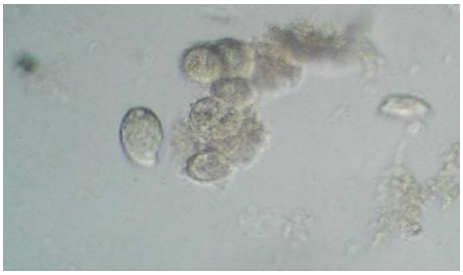

G

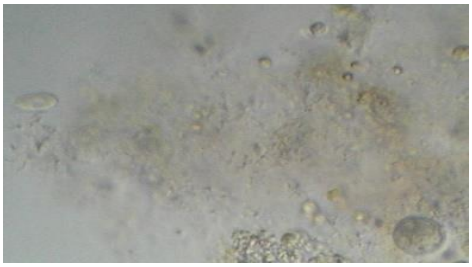

H

Figure 10. Microscopic view of the culture steps. Photos are performed by Opticalview program under optical microscope with 40X focus. A) *C. minutissima* culture 3 days after inoculum; B) *C. minutissima* mixed with *Tetrahymena* culture; C) Aggregates; D) Endosymbiosis with *Tetrahymena;* E) *Tetrahymena* cystis; F) Formation of aggregates composed by algal cells and cystis. G) Culture mix at 3 weeks after start.

In the **Figure 10** all the culture stages are reported. In particular, in the single culture of *Chlorella minutissima*, algal cells appeared homogeneous and without aggregates, but two days after addition of paramecia cultures, green aggregates were visible. The process can be important for our purpose as summarized: each symbiotic alga is enclosed in a special membrane called perialgal vacuole (PV) membrane derived from the host Digestive Vacuole (DV) membrane of the protozoan. The

perialgal vacuole is able to protect the algal cells preventing the fusion to the host lysosoms (Kodama & Fujishima, 2011; Mucibabic, 1957). Intact algal cells enclosed into PV can escape from the host cell. At this point, algal cells are free in the culture medium and are larger because enclosed by PV (Kodama & Fujishima, 2011).

Algae in the protozoan are subject to color changes from green to yellow from yellow to brown (Kodama & Fujishima, 2011; Mucibabic, 1957). As shown above (**Figure10** pictures F,G,H), after three weeks aggregates were large and brown and there were no motile paramecia, because in this phase *Tetrahymena* assumed a rounded shape form called cyst. Cysts are ciliated and larger compared to *Chlorella* cells.

Symbiosis determine various benefits both P*aramecium* and the algae. For the symbiotic algae, the host can supply the algae with nitrogen components and CO_2. Algal carbon dioxide fixation is enhanced by the host extracts. On the other hand, for the host paramecia, the algae can supply the host with a photosynthetic product, mainly maltose and sugars. Inside the host cell, the algae show a higher rate of photosynthetic oxygen production than in the isolated condition, thereby guaranteeing an oxygen supply for their host (Kodama & Fujishima, 2011; Sommaruga & Sonntag, 2009). Furthermore, alga-bearing *paramecium* cells can divide better than the alga-free cells. Alga-bearing *paramecium* cells show a higher survival rate than the alga-free cells under various stressful conditions. The host paramecia can receive protection against UV damage by their symbiotic algae, which contains protecting substances which confers their capability to thrive in sunlit UV-exposed waters (Kodama & Fujishima, 2011).

As mentioned above, symbiosis can occurs between some protozoa and some algae of the *Chlorella* genus. Until today, the reason why some algae are able to establish symbiosis and others do not, is not clear. Few hypothesis were proposed and the most reliable ones assume that presence of glucosamine in the rigid wall of algal species can be a prerequisite for realization of symbiotic association. On the contrary, the presence of glucose and mannose in the rigid walls of alga species characterizes “infection-incapable” algal species (Kodama & Fujishima, 2011). However, this proposal has been questioned by other authors (Takeda et al., 2011).

Experiments performed in our laboratories indicated that symbiotic algae have a lipid content different compared with non-symbiotic ones. Also, we thought that lipids could have a role in symbiotic mechanisms since lipids provide energy reserves and in the form of lipid/protein bilayers constituting the semi-permeable barrier that compartmentalize the various cellular organelles.

For our tests, we selected two symbiotic algae *Chlorella minutissima* and *Chlorella sorokiniana* H1986 and two non-symbiotic ones *Chlorella prototecoides* and *Chlorella mirabilis*. Lyophilized

samples of these cultures were used for total lipid extraction. The results obtained shown that the two symbiotic algae tested have a higher lipid content compared to the two non-symbiotic ones, as shown in **Table 6**.

Sample	% Yield of the lipid extract	SFA/MUFA
Chlorella minutissima **(symbiotic)**	**79.7**	**3.06**
Chlorella sorokiniana **(symbiotic)**	**74.4**	**3.60**
Chlorella prototecoides **(non-symbiotic)**	**58.9**	**1.69**
Chlorella mirabilis **(non-symbiotic)**	**59.0**	**3.24**

Table 6. Representation of the data obtained by GC for ratio between SFA and MUFA.

The gas chromatography analysis indicates that between the two symbiotic algae and the two non-symbiotic there are significant differences in total lipid content and also in the amount of the various classes of fatty acids between individual algal samples.

However, as shown in **Table 6** the results do not confirm differences in particular lipids between symbiotic and non-symbiotic algae and thus the different behavior of the algae in the symbiosis cannot be ascribed to the presence of a different quantity of saturated and unsaturated lipids, as we preliminary supposed. However, the difference could be due to other lipid classes, thus the next step will be to study the other lipids present in the green algae by FTIR.

As indicated before, symbiosis determines advantages for the involved species such as protection against biotic and abiotic stresses and longer life. In order to determine differences between the single algal culture and the symbiotic one in terms of duration, we cultivated the two cultures as described in result section. With the protocol of growth used, we obtained that symbiotic culture can survive with constant refresh for long time. Vitality was determined monitoring the fluorescence parameter Fv/Fm. Fv/Fm value for algae a value between 0.60 and 0.75 is indicative of an efficient photosynthesis while, lowered values indicate stress conditions (Maxwell & Johnson, 2000; Kitajima & Butler, 1975).

The culture *Chlorella minutissima+Tetrahymena pyriformis* was maintained more than 1 year with refresh every month. High levels of fluorescence activity was demonstrated by measurements of Fv/Fm ratio; on the contrary the *Chlorella minutissima* was healthy in liquid culture for a short period no longer than 15-20 days and it was not possible to regenerate it by refresh.

The analyses demonstrated that there is a more resistance of algae when establish endosymbiosis. For this reason, we decided to use symbiotic cultures as biomediators for pesticide detection, in order to determine if they are advantageous in this role.

Preliminary biosensing experiments were performed comparing the response of *Chlorella minutissima* culture to that of *Chlorella minutissima* mixed with *Tetrahymena pyriformis*. As analyte we have chosen diuron herbicide.

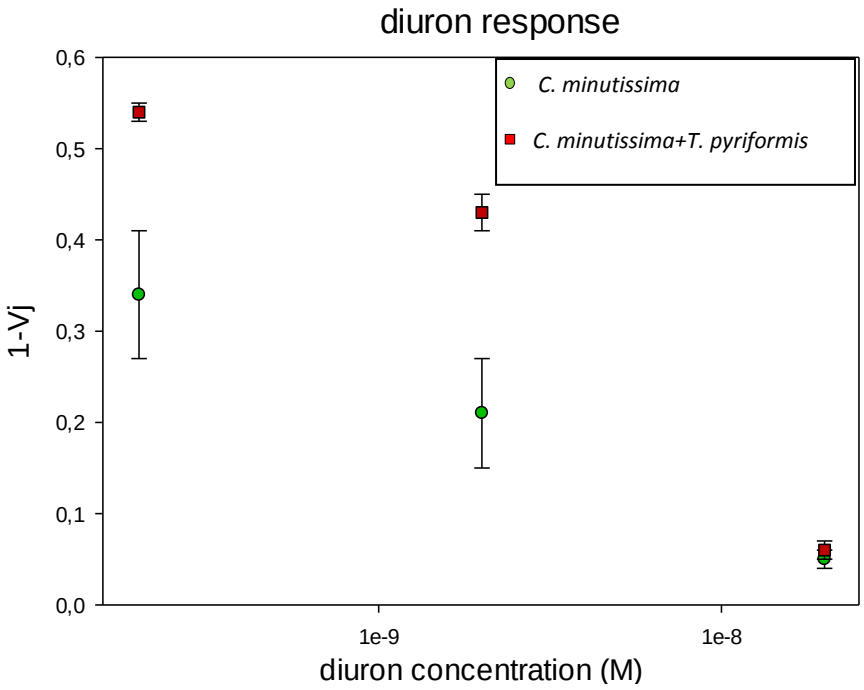

Figure 11. Comparison between diuron responses evaluated as 1-Vj fluorescence parameter variation of *C.minutissima* and *C.minutissima+T. pyriformis*. The measurements were performed by Multilight sensor. The points plotted in a semilogarithmic graph represent the averages of 1-Vj values for each diuron concentration. Standard error bars are shown for all values.

Comparison between diuron response of *Chlorella* alone and of the mixed culture, indicates that at the tested concentrations of pesticide the two cultures have a similar behavior. However, the results show that using the symbiotic culture, diuron detection already occurred at concentrations of 10^{-10}M. The measurements on the basis of the same chlorophyll content (data not shown) show that symbiotic culture have very higher fluorescence emission than culture alone that allows better reproducibility of the measurements (see **Figure 11**), perhaps due to a better connectivity of the chlorophylls. Due to the interesting preliminary results, other experiments with the other paramecia cultures and the other symbiotic and non-symbiotic *Chlorellae* are in progress.

CONCLUSIONS

In this part of the project thesis we studied a symbiosis process involving green alga *Chlorella minutissima* and the protozoa *Tetrahymena pyriformis* for biosensoristic purposes. We found that this mutualistic relationship determines changes in the culture and has positive effects on culture life. In order to discover the reasons why some organisms establish symbiosis and others do not, we studied lipid content of two *Chlorella* symbiotic algae and of two *Chlorella* non symbiotic ones. The results obtained in this contest reveal that total lipid content is highly different between the two algal classes, but fatty acid composition does not give difference for a particular class of lipids we suppose that the cause of the symbiosis establishment could be due to other lipid types; thus, other lipid analyses will be performed by FTIR. The study of behavior of *Chlorella minutissima* mutants modified on the lipid pathway is also in progress.

Finally, we used symbiotic cultures as biomediators to detect herbicides. The data obtained indicate that these cultures are able to reveal diuron presence at very low concentrations and that their response is higher than that obtained with single *Chlorella* cultures. At the present we are studying the use of *Chlorellae* in symbiosis with paramecia in liquid cultures and in immobilized forms with alginate, for monitoring biocides in marine environment (European project Bravoo, call FP7 Ocean of tomorrow). Also in that respect, others experiments are in progress to determine mixed culture response to diuron and to others herbicides.

Part IIb

Multiarray biosensors for milk safety assessment studies

INTRODUCTION

Milk and its derivate products are exposed to various chemicals and microbial safety problems, such as mycotoxins, veterinary drug residues, herbicide and pesticide residues and pathogens as *Lysteria monocytogenes*. Milk contamination may be due to food fed as in the case of alfatoxin B1 which is present in maize or in farm and industrial environment (Harvey et al., 1991).

In Europe, chemical and microbial food safety is regulated by EC legislations, which set the maximum levels for various contaminants in foodstuffs.

In order to guarantee the safety of milk, many studies are focused on analytical methods to detect contaminants and the right step of the product chain in which to perform analysis. For monitoring milk safety, in the last years many instruments have been produced, but it is now important to realize instruments which are able to monitoring the presence of various contaminants, in order to minimize the time analysis and the costs.

Chemical hazards present in raw milk can be determined with various analytical methods. In the case of biosensors it is possible to determine levels of chemical components, comparing sample concentration to the legislative limit, allowing if possible to carry out corrective actions on the milk production. The case of microbial contamination is more complex to monitor, because the contamination can occur at different stage of milk production chain, such as in the farm or during the transport etc. (Bennett & Klich, 2003**).** Between pathogen contaminations, the most important one is the presence of *Lysteria monocytogenes* which determines diseases in cows and safety problems in milk (Harvey et al., 1991).

For detection of milk pathogens electrochemical biosensors were previously developed. These instruments have the advantage of being sensitive, rapid, inexpensive and highly amenable towards microfabrication, specifically amperometric, potentiometric and impedimetric biosensors (Patel, 2002). Because most food hazards are introduced into the diary production chain at the dairy farm via feed, environment or farm conditions, it is important to determine the optimal sampling point on the basis of the component that has to be measured and its origin. Besides the sampling point, it is important to choose the monitoring system, in fact, monitoring systems can be characterized by on-line, off-line, non-invasive and in-line system. With on-line monitoring, a portion of the product is automatically analyzed and returned in the system. For off-line monitoring, a portion of the product

is manually taken away for analysis. Non-invasive method measures a signal in the production flow without physical contact with the product.

AIM OF THE WORK

The experiments performed in this work aimed at the realization of a multiarray biosensor based on fluorescence for milk safety and quality monitoring. This developed instrument is miniaturized, flexible, modular for on line measurements and can be performed directly in the cowshed.

The problem of analysis of milk for chemical contaminations is to develop a system for several classes of contaminants that can be present in the raw material; the measurements should be on line so that contaminated milk can be excluded from the production chain.

The first step of our work was the selection of suitable biomediators that can be useful for a broad range of milk contaminants such as *Chlamydomonas reinhardtii* for analyses of photosynthetic pesticides, Acetylcholinesterase for carbamates and organophosphates, Tyrosinase for phenolic compounds, Urease for urea concentration, β-galactosidase for lactose, and D-lactic dehydrogenase for D-lactic acid. The work was focus on the use of such biomediators for the development of a biosensor based on fluorescence that can be directly used on-line measurements of milk during production chain.

In the following we describe the selected biomediators and the analyses performed for making the measurement possible. The reasons for their selection are reported in the discussion section.

Chlamydomonas reinhardtii is a single-cell green alga about 10μm in diameter that swims with two flagella. The mechanism of recognition of photosynthetic herbicides by that microalgae is largely reported in the introduction of part IIa. It has a cell wall made of hydroxyproline-rich glycoproteins, a large cup-shaped chloroplast, a large pyrenoid, and an "eyespot" that senses light. Although widely distributed worldwide in soil and fresh water, *C. reinhardtii* is used primarily as a model organism in biology in a wide range of subfields. When illuminated, *C. reinhardtii* can grow in media lacking organic carbon and chemical energy sources, and can also grow in the dark when supplied with these. (Nickelsen, 2005). *C. reinhardtii* is also of interest in the biopharmaceuticals field and the biofuel field, as a source of hydrogen (Hemschemeier et al., 2008**)**.

Acetylcholinesterase, also known as AChE or acetylhydrolase, is a hydrolase (E.C. 3.1.1.7) that belongs to carboxylesterase family of enzymes. It is the primary target of inhibition by organophosphorus compounds such as nerve agents and pesticides (Witzemann & Boustead, 1983). Its function is hydrolyzing the neurotransmitter acetylcholine. AChE is found at mainly neuromuscular junctions and cholinergic brain synapses, where its activity serves to terminate synaptic transmission. Apart from its catalytic function, AChE affects cell proliferation, differentiation and responses to various insults, including stress (Tougu, 2001). It occurs in a wide variety of tissues and exists in various molecular forms which appear to be located at specific sites in tissue (Massouli & Bon, 1982).

Tyrosinase is an oxidoreductase (E.C. 1.14.18.1) that catalyzes sequential oxidation steps with various phenolic substrates. In the first reaction, often referred to as "monooxigenase" or "cresolase" activity, a hydroxyl group is introduced into the *ortho* position of the aromatic ring while in the second reaction, often referred to as the "diphenolase" or "catecholase" activity, the *o*-dihydroxy compound produced in the first reaction is oxidized to an *o*-quinone. Both reactions involve molecular oxygen (De Faria et al., 2007; Haghbeen & Tan, 2003)

Tyrosinases are distributed in microorganisms, plants and animals, much of the current interest in the development of biotechnological applications has focused on the use of mushroom ones. In higher plants and fungi, tyrosinases occur in various isoforms such as immature, mature latent and active forms (Seo et al., 2003; Sanchez-Ferrer et al. 1990; Sanchez-Ferrer et al. 1989).

Tyrosinase from *Agaricus bisporus* is a heterotetramer comprising two heavy and light chains with a molecular mass of 120kDa (De Faria et al., 2007; Strothkemp et al., 1976).

Urease (EC 3.3.1.5) belongs to hydrolase enzyme family and catalyzes the hydrolysis of urea to form ammonia and carbamate.

Urease is produced by bacteria, fungi, yeast and plants where it catalyzes the urea degradation in order to supply these organisms with a source of nitrogen for growth (Balasubramanian & Ponnuraj, 2010; Dixon et al., 1975). This enzyme is one of a small series of enzymes that require nickel for its functionality and it is know that binding of nickel to urease is very specific and tight (Balasubramanian & Ponnuraj, 2010).

In plants, urease is widely distributed in leguminous seeds and it is suggested to play an important role in seed germination and in seed chemical defense (Balasubramanian & Ponnuraj, 2010; Andrews et al., 1984).

Plant and fungal ureases are homo-oligomeric proteins of 90kDa identical subunits, while bacterial ureases are multimers of two or three subunit complexes.

β-galactosidase (β-D-galactohydrolase, EC 3.2.1.23) is an enzyme that hydrolyzes D-galactosyl residues from polymers, oligosaccharides or secondary metabolites. Polysaccharide specific β-galactosidases include β-galactanases, which attack pectic polymers and β-galactosidases that attack xyloglucans. These enzymes have two main applications: the removal of lactose from milk products for lactose intolerant people and production of galactosylated products (Husain, 2010; Neri et al., 2008; Heyman et al., 2006; Hsu et al., 2005).

β-Galactosidase is widely used in food industry to improve sweetness, solubility, flavor and digestibility of dairy products (Husain, 2010; Grosova et al., 2008; Richmond et al., 1981). Enzymatic hydrolysis of lactose by β galactosidase is one of the most popular technologies to produce lactose reduced milk and related dairy products for consumption by lactose intolerant people (Husain, 2010; Sener et al., 2006; Jurado et al., 2002; Ladero et al., 2001; Ladero et al., 2000).

D-lactic dehydrogenase. The enzyme D-lactic dehydrogenase (EC1.1.1.28) catalyzes the conversion of pyruvate to lactate and back, as it converts NADH to NAD^+ and back. Lactate dehydrogenases exist in four distinct enzyme classes. Each one acts on either D-lactate (D-lactate dehydrogenase) or L-lactate (L-lactate dehydrogenase). This enzyme is ubiquitous and found in animals, plants, and prokaryotes. The nicotinamide adenine dinucleotide (NAD)-linked lactic dehydrogenases (EC 1.1.1.27 and EC 1.1.1.28) of these organisms, which play an essential role in their energy-yielding metabolism, might be expected to share a substantial degree of homology with respect to primary structure (Gasser, F. & Gasser, S. 1971).

Bacteria can produce both D- and L-lactate and a group of bacteria commonly known as lactic acid bacteria (LAB) produce lactate as the major metabolic end product of carbohydrate fermentation (Salminen, von Wright, & Ouwehand, 2004).

MATERIALS AND METHODS

Algae cultures and fluorescence measurements

C. reinhardtii is a soil organism, it can be grown in laboratory either in liquid culture or on agar in simple mineral salts. Cultures of *C. reinhardtii* IL strain (intron less) (Johanningmeier & Heiss, 1993) were grown in liquid Tris–Acetate-Phosphate (TAP) medium pH 7.0÷7.2 at 50μmol/m^2s light intensity, 25°C temperature and 150rpm stirring (Harris, 2009).

For biosensoristic applications *C. reinhardtii* cultures with $A_{(750)}$ equal to 1 O.D. were employed.
Algal tests were carried out in the first walls of the instruments, with red LEDs. For the analyses, various diuron dilutions were prepared.
Analyses were carried out by Multiligth fluorometer. Measurement protocol consisted of the following steps:

- perform measurement of the baseline with TAP (in case of experiments performed in buffer) or with mixing milk and TAP in a 1:1 ratio setting instrument with the 11sec of light for 1 cycle at the maximum light intensity of 127u.a. (arbitrary units)
- for experiments in buffer, the first point of the curve was obtained measuring fluorescence of algal culture in TAP at 127a.u. after 10min of dark and 11sec of light. For milk experiments, algae were mixed with milk in a ratio 1:1. The measurement was performed with the same device parameters
- measurements with herbicide required 10min of incubation at 50μmol/m2s light intensity, 25°C temperature and 150rpm stirring after diuron addition. Experiments in milk provide the addition of diuron to milk and after mixing with algae, before 10min incubation in the light.

Acetylcholinesterase labeling with fluorophores and measurements

In order to use this enzyme as biomediator for optical biosensor is necessary to use FITC as fluorophore. Below, the labeling protocol is reported.

1. Solubilize 0.5mg of Fluorescein, 5-(6)-isothiocyanate (Sigma) in 50µl of DMSO
2. Solubilize 1mg of acetylcholinesterase from Electric eel ((*Electrophorus electricus*) (Sigma) in 0.5ml of 0.1M sodium hydrogen carbonate pH 9
3. Add dropwise the solubilized protein to the solubilized fluorophore. In this step it is important to prevent the formation of protein precipitates
4. Incubate the mix at 37°C for 1h in the dark, in order to prevent light exposure of fluorophore
5. Equilibrate column Sephadex G Biogel P with 20 or 30 ml 2mM of PBS pH8
6. Add dropwise the mix protein fluorophore into the column and add 2mM PBS pH8
7. Collect fraction of about 0.5ml and verify by spectrophotometer the conjugated presence, analyzing the spectrum between 220 and 550nm, because protein adsorbed at 280nm and the fluorophore at 495nm.

A stock of 15mM of acetylthiocoline chloride (Sigma) was prepared solubilizing 0.006g into 1ml 2mM PBS pH8.

The reaction mix was prepared using:

- 9µl of labeled protein with an absorbance at 280nm of 1.66OD
- 20.8µl of acetylthiocoline 5mM
- 250µl of milk
- Buffer 2mM PBS pH8 to get to total volume of 500µl

For measurements with spectrofluorimeter Jasco PF-8200 fluorimetric parameters used were:

- Excitation wavelength 495nm
- Emission wavelength 503nm

For organophosphorus detection, a stock of $1.4x10^{-6}$M of chlorpyrifos (Fluka) was prepared in 50% EtOH.

The mix was incubated for 15min in the dark and after chlorpyrifos was added. Measurements were performed 15min after analyte addition.

For experiments with Multilight the reaction mix was incubated for 15min in the dark and after pesticide was added. Measurement were performed in the cells with blue LEDs at light intensity of 01a.u. after 15min of dark and 11sec of light.

Using these experimental conditions is possible to obtain increases in fluorescence corresponding to increases of analyte concentration. Chlorpyrifos range tested was between $1.4x10^{-9}$ and $1.4x10^{-8}$M.

Tyrosinase labeling with fluorophores and measurements

In order to use tyrosinase as biomediator for optical biosensor is necessary to use FITC as fluorophore. Below, the labeling protocol is reported.

1. Solubilize 0.5mg of Fluorescein, 5-(6)-isothiocyanate (Sigma) in 50µl of DMSO
2. Solubilize 1.5mg of tyrosinase from mushroom (Sigma) in 0.5ml of 0.1M sodium hydrogen carbonate pH 9
3. Add dropwise the solubilized protein to the solubilized fluorophore. In this step it is important to prevent the formation of protein precipitates
4. Incubate the mix at 37°C for 1h in the dark, in order to prevent light exposure of fluorophore
5. Equilibrate column Sephadex G Biogel P with 20 or 30 ml 0.1M of PBS pH6.5
6. Add dropwise the mix protein fluorophore into the column and add 0.1M of PBS pH6.5
7. Collect fraction of about 0.5ml and verify by spectrophotometer the conjugated presence, analyzing the spectrum between 220 and 550nm, because protein adsorbed at 280nm and the fluorophore at 495nm.

The reaction mix was prepared using:

- 100µl of labeled protein with $A_{(280)}$ of 1.52O.D.
- 250µl of milk
- Buffer 0.1M of PBS pH6.5 to get to total volume of 500µl.

For measurements with spectrofluorimeter Jasco PF-8200 fluorimetric parameters used were:

- Excitation wavelength 495nm
- Emission wavelength 520nm

For experiments with Multilight the reaction mix was incubated for 10min and then catechol was added. Measurement were performed in the cells with blue LEDs at light intensity of 20a.u. after 10min of dark and 11sec of light. Using these conditions it was possible to obtain decreases in fluorescence corresponding to increases of analyte concentration. Catechol range $2x10^{-9}$-$2x10^{-8}$M.

Urease and measurements

For use urease as biomediator in optical biosensors, the protocol requires the following steps:

- Solubilize an amount of urease from *Canavalia ensiformis* (Sigma) corresponding to 20U for each measurement, in 0.1M PBS pH 4.5 for buffer tests ad in 0.14M PBS pH 4.5for milk tests
- Solubilize 2.8mg of 5(6)-carboxynaphthofluorescein (Sigma) in 50µl of DMSO and 950µl of ddH_2O in order to obtain a fluorophore stock of $1.3x10^{-3}$M
- Dilute this stock for 400times in 0.14M PBS pH 4.5.
- Solubilize $3x10^{-3}$g of urea (Sigma) in 0.1M PBS pH 4.5 to obtain urea stock of 5mM.

The reaction mix was prepared using:

- 100µl of protein
- 25µl of fluorophore
- 125µl of 0.14M PBS pH 4.5. or 125µl of milk.

For measurements with spectrofluorimeter Jasco PF-8200 fluorimetric parameters used were:

- Excitation wavelength 598nm
- Emission wavelength 610nm

For experiments with Multilight the reaction mix was incubated for 10min and after urea addition. Measurement were performed in the cells with yellow LEDs at light intensity of 0.1a.u. after 10min of dark and 11sec of light.

Using this protocol was possible to obtain fluorescence increases corresponding to the analyte concentration increases. Urea range tested was between 12 and 36mg/dl.

B-galacosidase labeling with fluorophores and measurements

The experiments performed with this enzyme required FITC as fluorophore. Labeling protocol used is summarized below:

1. Solubilize 0.5mg of Fluorescein, 5-(6)-isothiocyanate (Sigma) in 50µl of DMSO
2. Solubilize 2.5mg of acetylcholinesterase from Electric eel ((*Electrophorus electricus*) (Sigma) in 0.5ml of 0.1M sodium hydrogen carbonate pH 9
3. Add drop wise the solubilized protein to the solubilized fluorophore. In this step it is important to prevent the formation of protein precipitates
4. Incubate the mix at 37°C for 1h in the dark, in order to prevent light exposure of fluorophore
5. Equilibrate column Sephadex G Biogel P with 20 or 30 ml 0.1M of PBS pH4.5
6. Add dropwise the mix protein fluorophore into the column and add 0.1M of PBS pH4.5
7. Collect fraction of about 0.5ml and verify by spectrophotometer the conjugated presence, analyzing the spectrum between 220 and 550nm, because protein adsorbed at 280nm and the fluorophore at 495nm.

For experiments performed in buffer a stock of 10g/l of lactose anhydrous (Sigma) was prepared solubilizing in 0.1M of PBS pH4.5. The reaction mix was prepared using:

- 50µl of protein with $A_{(280)}$ of 1.51
- Buffer 0.1CM of PBS pH4.5 to get to total volume of 500 µl

For measurements with spectrofluorimeter Jasco PF-8200 fluorimetric parameters used were:

- Excitation wavelength 495nm
- Emission wavelength 510nm

Fluorimetric measurements were performed 15min after the addition of the lactose. With this protocol was possible to obtain fluorescence increase corresponding to the increase of lactose concentration. In this experiment lactose concentrations between $4.3x10^{-4}$ and $2.9x10^{-3}$M were tested.

For experiments with milk another protocol was used. Mix reaction was prepared using:

- 100µl of protein labeled with absorbance at 280nm of 1.51
- Buffer 0.1CM of PBS pH4.5 to get to total volume of 500µl

For measurements with spectrofluorimeter Jasco PF-8200 fluorimetric parameters used were:

- Excitation wavelength 495nm
- Emission wavelength 500nm

Fluorimetric measurements we performed 15min after the addition of skimmed milk used as analyte.

For experiments with Multilight the reaction mix is composed of 100µl of labeled protein with $A_{(280)}$ =1.51, 25µl of reaction buffer and 125µl of milk. At this mix lactose concentrations between 0 and 90g/l. Measurements were performed in the cells with blue LEDs at light intensity of 10a.u. after 10min of dark and 11sec of light.

With this protocol it was possible to obtain fluorescence increase corresponding to the increase of milk concentration. In this experiment skimmed milk concentrations between $2.6x10^{-7}$ and $1.5x10^{-6}$M were tested.

D-lactic dehydrogenase and measurements

Experimental protocol used for this enzyme provided various steps:

- Solubilize 1mg of D-lactic dehydrogenase from *Lactobacillus leichmannii* (Sigma) in 1ml of 75mM PBS pH8.9
- Prepare a NAD^+ stock of 40mM solubilizing 0.026g of NAD^+ (Sigma) in 1ml of 75mM PBS pH8.9
- Prepare stock of $1x10^{-2}$M of 5(6)-carboxynaphthofluorescein (Sigma) solubilizing 0.0035g in 50µl of DMSO+ 950µl of H_2O. From this stock a working dilution of $1x10^{-3}$M was obtained in 75mM pH8.9
- A stock of L and D-lactic acid 85+% solution water (Sigma) was diluted in 75mM pH8.9 in to obtain a working concentration of $1.66x10^{-1}$M

The reaction mix for 250µl of reaction mix was prepared using:

- 19.44µl of protein equal to 7U/ml
- 15µl of fluorophore
- 125µl of milk

- 90.5µl of 75mM PBS pH8.9

Reaction mix was incubated for 30min in the dark before adding lactic acid. After lactate addition the reaction mix was incubated for 15min before the measurements.

For measurements with spectrofluorimeter Jasco PF-8200 fluorimetric parameters used were:

- Excitation wavelength 505nm
- Emission wavelength 513nm

For experiments with Multilight, the measurement were performed in the cells with yellow LEDs at light intensity of 127a.u. after 15min of dark and 11sec of light.

Using these experimental conditions it was possible to obtain fluorescence decreases corresponding to the analyte concentration increases. D-Lactic acid range tested was between 1.6 and 5.8×10^{-4}M.

RESULTS

In this study, we analyzed photosynthetic pesticides, carbammate and organophosphorus pesticides and phenolic compounds for milk safety assessment and urea, lactose and lactic acid for milk quality assessment. The analyses with photosynthetic pesticides were realized by green algae that are autofluorescent while other analytes were analyzed using enzymes. In order to use enzymes as biomediators in optical biosensors, it is necessary to mark them with fluorescent molecules (fluorophores). Each fluorophore has a specific excitation wavelength and after radiation absorption it re-emits the radiation at a higher wavelength.

In this work two fluorophores were used: FITC (Fluorescein 5(6)-isothiocyanate) and 5(6)-Carboxynaphthofluorescein. The first one binds proteins stably being able to establish a covalent bond between the thiocyanate radical and the primary amino groups of proteins; instead the 5(6)-Carboxynaphthofluorescein is a dual emission ratiometric pH probe that is functional at near-neutral conditions (pKa=7.6). In its acidic form, this compound absorbs and fluoresces at 509mn and

572nm, respectively. Its basic form has a red-shifted (batho-chromic) absorption and emission with maxima peaks at 598 and 668nm, respectively (Han & Burgess, 2009).

Photosynthetic pesticides analyzed by algae

In the last decades, herbicides and pesticides target to photosynthesis have been used massively in agriculture. Their accumulation and persistence in the environment determine a toxic effect on human and animal health.

In this work, we used whole cells of the green alga *Chlamydomonas reinhardtii* as biomediator to detect photosynthetic herbicides in milk, because these compounds act directly on the D1 protein of the photosystem II interfering with photosynthetic process. Various studies demonstrated that, transferring photosynthetic material from dark to light, the fast fluorescence is not constant, but it has a fast increase, reaching a maximum within a few seconds. The fast fluorescence produced by photosynthetic organisms due to the sun light energy dissipation can be detected. The energy dissipated correspond to the energy that is not converted in chemical one, inversely proportional to the photosynthetic efficiency. After, in a few minutes a steady state is reached. As reported in the Introduction of IIa part (pag. 50). The parameters important in this work are F0: initial fluorescence, FM: maximum fluorescence, Vj: Vj= (Fj−F0)/(Fm−F0).

According to European legislations, herbicide content in agrifood should not exceed 0.05-0.1mg/kg. For diuron herbicide, the safe limit corresponds to 10^{-7}M. Therefore, the herbicide concentration range analyzed is between 10^{-10} and 10^{-6}M. In **Figure 1** the results obtained in buffer are shown.

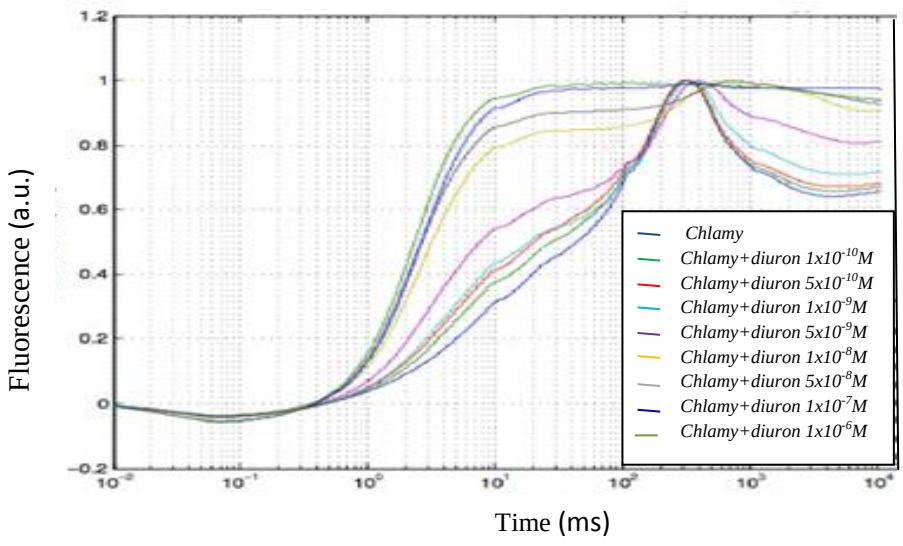

Figure 1. Fluorescence comparison between Chlamydomonas curves in buffer in presence of various diuron concentrations. In this graph, fluorescence expressed as arbitrary units is related to time expressed as ms (milliseconds).

From these data is possible to see that in presence of increasing diuron concentrations from 10^{-10}M to 10^{-6}M there are changes in the fluorescence curve, indicating that *Chlamydomonas* undergoes an inhibition of the photosynthetic activity at the level of photosystem II.

The data obtained in this experiment are shown in **Table 1**

Diuron concentration (M)	1-Vj	Photosynthesis inhibition %
0	**0.81±0.01**	
10^{-10}	**0.78±0.02**	**3.70**
$5x10^{-10}$	**0.76±0.05**	**6.17**
10^{-9}	**0.70±0.03**	**13.50**
$5x10^{-9}$	**0.54±0.01**	**33.33**
10^{-8}	**0.32±0.08**	**60.49**
$5x10^{-8}$	**0.30±0.01**	**62.96**
10^{-7}	**0.27±0.05**	**66.66**
10^{-6}	**0.21±0.05**	**74.07**

Table 1. Average of 1-Vj values and as % of photosynthesis inhibition at various diuron concentrations, obtained in Multilight experiments

The data show that increasing diuron concentration there is a decrease of the 1-Vj value and relative photosynthetic inhibition. The limit of detection is in the order of 10^{-9}M

To evaluate the reaction between algae and milk, comparisons between fluorescence curve obtained when algae are in presence of their medium and when they are mixed with milk in a ratio of 1:1 were performed.

A list of the experiments performed in milk, is presented below.

1) Algae incubation in milk for 10min under light.
   Algae were incubated in agitation in the presence of milk. After were centrifuged and algal pellet was collected separated from milk, washed in TAP medium and used for the measurements.

In **Figure 2** comparison between the curves obtained in TAP and that obtained in milk is shown.

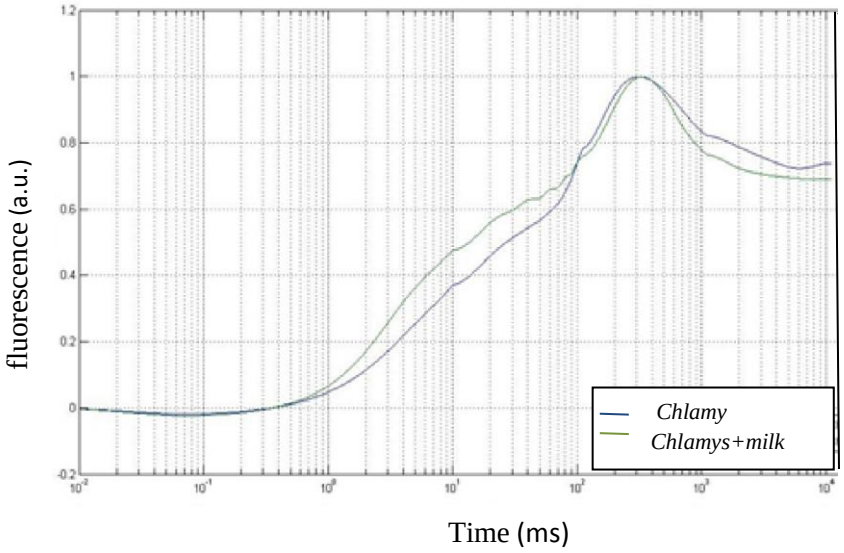

Figure 2. Comparison between *Chlamydomonas* (TAP) and *Chlamydomonas* (TAP) + milk.

The comparison of the two fluorescence curves, indicates that milk interferes with algal fluorescence.

2) <u>Addition of herbicide to milk.</u>

In this experiment, herbicide concentrations of 10^{-9}, 10^{-8} and 10^{-6}M were added to milk before incubation with algae. In **Figure 3** the results of this experiment are represented.

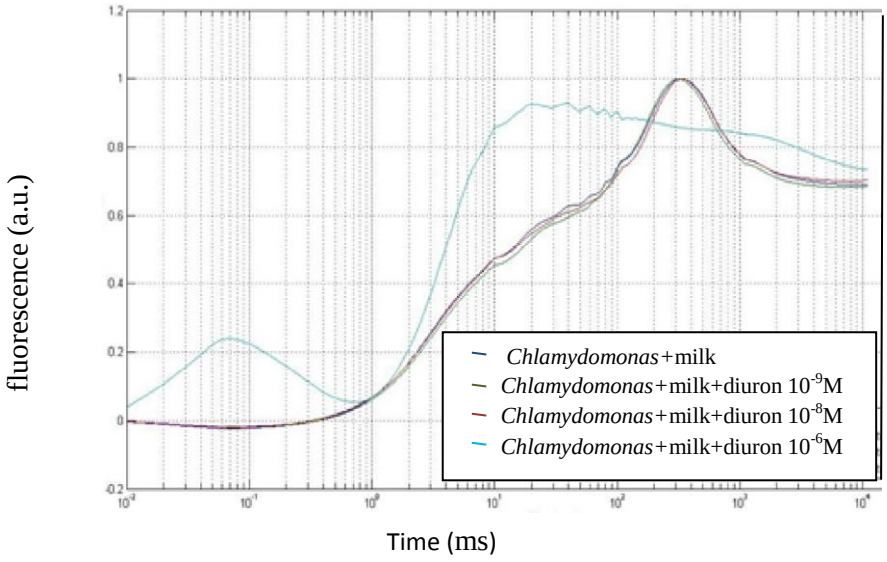

Figure 3. Comparison between fluorescence curve of *C. reinhardtii* in 50% milk in TAP with pesticide added at three different concentrations.

The data obtained in this experiment are shown in **Table 2**.

	1-Vj algae	1-Vj Algae+milk 1:1	1-Vj algae+milk+ diuron 10^{-9}M	1-Vj algae+milk+ diuron 10^{-8}M	1-Vj algae+milk+ diuron 10^{-6}M
	0.58	**0.46**	**0.48**	**0.46**	**0.08**
	0.52	**0.42**	**0.45**	**0.45**	**0.03**
	0.48	**0.4**	**0.42**	**0.42**	**0.03**
	0.53	**0.44**	**0.48**	**0.46**	**0.05**
	0.48	**0.4**	**0.43**	**0.42**	**0.09**
Av	**0.52**	**0.42**	**0.45**	**0.44**	**0.06**
Main inh%		**17%**	**0%**	**0%**	**92%**

Table 2. Comparison between fluorescence parameter 1-Vj of *C. reinhardtii* after incubation in milk and in the presence of various diuron concentrations.

Values in this table reveal that the milk influences the algal fluorescence (from 14% to 40%) but in these tested conditions, the presence of the pesticide gives significant variations in fluorescence only at relatively high concentrations of 10^{-6}M.

3) Milk incubation with diuron.

Experiments were performed in order to determine if there is an interaction between diuron and the milk lipid component. Diuron at 10^{-8}M for 5, 30 min and 4 hours was incubated in milk before or after centrifugation. A small variation in the fluorescence curve of algae treated with milk+herbicide, was determined. The value of 1-Vj showed no significant changes. In **Figure 4** the graph resultant from this experiment is shown.

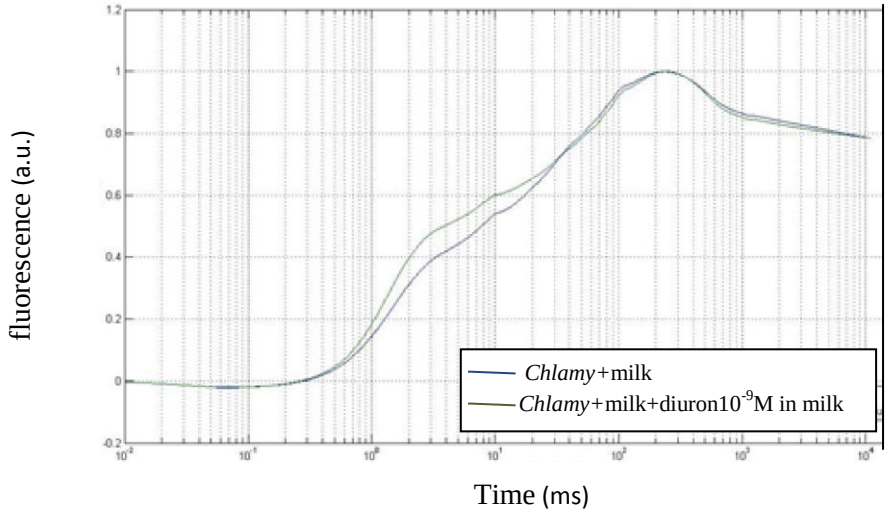

Figure 4. Comparison between the curve emissions obtained with *C.reinhardtii* in milk with added 10^{-8}M diuron.

In **Figure 5** the curves obtained incubating algae with milk+diuron at various times are shown.

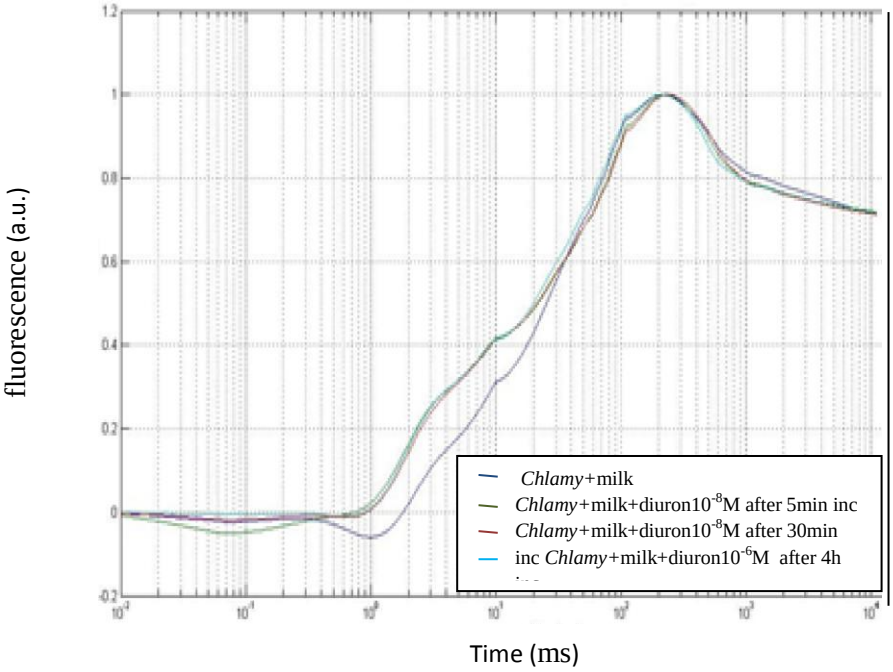

Figure 5. Comparison between the curves obtained with *C. reinhardtii* in milk with added 10^{-8}M diuron at various incubating times and without.

Comparing the curves obtained in this experiment, it is possible to determine that there are no relevant differences between the curves obtained at different incubation times with pesticide in milk. This result might be explained in two ways: either the herbicide is not absorbed by the lipid component or the adsorption is fast so that over time there are no differences in the profile of fluorescence.

In the graph below the curves obtained with and without pesticide and with diuron added before or after centrifugation of milk are compared.

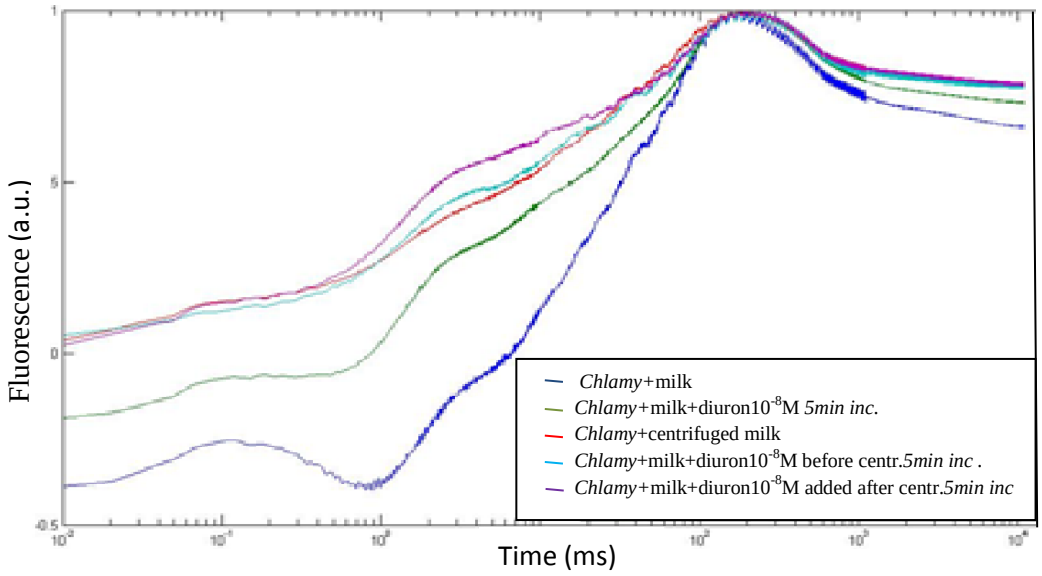

Figura 6. Comparison between the fluorescence profiles of algae+milk without and with pretreatment and with herbicide.

The red curve corresponds to the sample with centrifuged milk without diuron and the curve deep blue (sample with centrifuged milk and diuron) are stackable, indicating that herbicide was reduced by centrifugation with the milk fat component. But, the two curves are not comparable with the green and the blue ones, that correspond to the sample with milk + herbicide and to the sample only with milk, respectively.

These results may indicate that only a part of pesticide is absorbed by the lipid fraction of the milk. It also is possible that discarding lipid fraction of milk, the solution becomes less turbid changing the optical behavior.

The next graph represents fluorescence curves of *C. reinhardii* with milk centrifuged and incubated with diuron at times of 5, 30 min and 4 hours, added before and after centrifugation.

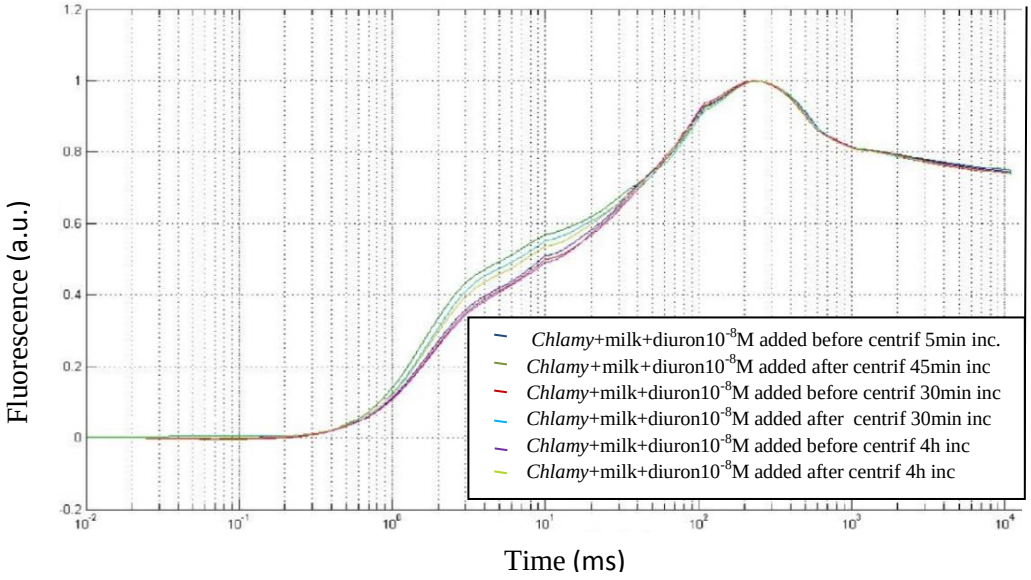

Figure 7. Comparison between fluorescence curves of *C. reinhardtii* incubated with pretreated milk and inoculated at various times with 10^{-8}M before or after centrifugation.

The data indicate that if the herbicide is added after milk centrifugation, fluorescence inhibition is greater than when diuron is added before centrifugation. Furthermore, the adsorption of the herbicide by lipid fraction of milk occurs immediately and independently of the incubation time.

Thus, further experiments were performed using whole milk but changing the geometry of the cell to reduce the distance between the excitation source and the photodiodes (see **Figure 42** of the biosensor device in the last discussion paragraph page.148)

Tests with various diuron concentrations were performed, as shown in **Figure 8**.

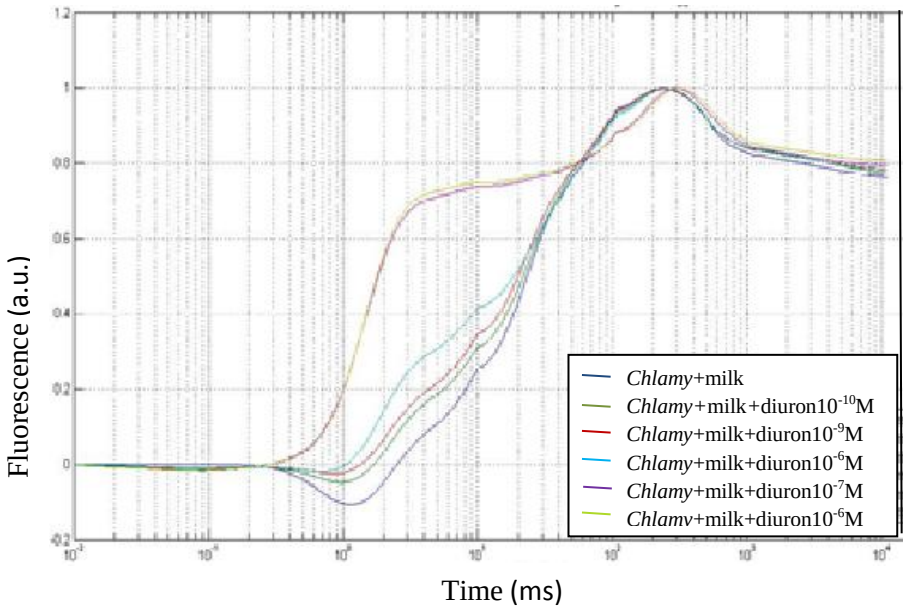

Figure 8. Comparison between *C. reinhardtii* fluorescence curves in milk at various pesticide concentrations.

In **Table 5**, data obtained in this experiments are shown.

Diuron concentration (M)	1-Vj	Inhibition %
10^{-10}	0.84±0.03	54.33
10^{-9}	0.86±0.05	58.70
10^{-8}	0.71±0.03	65.97
10^{-7}	0.30±0.01	85.70
10^{-6}	0.28±0.01	86.50

Table 5. Results obtained in milk. For each measurement average of 1-Vj and % of photosynthesis inhibition was calculated

The data obtained in this experiment indicate that in these conditions is possible to detect the presence of small concentrations of herbicide.

Organophosphorus and carabammetes pesticides analyzed by acetylcholinesterase

Acetylcholinesterase, as it is reported in the first section, is an enzyme normally presents in mammalian organisms localized in the post-synaptic membrane of the cholinergic junctions. The activity of this enzyme can be inhibited by various substances, for example organophosphorus

pesticides. For instance, chlorpyrifos (*O*,*O*-diethyl *O*-3,5,6-trichloro-2-pyridyl phosphorothioate) is a crystalline organophosphate pesticide which was used in massive way in Europe, not only in agriculture but also in gardening. This pesticide inhibits the activity of acetylcholinesterase determining an accumulation of acetylthiocoline and the modification of environmental pH.

Because of its wide use, many areas are contaminated and many foods are contaminated. In fact, it has been demonstrated that cholpyrifos can be accumulate in vegetables, meat and presumably also in milk.

In our experiments 5-(6)-Carboxynaphthofluorescein was used as probe. In buffer the first tests were performed using the protocol indicated in the literature (Scognamiglio et al., 2012). In particular, a pH 8 buffer PBS 2mM was used. Because the pesticide acts inhibiting the enzyme reaction, the first measurement was performed mixing enzyme fluorophore with the substrate acetylthiocoline. After, in order to determine the reaction progress, concentrations of chlorpyrifos between $2x10^{-7}$ and $2x10^{-4}$M were added. To establish the best time of measurement, four different times (5, 10, 15 and 30min) for all concentrations were tested. In **Figure 9**, the results of this experiment are shown.

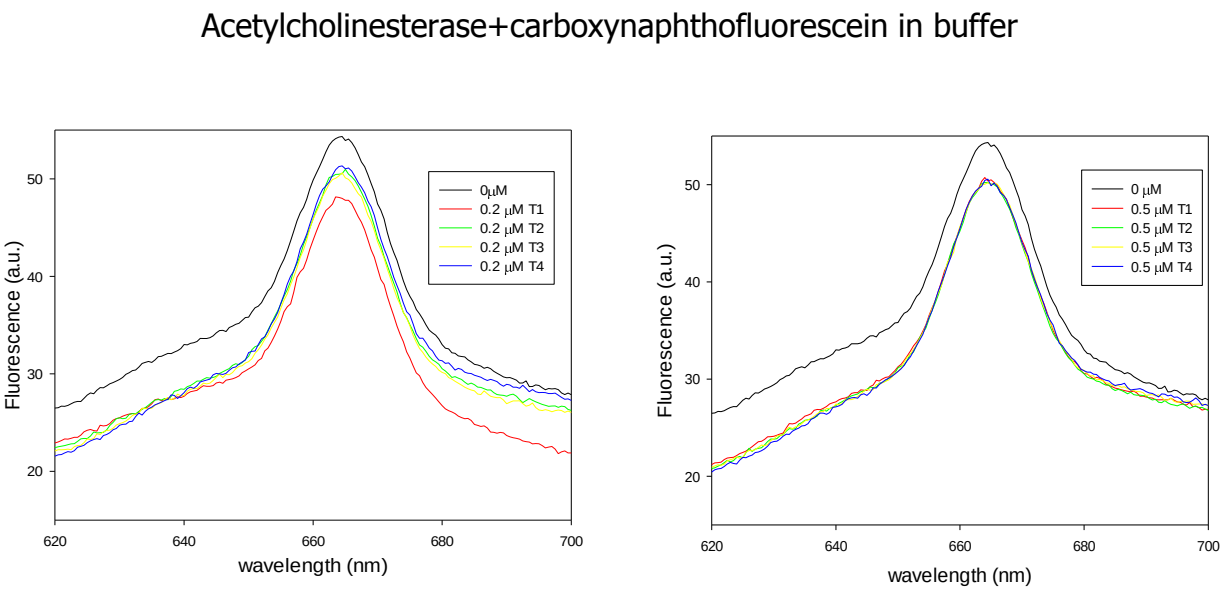

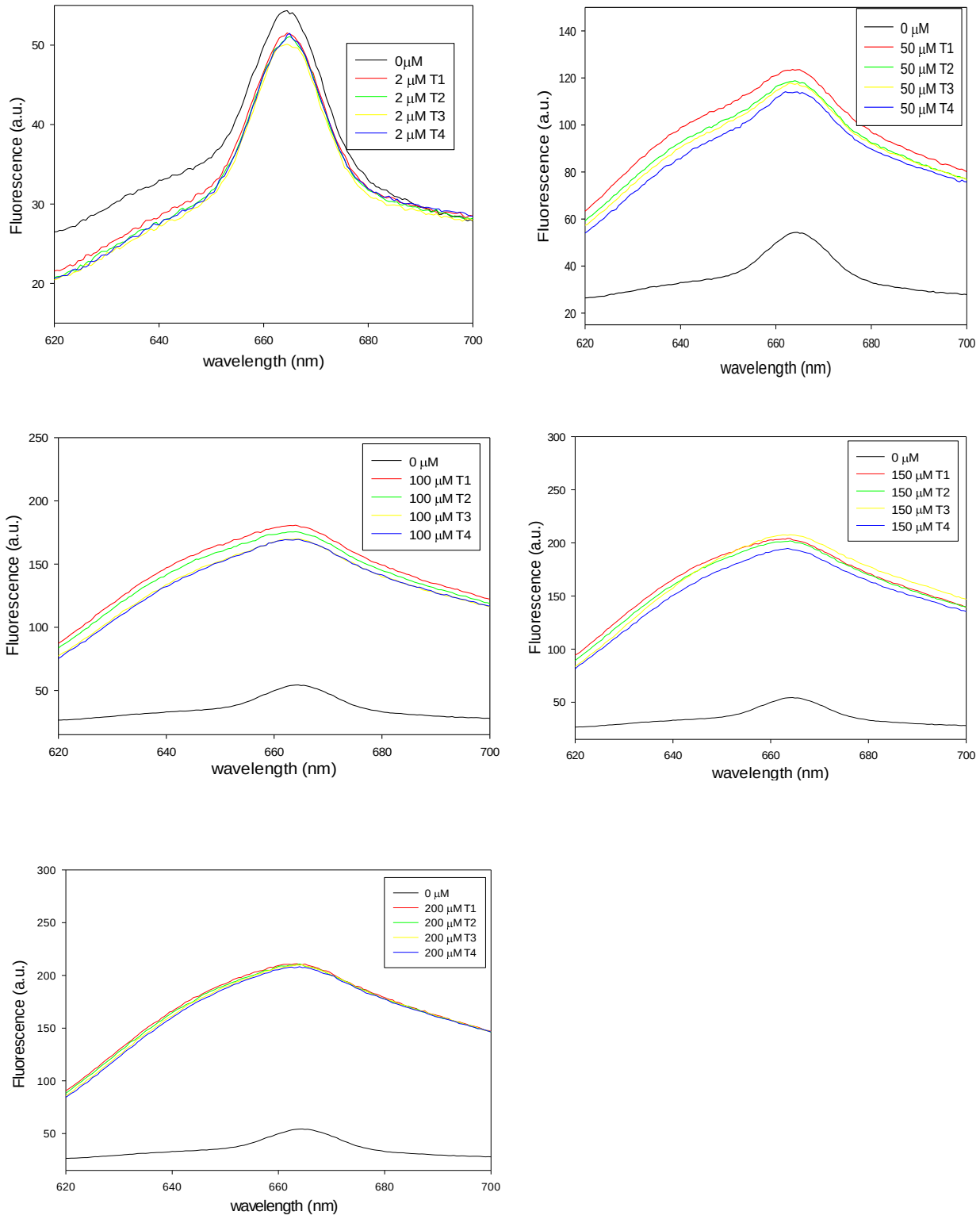

Figure 9. Comparison of the fluorescence emissions at various exposure times and various concentrations of pesticide. Fluorimetric parameters: excitation 598nm; emission 610nm; excitation and emission bandwidth 5nm. Maximum fluorescence 665nm.

The graphs indicate that fluorescence already changes after 5min from herbicide addition and that the results obtained at 15 and 30min are similar. Thus time chosen for the measurements was T3=15min, as represented in **Figure 10**.

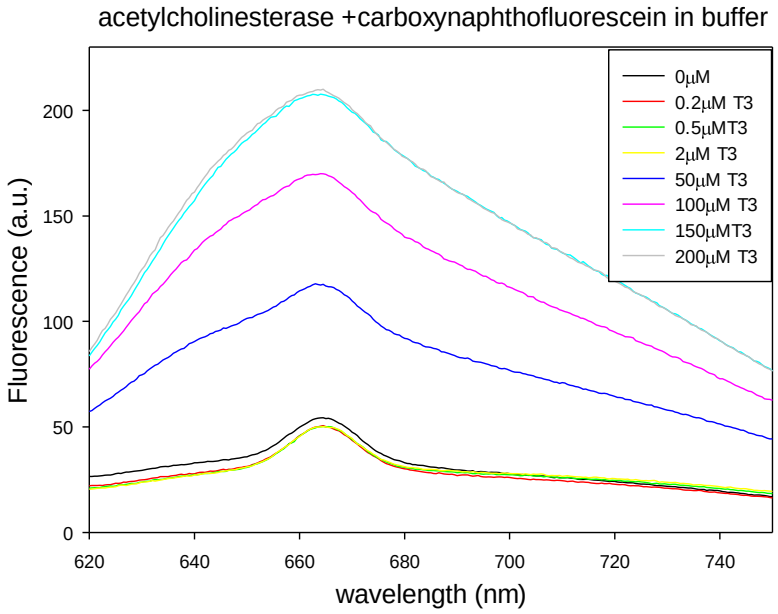

Figure 10. Comparison of the fluorescence emissions obtain after 15min from chlorpyrifos addition at various concentrations. Fluorimetric parameters: excitation 598nm; emission 610nm; excitation and emission bandwidth 5nm. Maximum fluorescence 665nm.

It is possible to see that the addition of small herbicide concentrations do not affect significantly the fluorescence signal, but from $5x10^{-5}$M until $2x10^{-4}$M, the fluorescence variation is remarkable increasing with the increase of the pesticide concentration.

Because the concentration of organophosphorus in foods according to EU legislations must not exceed 1μg/l, we performed experiments using this value as reference. For experiments a range between $1.4x10^{-9}$ and $1.4x10^{-8}$M of pesticide was tested.

The first experiment was performed using the same experimental conditions selected for the test above: 13U of enzyme, $5x10^{-3}$M of acetylthiocoline and $5x10^{-4}$M of fluorophore, but no fluorescence variations was obtained. After, various experiments were performed changing the reaction mix, the concentrations of enzyme to 3.2U and of the substrate to $1.2x10^{-3}$M.

With these experimental conditions it was possible to obtain variations of fluorescence signal at low pesticide concentrations, as shown in **Figure 11**.

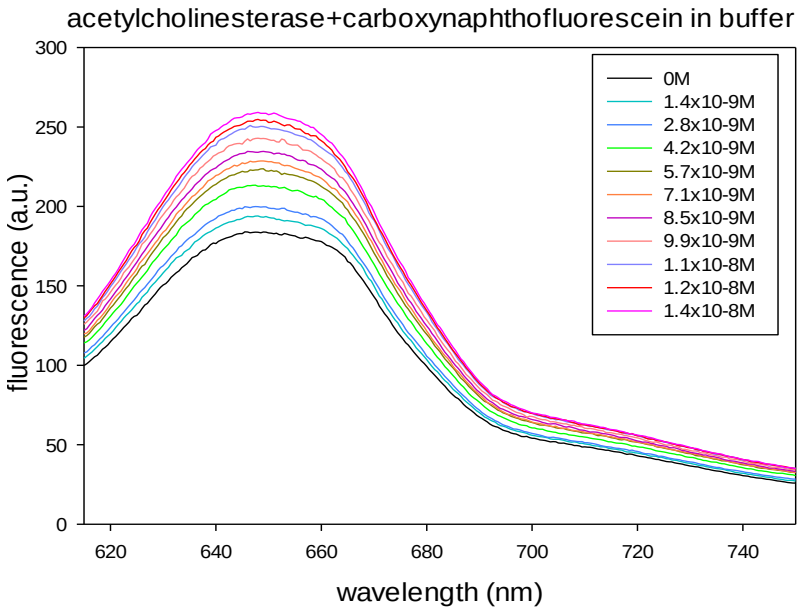

Figure 11. Fluorescence emissions obtained with various chlorpyrifos concentrations. Fluorescence parameters: excitation 598nm; emission 615nm; excitation and emission bandwidth 10nm. Maximum fluorescence 650nm. Measurements were carried out after 15min incubation.

It is possible to see that the increase of chlorpyrifos concentration determines an increase of fluorescence signal. In **Table 6** numerical results are shown.

Chlorpyrifos concentration (M)	**Fluorescence emissions (a.u)**
0	**184.35±0.4**
$1.4x10^{-9}$M	**194.22±1.8**
$2.8x10^{-9}$M	**200.53±0.46**
$4.2x10^{-9}$M	**213.80±0.45**
$5.7x10^{-9}$M	**223.81±0.13**
$7.1x10^{-9}$M	**228.99±0.4**
$8.5x10^{-9}$M	**235.28±0.33**
$9.9x10^{-9}$M	**243.08±0.57**
$1.1x10^{-8}$M	**251.17±0.37**
$1.2x10^{-8}$M	**255.00±0.16**
$1.4x10^{-8}$M	**259.71±0.13**

Table 6. Averages of the fluorescence emissions in arbitrary units at the maximum peak at various concentrations of pesticide with the relative standard error.

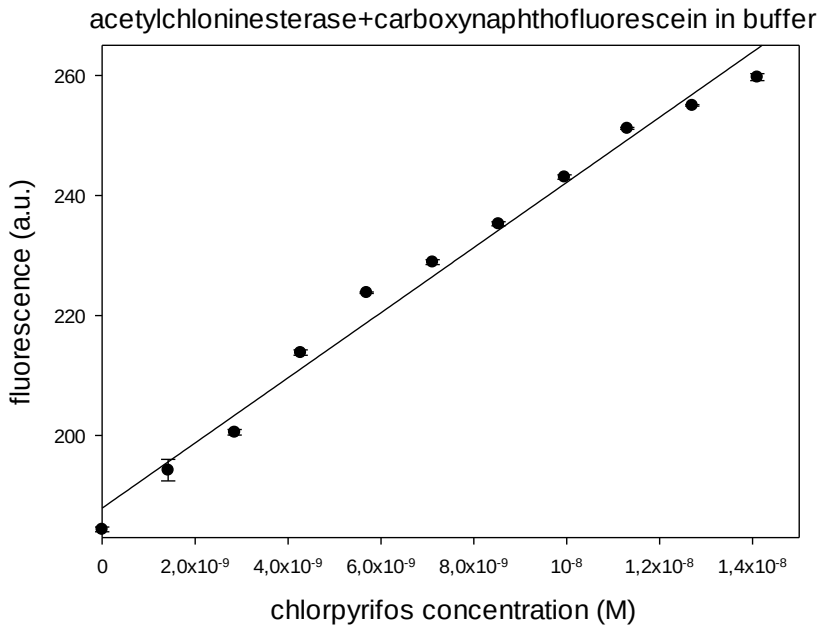

Figure 12. Relationship between pesticide concentration expressed as molarity and fluorescence emission at 650nm at T3=15min. Experiments were performed three times for each analyte concentration and the points represent the average of the fluorescence emissions at the maximum peak with standard error bars shown. Fluorescence parameters: excitation 598nm; emission 615nm; excitation and emission bandwidth 10nm. Maximum fluorescence 650nm.

However, the experiments in milk using the 5-(6)-carboxynaphthofluorescein did not yield positive results thus, we tried to use FITC.

As reported above, after the marker procedure, fractions of protein labeled were analyzed by spectrophotometer in order to quantify the protein and the fluorophore. The range analyzed was between 550 and 220nm, since FITC absorption wavelength is 495nm while protein absorption is 280nm, respectively. In **Figure 13** an example of graph obtained in the range of interest is reported.

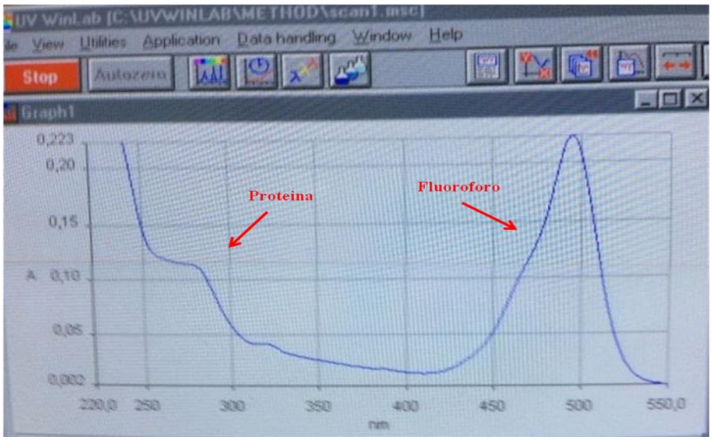

Figure 13. Spectrophotometer graph analysis of protein marked with FITC. Protein peak at 280nm and the fluorophore peak at 495nm.

Before using labeled enzyme in fluorimetric assays it is important to determine labeling efficiency. For this reason DOL (degree of labeling) was calculated with the following formula:

$$DOL = \frac{\text{Amax(dye)} * \text{MW (prot)}}{[\text{prot}] * \varepsilon \text{ dye}}$$

Where:

- A_{max} is the maximum absorbance of fluorophore
- MW is the protein molecular weight
- ε dye is the molar extinction coefficient of FITC
- [prot] is the protein concentration

Protein concentration is calculated with the Lambert Beer low:

$A = \varepsilon * C \quad C = \frac{A}{\varepsilon}$

Where:

- A is the absorbance
- C is the protein concentration
- ε is the protein molar extinction coefficient.

For an optimal labeling DOL value should be as close as possible to 1.

Experiments performed with the acetylcholinesterase enzyme indicated that a small concentration of enzyme is required in order to detect the enzymatic inhibition due to small concentrations of pesticide used. To determine the right quantity of labeled protein, spectrophotometer measurements of 3.25U of protein in pH 8 PBS 2mM, at 280nm were performed.

The results are shown in **Figure 14**.

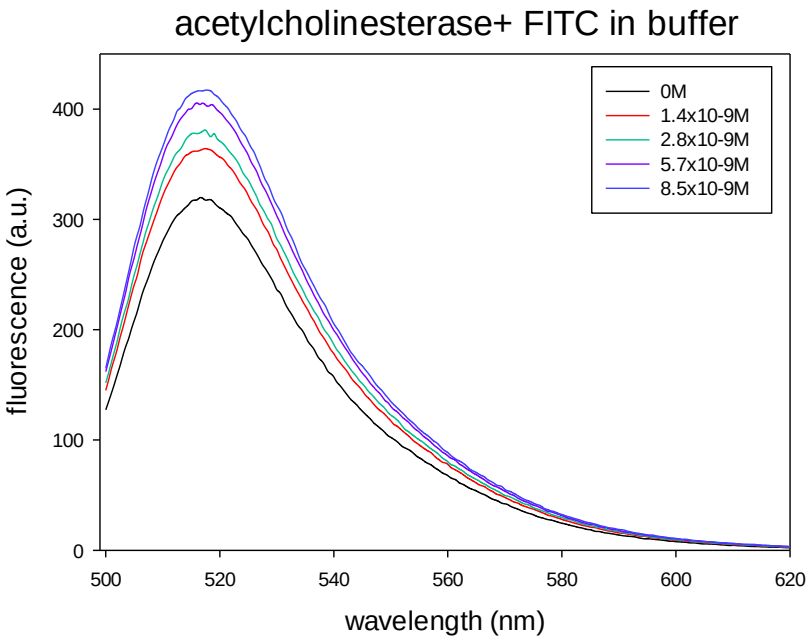

Figure 14. Fluorescence emissions with various chlorpyrifos concentrations and FITC as fluorophore. Fluorescence parameters: excitation 495nm; emission 503nm; excitation bandwidth 2.5nm and emission bandwidth 5nm. Maximum fluorescence 520nm. Measurements were carried out after 15 min of incubation.

Numerical results are shown in **Table 7**.

Chlorpyrifos concentration (M)	**Fluorescence emissions (a.u)**
0	**319.94±0.78**
1.4x10^{-9}M	**364.91±0.46**
2.8x10^{-9}M	**379.87±0.83**
5.7x10^{-9}M	**407.50±2.33**
8.5x10^{-9}M	**417.50±2.33**

Table 7. Averages of the fluorescence emissions in arbitrary units at the maximum peak at various concentrations of pesticide with relative standard errors.

In this experiment, the major fluorescence increase was obtained from 0 to 1.4x10^{-9}M of pesticide concentrations. After this pesticide concentration, fluorescence increase was less relevant.

In the first experiments performed in milk, relatively high chlorpyrifos concentrations were used. In particular, $5x10^{-5}$M, $1x10^{-4}$M and $1.5x10^{-4}$M of chlorpyrifos in a reaction mix with 250μl milk, 13U enzyme and $5x10^{-3}$M acetylthiocoline were added. For each concentration, measurements at 5, 10, 15 and 30min were carried out. However, the fluorescence signals in the presence of various pesticide concentrations did not change (**Figure 15**).

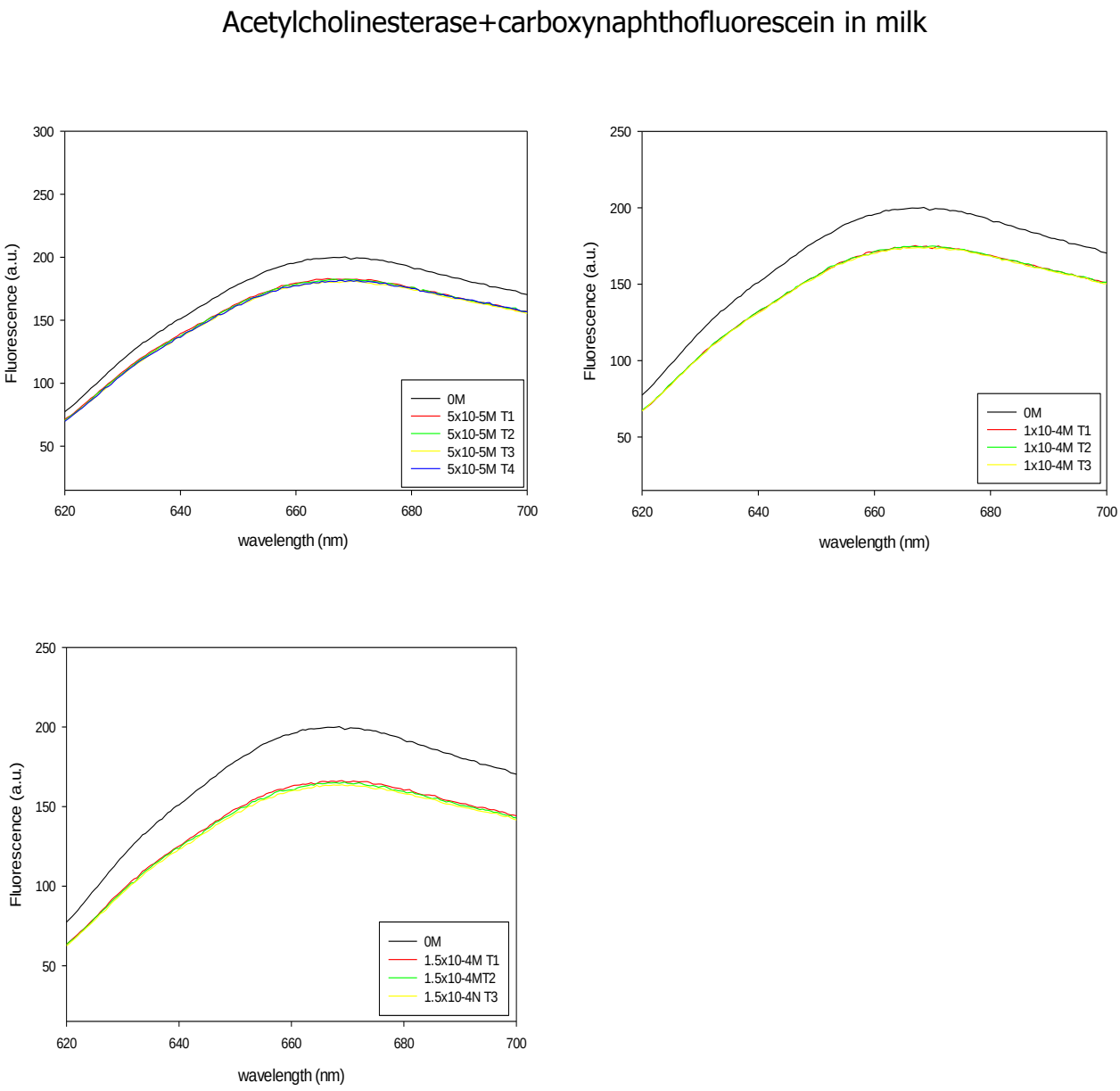

Figure 15. Comparison of the curves of fluorescence at various exposure times and various concentrations of pesticide. Fluorimetric parameters: excitation 598nm; emission 620nm; excitation and emission bandwidth 10nm. Maximum fluorescence 665nm.

Other experiments were carried out in order to determine the best conditions to obtain positive results. All tests performed in milk are listed below:

1) Modification of fluorophore concentration

   a) a double amount of fluorophore (from 3µl to 6µl) was used in mix reaction, but in this case, increasing chlorpyrifos concentration a decrease of fluorescence signal was obtained;

   b) a half amount of $1.5x10^{-4}$M fluorophore (from 3µl of to 1.5µl) was added in the mix reaction, but no fluorescence modification was obtained.

2) Modifications of buffer concentration and pH

   a) An experiment increasing the buffer concentration from $2x10^{-3}$M to $5x10^{-3}$M was performed, but no changes in fluorescence signals were obtained.

   b) Because the enzyme data sheet indicates that the optimal pH is 7.5 the pH of buffer from 8 to 7.5 was modified. However, no results were obtained.

   c) Other experiments were carried out using a pH 7.5 buffer $5x10^{-3}$M, but negative results were obtained.

3) Modification of milk in type and concentration

   a) Milk type. In literature, tests of the pesticide presence experiments were reported with centrifuged milk. (ref). In our experiment, we centrifuged milk at 5000rpm for 15min, allowing to obtain a milk with low fat. However, the results were negative, so after this test, milk skimmed was used but again without results.

   b) Others experiments with a ratio between mix and milk of 2:1 were carried out, but also in this case without results.

Thus, experiments using FITC as fluorophore were tried. Using a ratio milk:buffer of 1:1 an increase of fluorescence in presence of various pesticide concentrations was obtained for all milk conditions of reported in the paragraph before.

Results of this experiment are shown in **Figure 16**.

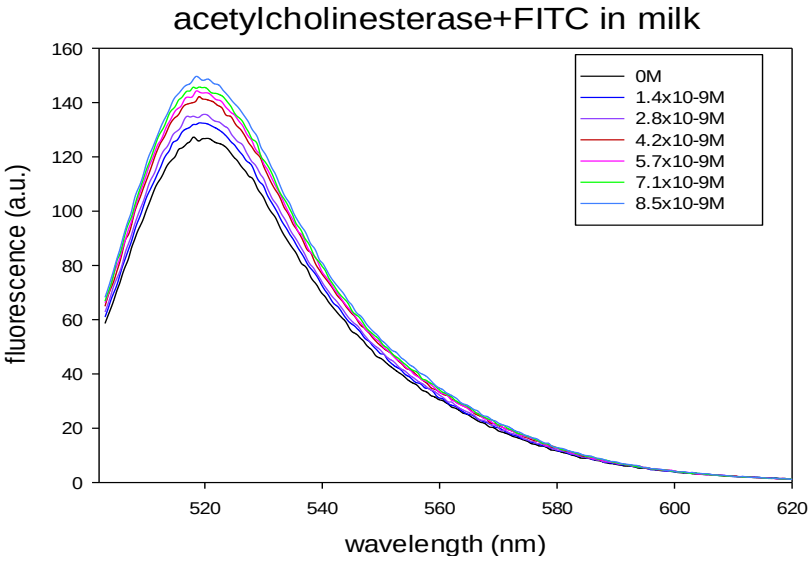

Figure 16. Fluorescence emissions in milk with various chlorpyrifos concentrations and FITC as fluorophore. Fluorescence parameters: excitation 495nm; emission 503nm; excitation bandwidth 2.5nm and emission bandwidth 5nm. Maximum fluorescence 525nm. Measurements were carried out after 15 min of incubation.

In **Table 8**, data obtain in this experiments are shown.

Chlorpyrifos concentration (M)	Fluorescence emissions (a.u)
0	**127.40±1.17**
$1.4x10^{-9}$M	**133.18±0.18**
$2.8x10^{-9}$M	**135.93±0.18**
$4.2x10^{-9}$M	**142.24±0.17**
$5.7x10^{-9}$M	**144.54±0.18**
$7.11x10^{-9}$M	**146.60±0.45**
$8.5x10^{-9}$M	**150.00±0.41**

Table 8. Averages of the fluorescence emissions in arbitrary units at the maximum peak at various concentrations of pesticide with relative standard error.

Phenolic contaminants analyzed by Tyrosinase

Tyrosinase belongs to oxidase enzyme class. This enzyme is commonly present in humans where controls the melanin production. It acts oxidizing phenolic compounds to correspondent benzoquinones.

In this work, tyrosinase from mushroom was used to detect toxic phenolic compounds in milk. These substances are commonly present in the environment and their persistence and their presence in agrifoods may cause serious damages to human health.

The presence of phenolic compounds in the environment is due to their massive use in many application fields in fact, they are important raw materials and additives for industrial purposes in laboratory processes, chemical industry, chemical engineering processes, wood processing and plastics processing. To this class of compounds belong substances like bisphenol A [4,4'-(propane-2,2-diyl)diphenol] and 4-nonylphenol [4-(2,4-dimethylheptan-3-yl)phenol] that are extremely toxic. According to European legislations, foods can contain an amount of phenolic compounds not exceeding 0.02-0.05mg/kg.

In particular, catechol the precursor of phenolic compounds was used as analyte. Approximately 50% of synthetic catechol (benzene-1,2-diol) is consumed in the production of pesticides, the rest being used as a precursor to fine chemicals such as perfumes and pharmaceuticals.

FITC was used as probe in these fluorescence experiments.

Experiments in buffer using a range of catechol between $5x10^{-9}$M and $4x10^{-8}$M were performed.

To determine the best protocol the method of Scognamiglio et al. (2012) was used with small modifications. In our work, various enzyme concentrations were tested in order to determine the right amount of enzyme useful for catechol detection. Data obtained in the experiments using a protein concentration corresponding to $A_{(280)}$ 0.17 are shown in **Figure 17** and **Table 9**.

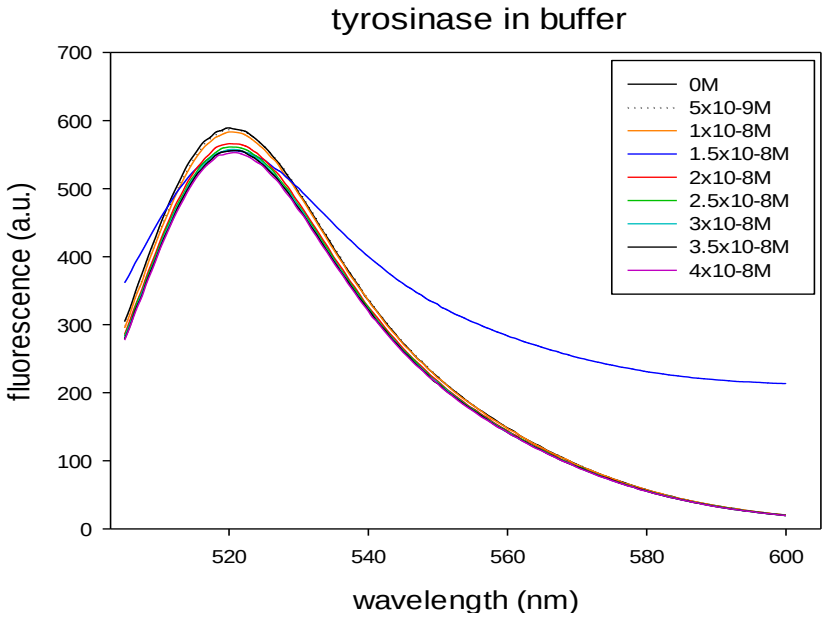

Figure 17. Fluorescence emissions in buffer with various catechol concentrations and FITC as fluorophore. Fluorescence parameters: excitation 495nm; emission 505nm; excitation bandwidth 2.5nm and emission bandwidth 5nm. Maximum fluorescence 525nm. Measurements were carried out after 15 min of incubation.

Catechol concentration (M)	Fluorescence emissions (a.u)
0	**589.3±1.6**
$5x10^{-9}$M	**588.1±0.1**
$1x10^{-8}$M	**582.3±1.5**
$1.5x10^{-8}$M	**572.8±1.0**
$2x10^{-8}$M	**566.0±0.7**
$2.5x10^{-8}$M	**561.3±0.6**
$3x10^{-8}$M	**557.6±0.6**
$3.5x10^{-8}$M	**555.9±0.3**
$4x10^{-8}$M	**553.0±0.5**

Table 9. Average of three repetitions of fluorescence emissions in arbitrary units at the maximum peak obtained at various catechol concentrations. Standard errors are shown. Fluorimetric parameters: excitation 495nm; emission 505nm; excitation and emission bandwidth 5nm. Maximum fluorescence 525nm.

Thus, with tyrosinase concentration reported above it is possible to detect catechol concentrations in a narrow range.

Various tests in milk were performed. In the first experiments, the same concentration of tyrosinase reported for buffer was used however, in milk no fluorescence variations in the presence of catechol were obtained. For this reason, other experiments were carried out. As demonstrated in the figure and table below, using tyrosinase concentration corresponding to $A_{(280)}$ 0.34 it was possible to obtain a fluorescence signal variation in the catechol concentration range between $2x10^{-9}$ and $2x10^{-8}$M.

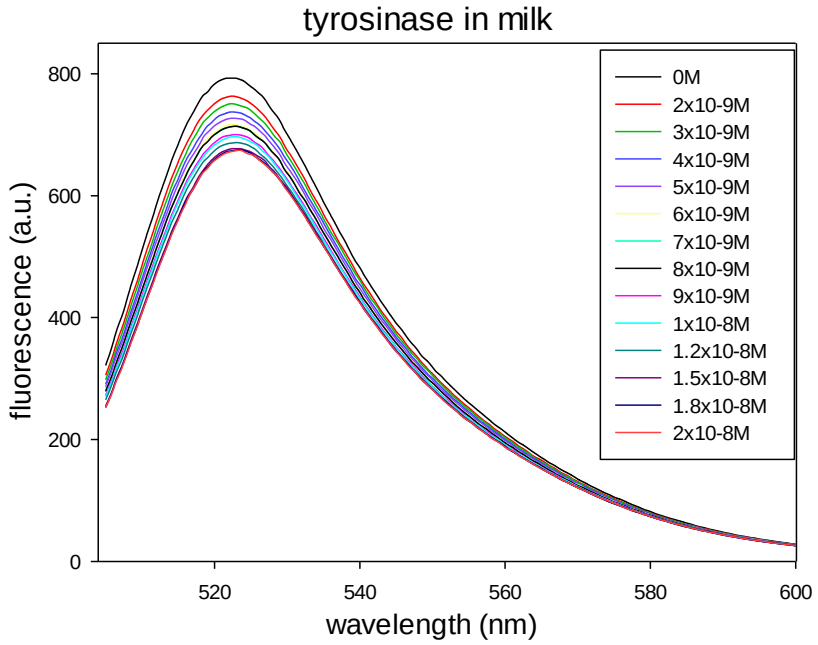

Figure 18. Fluorescence emissions in buffer with various catechol concentrations and FITC as fluorophore. Fluorescence parameters: excitation 495nm; emission 505nm; excitation and emission bandwidth 5nm. Maximum fluorescence 525nm. Measurements were carried out after 15 min of incubation.

Catechol concentration (M)	Fluorescence emissions (a.u)
0	**793.0±1.3**
$2x10^{-9}$M	**763.4±0.2**
$3x10^{-9}$M	**750.8±0.5**
$4x10^{-9}$M	**737.5±0.4**
$5x10^{-9}$M	**727.4±1.0**
$6x10^{-9}$M	**716.8±0.7**
$7x10^{-9}$M	**714.1±0.7**
$8x10^{-9}$M	**709.8±0.5**
$9x10^{-9}$M	**700.6±0.2**
$1.1x10^{-8}$M	**697.4±0.8**
$1.2x10^{-8}$M	**687.2±0.4**
$1.5x10^{-8}$M	**677.4±0.6**
$1.8x10^{-8}$M	**675.5±0.9**
$2x10^{-8}$M	**674,5±0.4**

Table 10. Average of three repetitions of the fluorescence emissions in arbitrary units at the maximum peak obtained at various catechol concentrations. Standard errors are shown. Fluorimetric parameters: excitation wavelength 495nm; emission wavelength 505nm; excitation and emission bandwidth 5nm. Maximum fluorescence 525nm.

As shown in **Table 10** the increase of the analyte concentration determines a decrease in fluorescence signal.

Urea content detection by Urease

In order to determine the best urease performance, fluorescence experiments were made with both fluorophores previously mentioned. The first experiments were performed with FITC.

After the first measurement, urea was added at different concentrations chosen on the basis of the range content indicated for milk quality. This range for milk is between 24 and 35mg/dl, thus the urea range used for our test was between 15 and 100mg/dl.

For all urea concentrations, fluorescence measurements were performed at various times in order to determine the best reaction time at which the greatest fluorescence change at the maximum occurs. The measurements were performed at 0, 5, 10, 15 and 30 min after addition of urea.

In the following table the averages of three repetitions for each concentration and each time are shown.

Fluorescence emissions (a.u.)					
UREA mg/dl	**T0**	**T1=5min**	**T2= 10min**	**T3= 15min**	**T4= 30min**
15	**817.0±0.5**	**814.5±0.3**	**816.0±0.02**	**830.5±0.04**	**852.5±0.6**
18	**857.3±0.3**	**854.0±0.08**	**860.0±0.7**	**863.6±0.1**	**871.0±0.07**
21	**890.0±1.2**	**883.5±0.5**	**881.5±0.4**	**892.0±0.5**	**903.0±0.2**
27	**907.0±1.9**	**913.0±1.6**	**921.5±0.9**	**918.0±0.6**	**923.5±0.6**
33	**919.0±2.2**	**928.0±0.9**	**934.5±0.2**	**938.0±0.04**	**939.5±0.5**
36	**941.0±1.5**	**949.0±0.6**	**943.3±0.4**	**941.0±0.4**	**947.0±0.7**
50	**939.6±1.1**	**944.5±2.3**	**940.5±2.5**	**942.0±0.2**	**933.0±1.4**
75	**960.0±1.0**	**930.0±1.5**	**920.5±2.6**	**927.5±1.7**	**n.d**
100	**916.0±2.1**	**910.5±1.9**	**905.0±1.8**	**n.d**	**n.d.**

Table 11. Values of fluorescence emissions at the maximum for tested concentrations and times. For each measurement three repetitions were performed and the standard errors are presented. Fluorimetric parameters used: excitation 495nm and emission 500nm; emission and excitation bandwidth 2.5nm. Maximum values at 520nm.

In this table it is clear that increasing urea concentration there is an increase in fluorescence, but after 36mg/dl of urea the fluorescence decreases probably because at those high substrate concentrations the enzyme is saturated.

Urease+FITC response in buffer

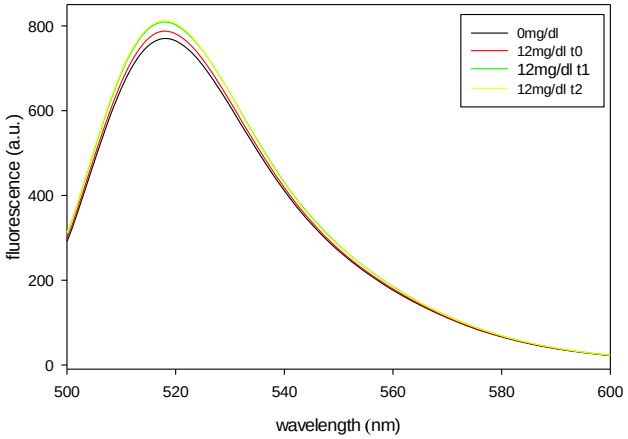

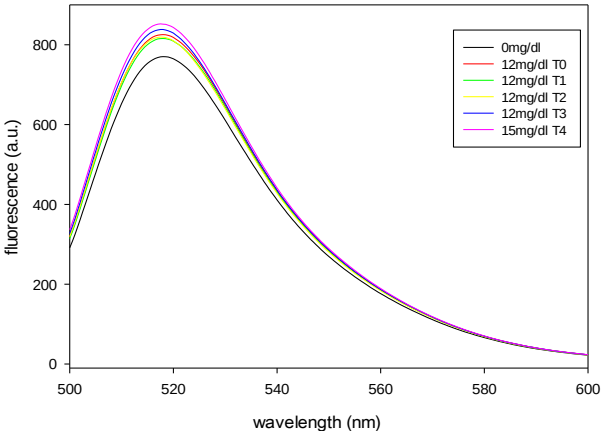

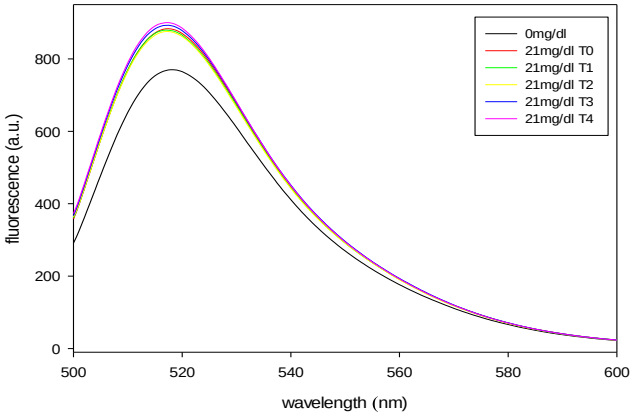

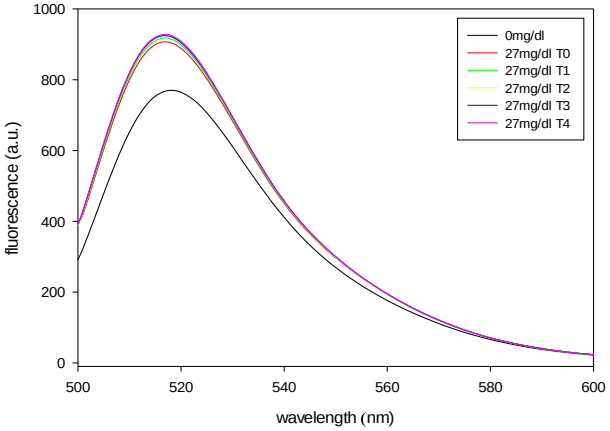

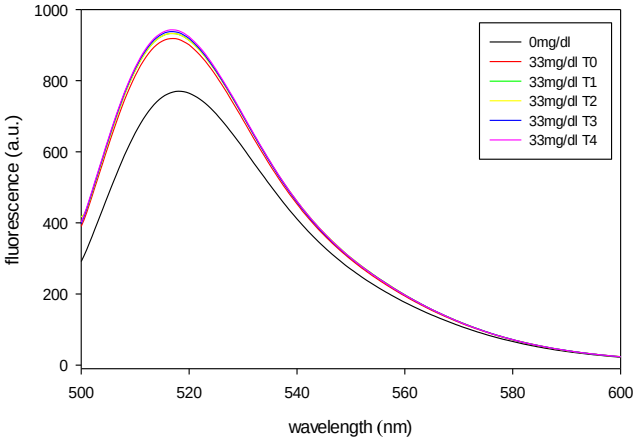

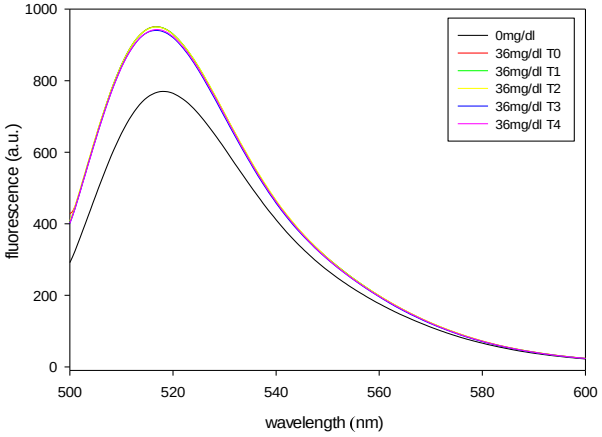

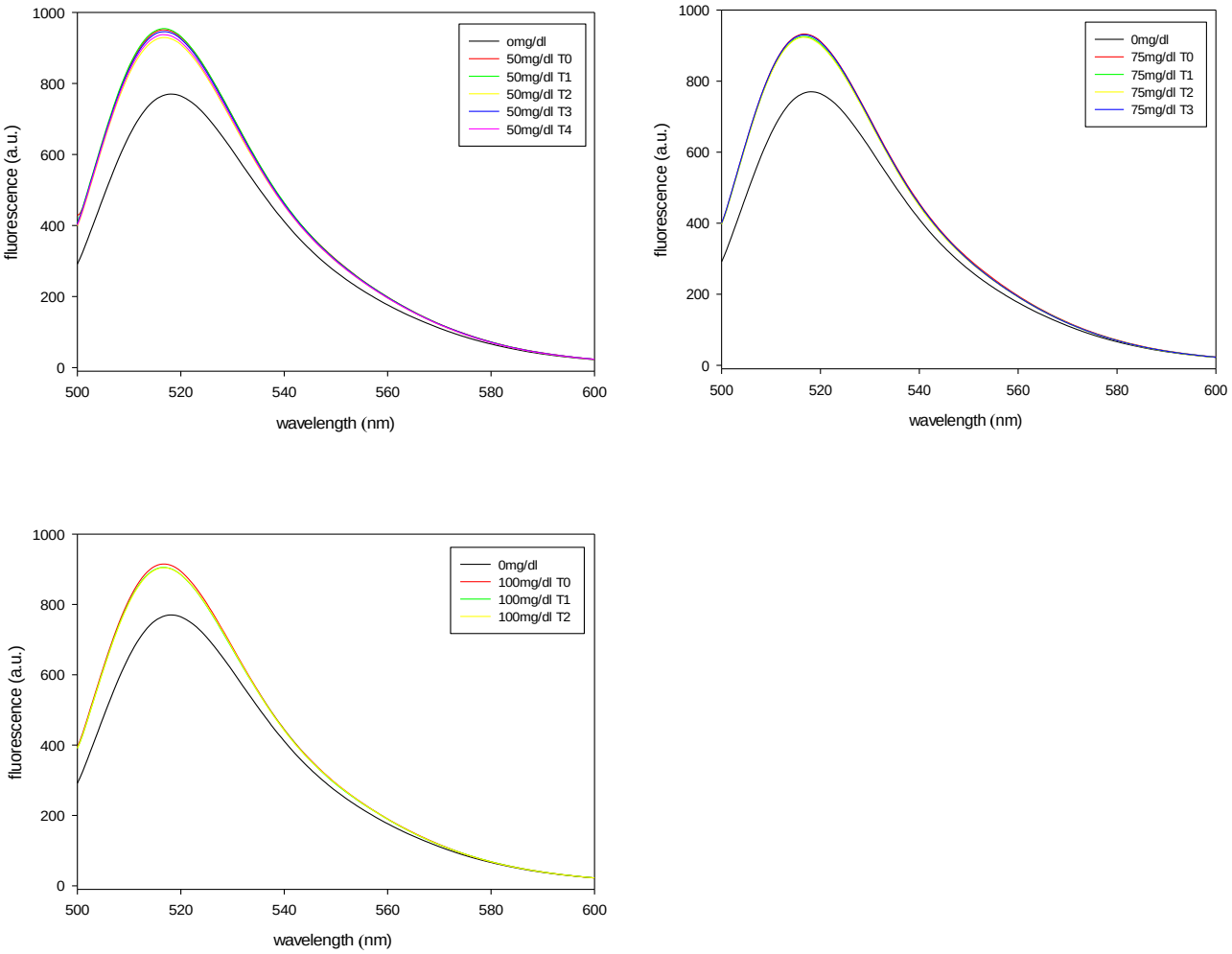

Figure 19. Fluorescence curves obtained at various urea concentrations and different times of incubation. Fluorimetric parameters: excitation 495nm; emission 500nm; emission and excitation bandwidth 2.5nm. Maximum fluorescence value at 520nm.

The previous figure show data obtained for various concentrations of urea at different times of incubation. In these graphs it is possible to note that at each concentration of substrate there is an increase of fluorescence with increasing time of reaction. The best results were obtained at 10 and 15 min, T2 and T3, respectively. At 30 min, the fluorescence increase is no significant compared to T3. The following figure shows the fluorescence curves at various concentrations of urea at the same time of 15 min. It is possible to observe that at the same time, the increase of substrate determines an increase of fluorescence emission signal.

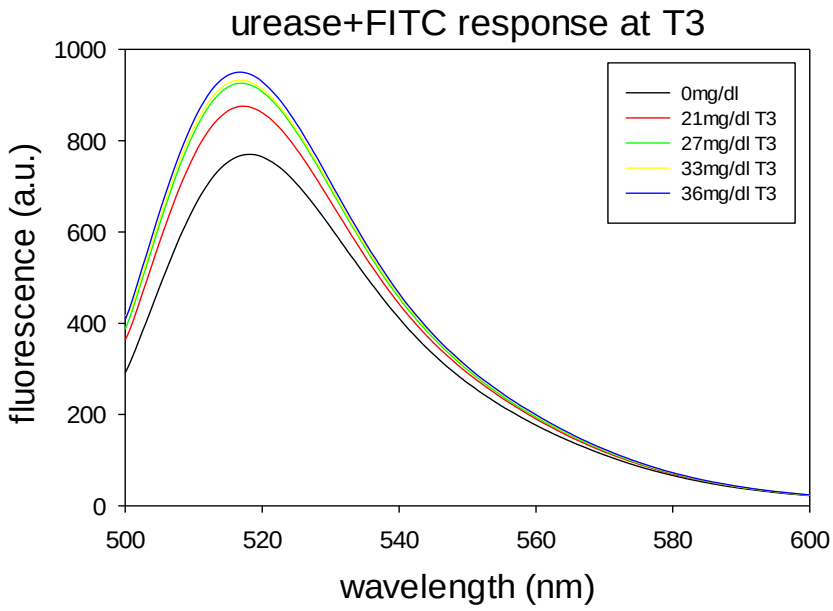

Figure 20. Fluorescence emissions at various urea concentrations and 15min of incubation. Fluorimetric parameters: excitation 495nm; emission 500nm; emission and excitation bandwidth 2.5nm. Maximum fluorescence value at 520nm.

The same data were analyzed in the following graph as urea molarity vs. fluorescence emission.

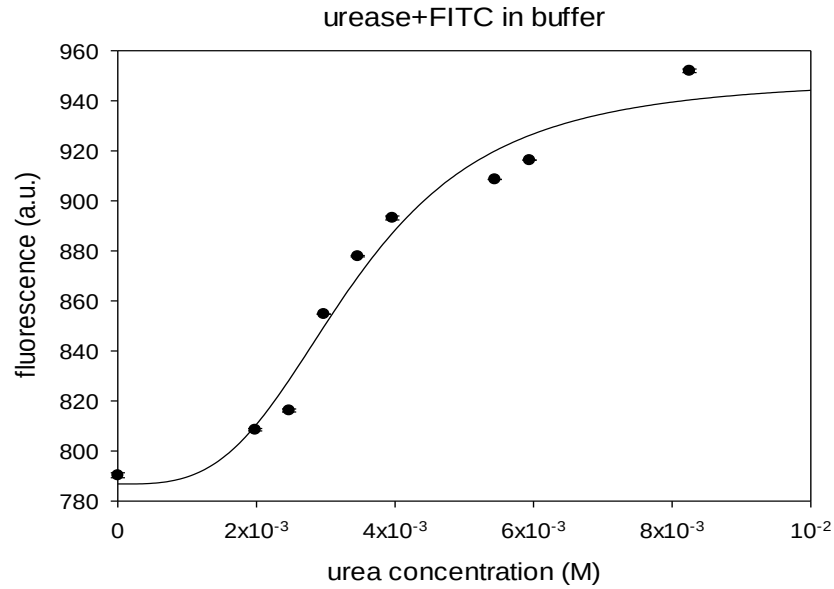

Figure 21. Relationship between urea concentration expressed as molarity and fluorescence emission at 15min. Experiments were performed three times for each analyte concentration. The points represent the averages of the fluorescence emissions at the maximum peak for each analyte concentration. Standard error bars are shown for all values. Fluorimetric parameters: excitation 495nm; emission 500nm; emission and excitation bandwidth 2.5nm. Data are represented as a sigmoid dose-response curve.

As previously reported, the enzyme urease is able to hydrolyze urea into carbon dioxide and two molecules of ammonia. The reaction determines a pH variation. For this reason, it is possible to use as fluorophore the 5(6)-Carboxynaphthofluorescein.

However, in this case the selection of the suitable reaction buffer is important in fact, because the reaction determines an accumulation of ammonia the initial pH must be acid. The buffer selected in this experiment was a 4.5 pH phosphate buffer (PBS). In order to determine the optimal buffer concentration tests were performed with the PBS 0.5M and 0.1M. In the experiment performed with the first buffer concentration, the results obtained were different from those obtained in experiments performed with FITC; in fact with increasing concentration of urea, the fluorescence was found to decrease as shown in **Figure 22**. This result indicates that this buffer is no well adapt for this test.

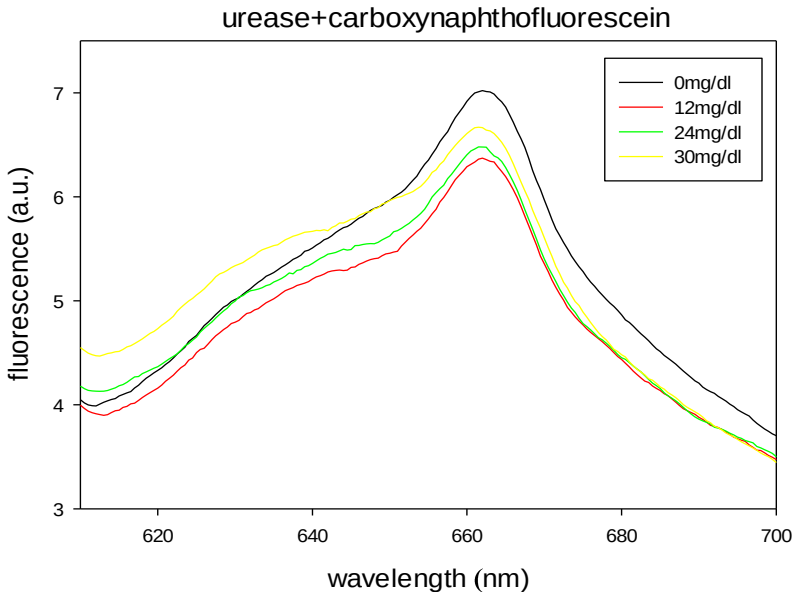

Figure 22. Fluorescence emissions in 4.5 pH PBS 0.5M at various concentrations of urea. Fluorimetric parameters: excitation 598nm; emission 610nm; excitation and emission bandwidth 5nm. Maximum fluorescence value at 663nm.

Subsequently, an experiment was performed using a phosphate buffer 0.1M. In this case, adding various urea concentrations in the range between 12 and 36mg/dl, it was possible to observe an increase of fluorescence. The measurements were performed at 0, 10 and 15 min of incubation and the results are shown in **Figure 23**.

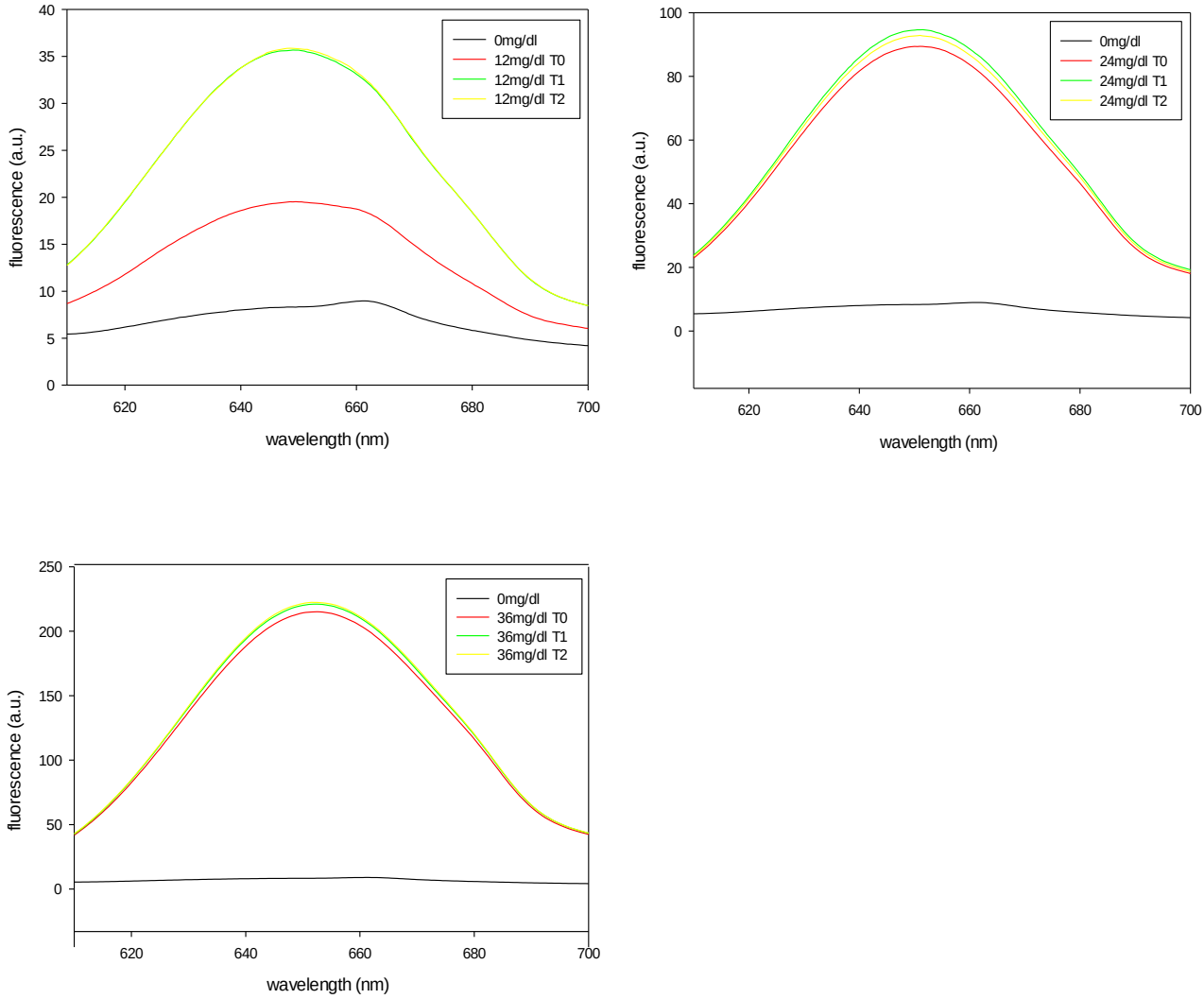

Figure 23. Fluorescence curves in the presence of various urea concentrations at times T0, T1 and T2.

From the data obtained it was possible to obtain a dose-response curve as shown in the **Figure 24**.

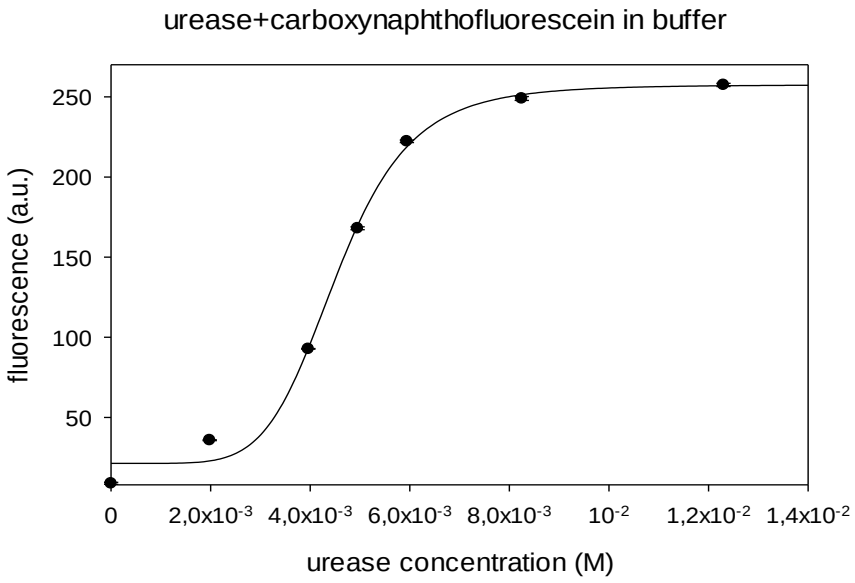

Figure 24. Relationship between urea concentration expressed as molarity and fluorescence at T3=15min. Experiments were performed three times for each analyte concentrations and reproduced three times. The points represent the averages of the fluorescence emissions at the maximum peak. Standard error bars are shown for all values. Fluorimetric parameters: excitation 598nm; emission 610nm; excitation and emission bandwidth 5nm. Maximum fluorescence value at 650nm.

To validate the data and the method, the experiment was repeated using higher concentrations of urea compared to the experiment above. In this case, the fluorescence was measured at four incubation times.

The results obtained in this test are summarized in the table below and numerical data correspond to the average of three repetitions for each value (**Table 12**).

Fluorescence emissions (a.u.)				
UREA mg/dl	**T0**	**T1**	**T2**	**T3**
12	**10.3±1.6**	**23.0±0.8**	**25.1±0.8**	**29.2±0.6**
15	**33.3±1.2**	**67.0±0.9**	**38.3±0.5**	**39.2±0.4**
18	**48.0±1.0**	**46.0±10.**	**48.3±0.3**	**51.2±0.05**
21	**61.8±1.3**	**64.3±0.7**	**69.0±0.6**	**72.0±0.6**
24	**97.7±0.9**	**94.4±0.9**	**97.2±0.2**	**100.0±0.4**
27	**132.3±1.0**	**130.0±1.1**	**140.5±0.7**	**145.4±0.3**
30	**189.4±2.1**	**192.9±1.3**	**195.6±0.4**	**196.9±0.08**
33	**224.6±1.5**	**226.2±1.1**	**227.2±0.05**	**226.5±0.02**
36	**280.0±1.0**	**281.6±0.8**	**286.3±0.03**	**289.2±0.12**
43	**244.12±1.8**	**243.99±1.2**	**244.59±2.3**	**243.88±1.8**

Table 12. Average of the fluorescence emissions at maximum peak for various urea concentrations and the various times tested with relative standard errors. For each measurement three repetitions were performed. Fluorimetric parameters: excitation 598nm; emission 610nm; excitation and emission bandwidth 5nm. Maximum fluorescence 650nm.

In this table it is possible to observe that with increasing concentration of urea an increase of the fluorescence signal is obtained till 36mg/dl concentration of urea. After that concentration, the fluorescence emission decreases, perhaps because the enzyme is saturated. The table also shows that there is a constant increase of fluorescence from time T0 to T3.

In **Figure 25** the curves of fluorescence obtained in this experiment are shown, in particular the fluorescence responses obtained at each concentration of urea for the different times are compared.

Urease+carboxynaphthofluorescein response in buffer

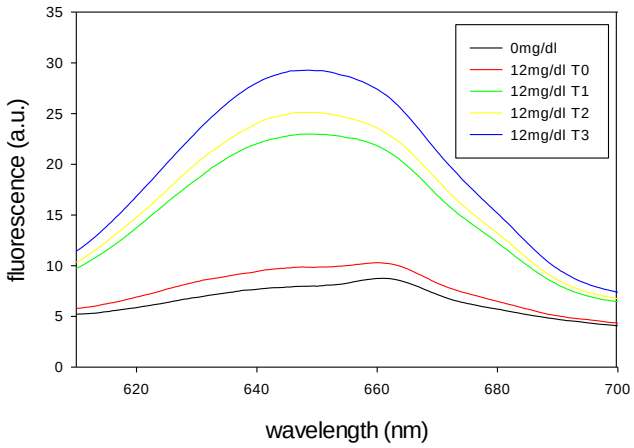

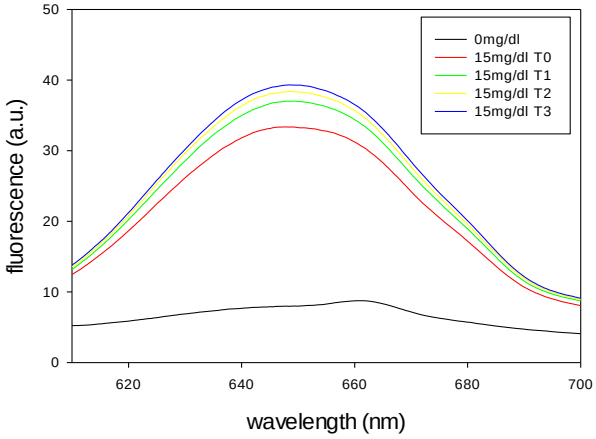

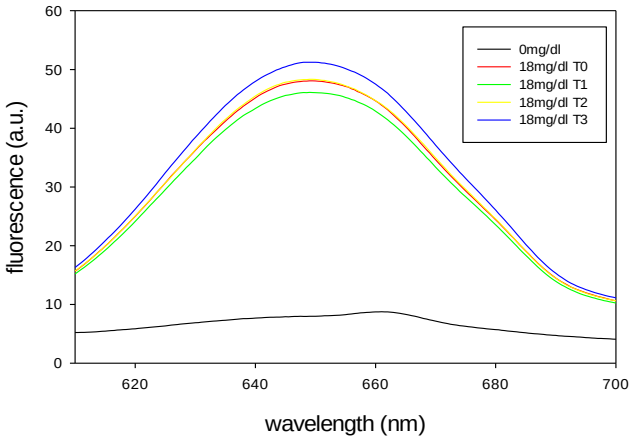

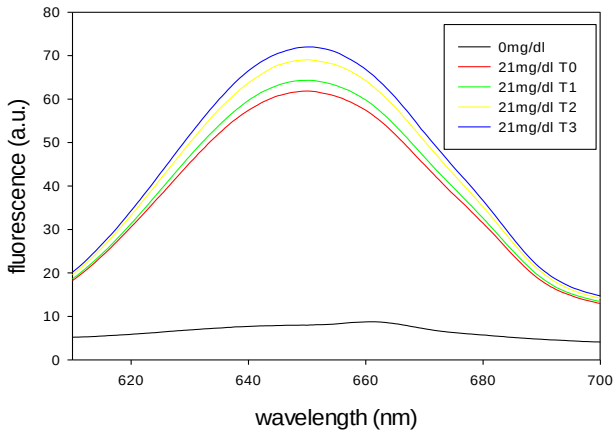

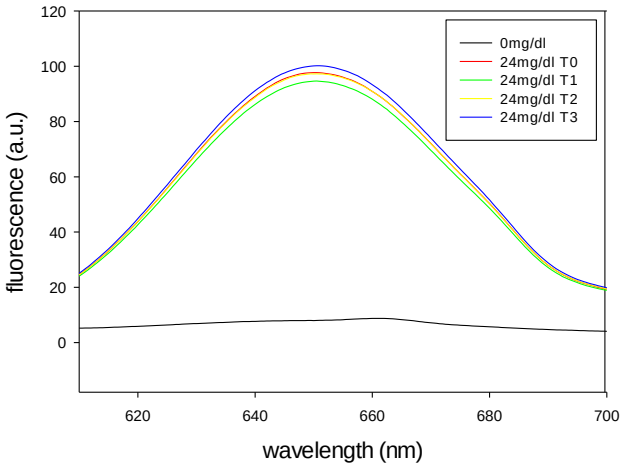

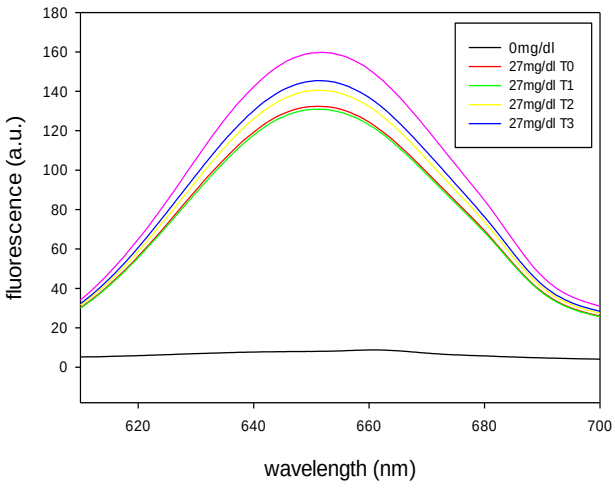

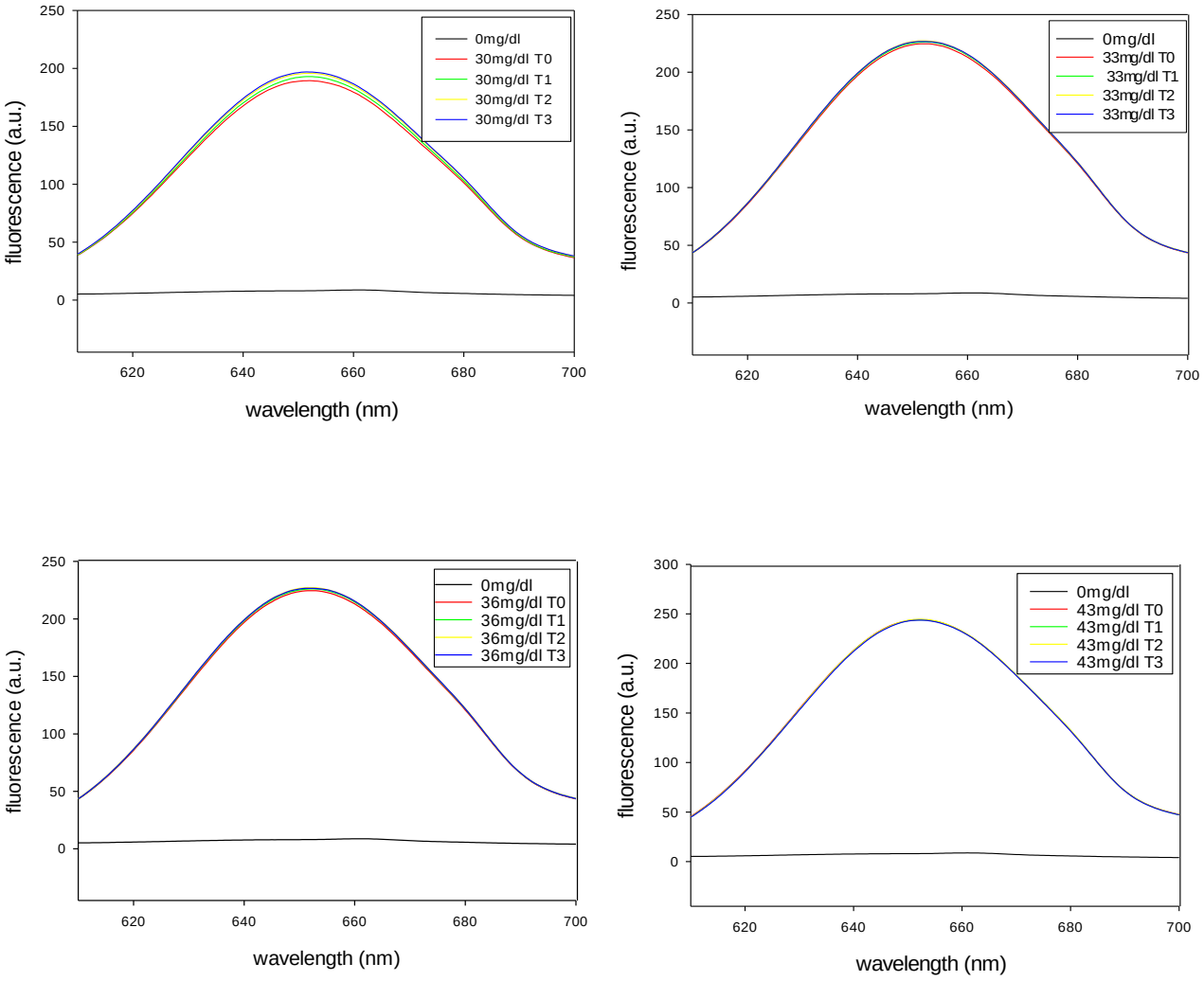

Figure 25. Comparison of the fluorescence emissions at various exposure times and concentrations of urea. Fluorimetric parameters: Excitation 598nm; emission 610nm; excitation and emission bandwidth 5nm. Maximum fluorescence 650nm.

In the **Figure 26** the curves of fluorescence obtained at different substrate concentrations and incubation time of 15min are shown.

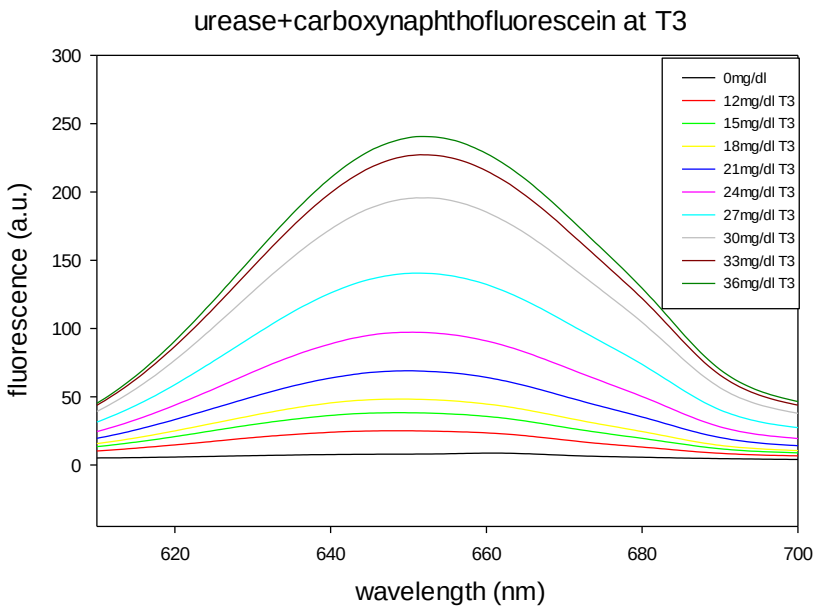

Figure 26. Comparison of the fluorescence emissions at time T3 and at various concentrations of urea. Fluorimetric parameters: Excitation 598nm; emission 610nm; excitation and emission bandwidth 5nm. Maximum fluorescence value at 650nm.

After verifying that it was possible to monitor the reaction catalyzed by urease with urea using the fluorescence probe, the next step was to repeat the experiments in milk.

In all the experiments carried out the ratio 1:1 for milk and reaction mix was used. Experiments with urease in milk were carried out with 5(6)-Carboxynaphthofluorescein as fluorophore because, as already stated, it is easier to use it compared to the other fluorophore.

In the first experiments the same conditions of the last experiment in buffer (250µl of mix enzyme+ fluorophore in PBS 0.1M and 250µl of milk, see materials and methods) were used but unfortunately it was not detected any variation of the fluorescence emission.

The experiments performed in milk are listed below:

1) <u>Acidification of milk</u>

   This test was performed because milk added in the reaction mix determines a change in the initial pH. pH5 was chosen since close to the milk coagulation of pH4.6. However, adding 12mg/dl of urea there were no results.

2) <u>Modification of the fluorophore concentration</u>

a) a double amount of fluorophore was diluted in acidified water at pH4.5, but it has been obtained an increase of fluorescence only with the addition of 12mg/dl and 24 mg/dl; after the last value the saturation was reached.

b) 250µl of the stock of $1.5x10^{-4}$fluorophore was diluted in 0.1M PBS pH4.5. In addition, in order to increase the chance of detecting the fluorescence, the bandwidth increase so that the excitation light was greater than that emitted. In these conditions, it was possible to obtain fluorescence modifications until 33mg/dl of urea; after this concentration the reaction reached the saturation.

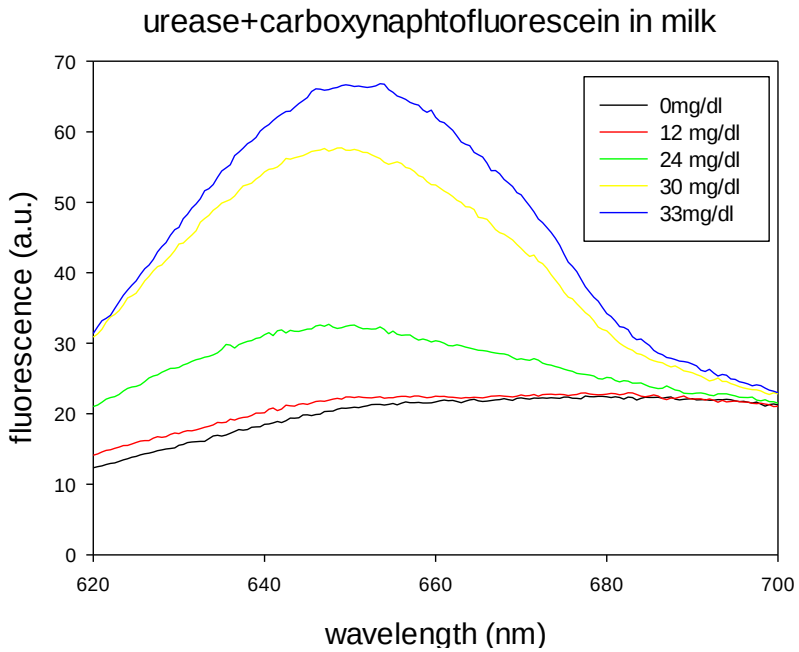

Figure 27. Fluorescence curves obtained in the experiment 2b. Fluorescence parameters: excitation 598nm; emission 610nm; excitation bandwidth 10nm and emission bandwidth 5nm. Measurements were carried out after 15 min of incubation. Maximum fluorescence value at 650nm.

c) Fluorophore concentration was further doubled and at 30mg/dl of urea the plateau was reached.

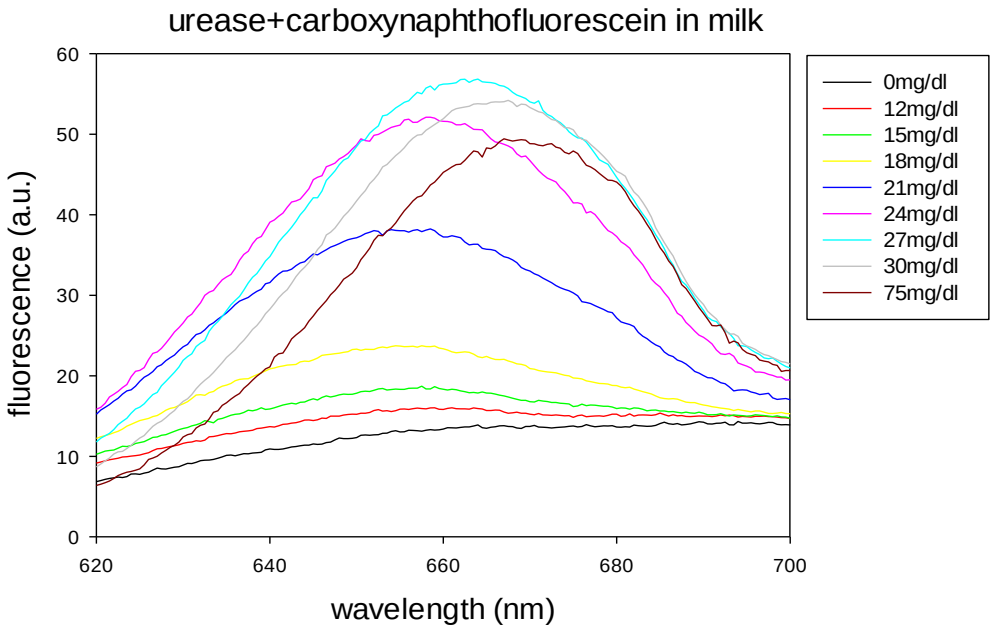

Figure 28. Fluorescence curves with various urea concentrations. Fluorescence parameters: excitation 598nm; emission 610nm; excitation bandwidth 10nm and emission bandwidth 5nm. Measurements were carried out after 15 min of incubation. Maximum fluorescence value at 660nm.

In **Figure 28** is possible to observe that there is a constant increase of fluorescence emission with increasing urea concentrations, but at 75mg/dl there is a decrease perhaps due to the saturation of the enzyme.

Next table shows the average of three repetitions for each urea concentration.

Urea concentration (mg/dl)	Fluorescence emissions (a.u)
0	**13.10±0.11**
12	**15.90±0.08**
15	**18.70±0.08**
18	**23.70±0.02**
21	**38.00±0.1**
27	**51.10±0.01**
30	**56.80±0.33**
33	**54.00±0.15**
75	**48.80±N.D.**

Table 13. Averages of the maximum values of fluorescence emission at various concentrations of urea. Measurement values are in arbitrary units.

In the experiments before, to improve the performance of the reaction, the experiments were repeated looking at the right concentrations of fluorophore, while in the subsequent tests different concentrations of buffer were tested to check whether by changing the buffer concentration it would be possible to achieve better results.

In the next experiment, the buffer concentration was increased from 0.1 to 0.12M, but the saturation was reached at 33mg/dl urea. The same results were obtained with PBS 0.13M and 0.14M. Using a 4.5 pH PBS 0.14M the fluorescence signal is increased with increasing concentration of urea until 39mg/dl. This result indicates that by increasing the concentration of the buffer, there is an increase of the buffering effect which allows to delay the saturation of the reaction.

The data are shown in **Figure 29**.

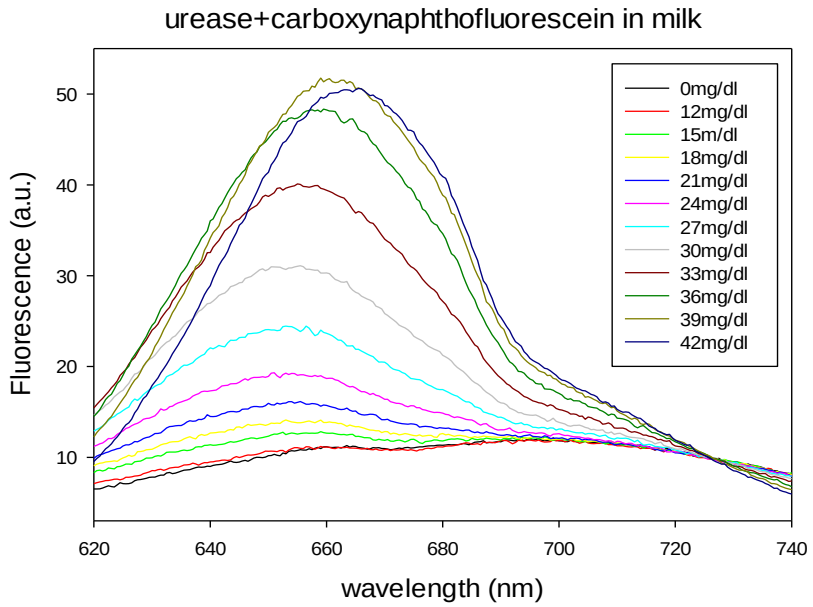

Figure 29. Comparison of the fluorescence emission curves at various concentrations of urea.

In the next table the data obtained in this experiment are reported. Also in this case the data are the results of three repetitions of each urea concentration.

Urea concentration (mg/dl)	Fluorescence emissions (a.u)
0	**12.2±0.5**
12	**12.0±1.4**
15	**12.9±1.0**
18	**14.2±0.4**
21	**16.3±1.0**
24	**19.4±0.2**
27	**24.6±0.9**
30	**31.2±0.8**
33	**40.1±0.6**
36	**48.5±0.8**
39	**51.9±0.8**
42	**50.8±0.4**

Table 14. The averages of the fluorescence emissions at the maximum peak at various concentrations of urea with the standard errors.

Lactose content analyzed by β-galactosidase

Milk quality is determined by several parameters. In particular, lactose concentration is an important parameter, since for a high quality milk must have a concentration between 45 and 50g/l. Therefore, experiments with the enzyme *β-galactosidase* were performed. This enzyme catalyzes the lactose hydrolysis in the two monomers: galactose and glucose. In this study, fluorescence studies using FITC as probe were performed.

In our experiments it was not possible to test the high concentrations necessary to detect quality of milk. Since to detect these quantities, a big volume of reaction mix and a great amount of enzyme are requested. For this reason, we tested a range of concentrations between 0.1 and 1g/l. To determine the best time of reaction, measurements at 0, 5,10, 15 and 30min after analyte addition were performed. The data obtained, are shown in **Figure 30**.

B-galactosidase in buffer

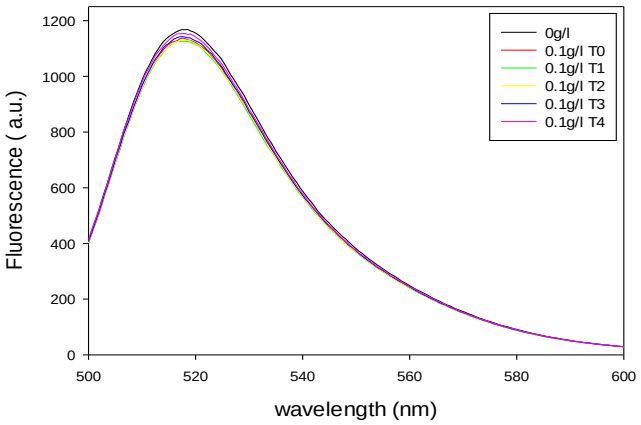

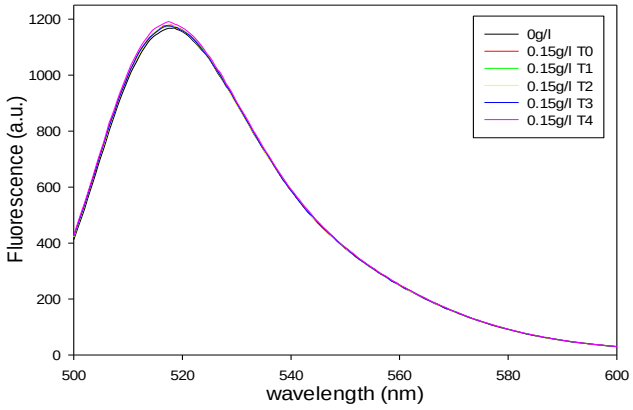

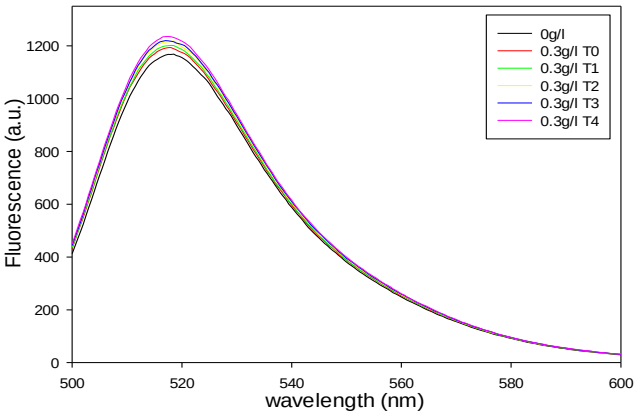

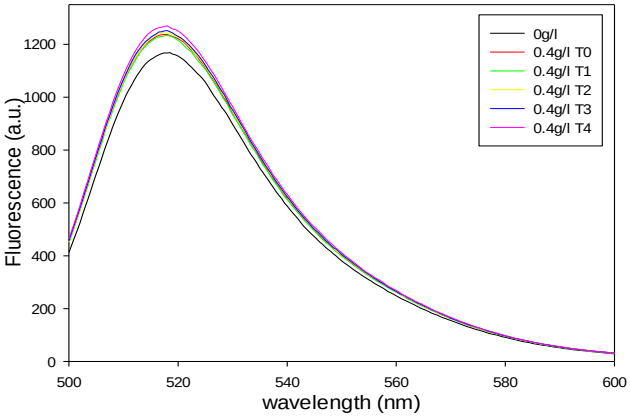

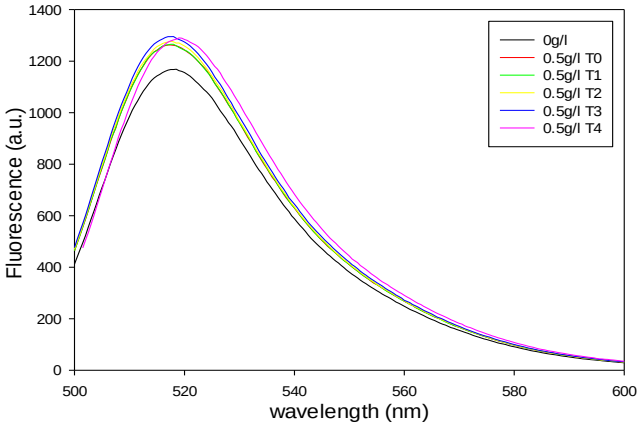

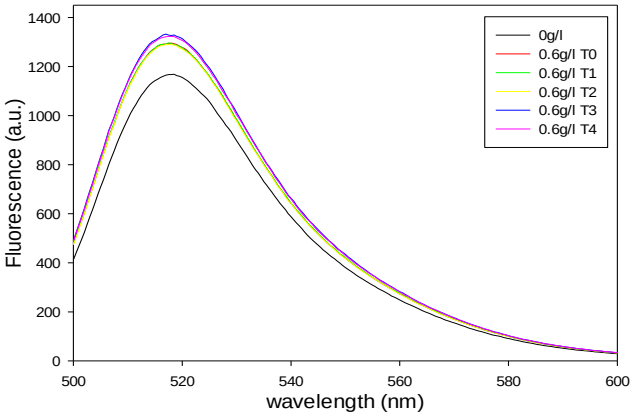

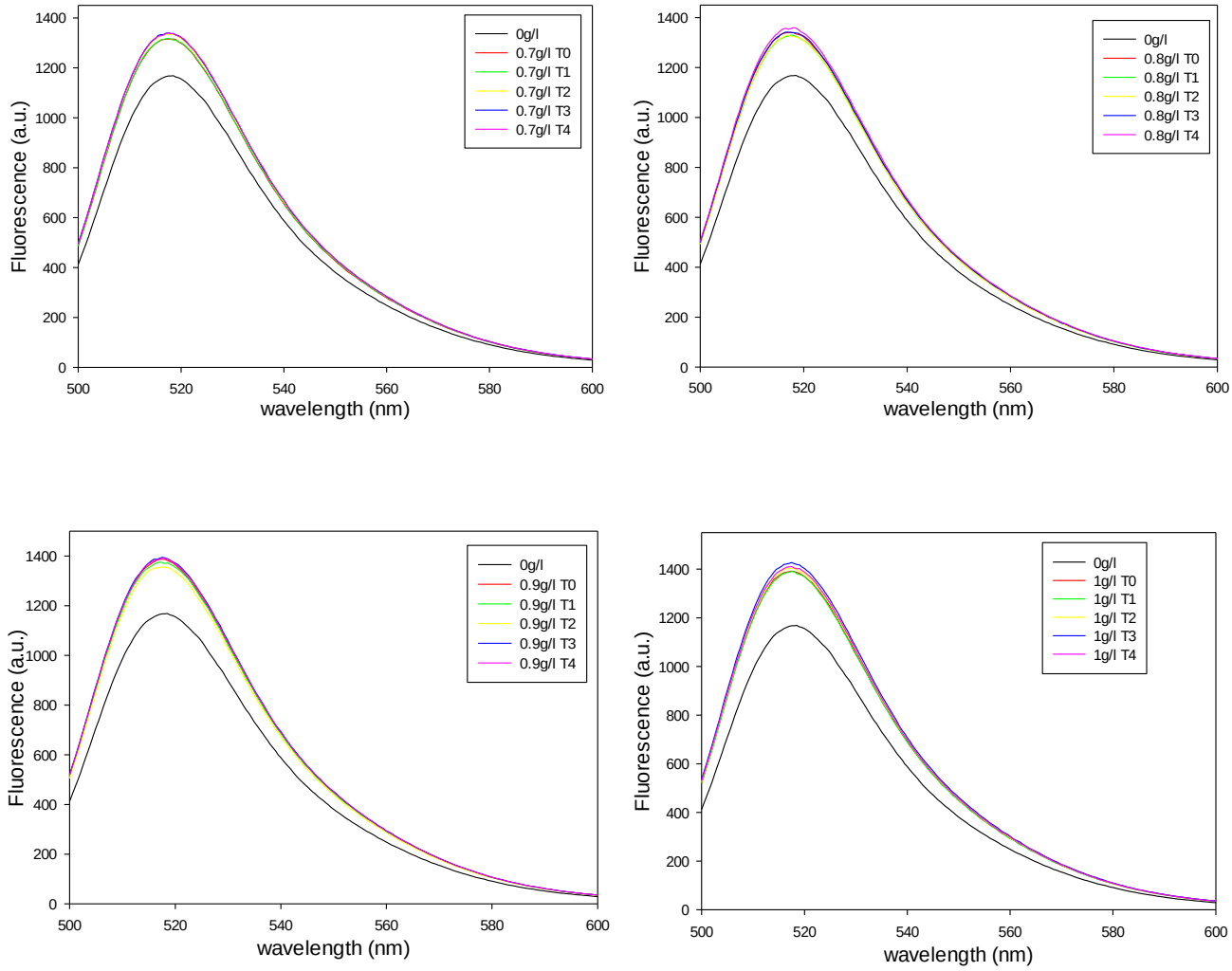

Figure 30. Comparison of the fluorescence emission curves at various exposure times and analyte concentrations. Fluorimetric parameters: excitation 495nm; emission 500nm; excitation and emission bandwidth 5nm. Maximum fluorescence value at 518nm.

The results obtained in this experiment show that using small amounts of analyte it is possible to obtain fluorescence emission variations already after 5min from lactose addition. Fluorescence signal increases with the increase of analyte concentration with best time of measurement T3.

In **Figure 31** the comparison between fluorescence curves obtained at various lactose concentrations at the time of 15min is shown.

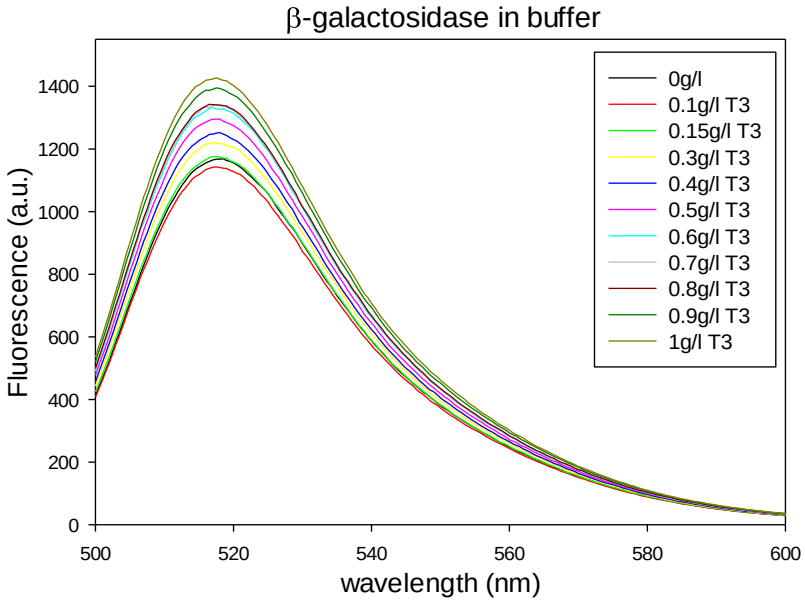

Figure 31. Comparison of the fluorescence emission curves at various concentrations of analyte at 15min from lactose addition. Fluorimetric parameters: excitation 495nm; emission 500nm; excitation and emission bandwidth 5nm. Maximum fluorescence value at 518nm.

In **Table 15** the data obtained in this experiment are summarized.

lactose concentration (g/l)	Fluorescence emissions (a.u)
0	**1169.7±32.1**
0.1	**1142.9±5.03**
0.15	**1177.7±1.7**
0.3	**1220.3±3.7**
0.4	**1252.3±3.1**
0.5	**1297.3±6.2**
0.6	**1333.5±3.6**
0.7	**1346.7±2.7**
0.8	**1349.2±5.6**
0.9	**1396.5±2.2**
1	**1427.4±5.0**

Table 15. Averages of three repetitions of fluorescence emission (in arbitrary units) at the maximum peak obtained at various lactose concentrations. Error standards are shown. Fluorimetric parameters: excitation 495nm; emission 500nm; excitation and emission bandwidth 5nm. Maximum fluorescence value at 518nm.

The data indicate that an increase in the concentration of lactose corresponds to an increase of the fluorescence emission signal.

In the first experiments in milk, lactose in a range between 0.2and 1g/l was added. In this experiment milk represents the 50% of the reaction mix, but unlike in the buffer, with increasing concentration of the analyte a decrease of fluorescence emission was observed.

This result could be due to an excess of exogenous lactose added to milk so that the enzyme immediately saturated. Experiments with milk deprived of lactose were performed, but adding further lactose no results were obtained. A list of other experiments is shown in the following.

1) Use of milk without lactose

   In this experiment, exogenous lactose was added to deprived lactose milk, however no results were obtained. Reducing the quantity of milk in the reaction mix from a ratio of 1:1 to a 1:2 or 1:4 and further adding lactose, negative results were obtained.
2) Modification of protein concentration

   Experiments with a double enzyme concentration were performed, but using lactose-free milk and adding lactose to the mix, however fluorescence signal did not change.

   Using a double β-galactosidase concentration and reducing milk from a ratio of 1:4 to 1:5, no fluorescence variations were obtained.
3) Buffer modification

   Next step was to modify buffer concentration from 0.1 to 0.05M and pH from 4.5 to 6.5, that is reported as optimal pH for this enzyme. In these conditions, using lactose-free milk no results were obtained.

Use of the milk as lactose

Because adding exogenous lactose no results were obtained, new experiments adding whole milk at reaction mix in the buffer were performed. In this case, fluorescence decrease was obtained when milk was added.

Other tests were performed using skimmed milk and semi-skimmed. Using a double enzyme concentration and adding semi-skimmed milk to the reaction mix, a reduction of fluorescence was obtained; on the contrary, adding skimmed milk, a fluorescence increase was obtained.

Experiments with skimmed milk were performed in order to determine the best reaction conditions. The results obtained in these experiments are shown in **Figure 32**.

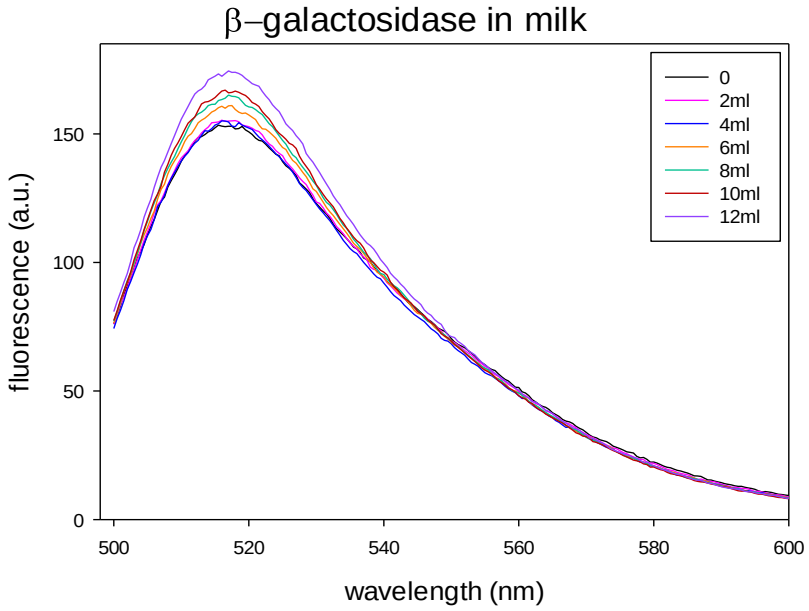

Figure 32. Comparison of the fluorescence emissions at various concentrations of semi-skimmed milk. Fluorimetric parameters: Excitation 495nm; emission 500nm; excitation and emission bandwidth 10nm. Maximum fluorescence 518nm.

In this experiment, adding skimmed milk a reaction progress in line with what happened in the lactose in buffer, was obtained.

D-Lactic acid content analyzed by D-lactic dehydrogenase

Another important parameter to determine high quality and safety of milk is the concentration of lactic acid. According to European legislation, a milk with high quality presents a lactic acid content no more than 30ppm ($3.3x10^{-4}$M). D-lactic dehydrogenase is the enzyme used as biomediator in order to monitor lactic acid content in milk. This enzyme is normally present in mammalian and in some bacteria, called lactic acid bacteria (LAB). They are responsible of milk fermentation and are used for production of fermented foods. D-lactic dehydrogenase catalyzes the conversion of D-lactic acid to pyruvate, with the contemporary reduction of a NAD^+ molecule with production of $NADH+H^+$.

The reaction catalyzed by this enzyme determines a change of the pH in the environment thus, the fluorophore 5-(6)-carboxynaphthofluorescein was employed in our experiments.

A lactic acid concentration range between 1.6 and $5.8x10^{-4}$M was tested. The lactic acid used in this work is a solution in which there are both L and D-lactic acid in a ratio of 1:1. We considered that in the calculation of the analyte concentration. According to literature, before analyte addition, the reaction mix was incubated in the dark for 30min, to guarantee the interaction between enzyme and the co-factor NAD^+. In **Table 16** it is possible to see that an increase of lactate concentration corresponds to a decrease of fluorescence signal.

Lactic acid concentration (M)	Fluorescence emissions (a.u)
0	**64.00±0.06**
1.66x10-4M	**80.12±0.1**
2.49x10-4M	**79.24±0.19**
3.33x10-4M	**78.44±0.04**
4.15x10-4M	**75.73±0.01**
4.98x10-4M	**74.77±0.04**

Table 16. Averages of fluorescence emissions at the maximum peak in presence of various D-lactic acid concentrations and after 15min from the analyte addition. Fluorimetric parameters: excitation 505nm; emission 513nm; excitation and emission bandwidth 5nm. Maximum fluorescence value at 525nm.

The first experiments in milk were performed in the same conditions as in buffer, but no fluorescence variations were obtained. Other experiments were performed using the same reaction conditions, but changing pH and fluorimetric parameters. In fact, we observed that in the experiments without milk the initial pH is highly basic, while in presence of milk the initial pH is neutral. Also the excitation wavelength in these experiments was changed from 598nm to 512nm. With this modification of the protocol, the progress of the reaction was found to be equal to that obtained in experiments in buffer, where the increase of D-lactate concentration determines a decrease in the fluorescence signal. The results are shown in **Figure 33** and **Table 17**.

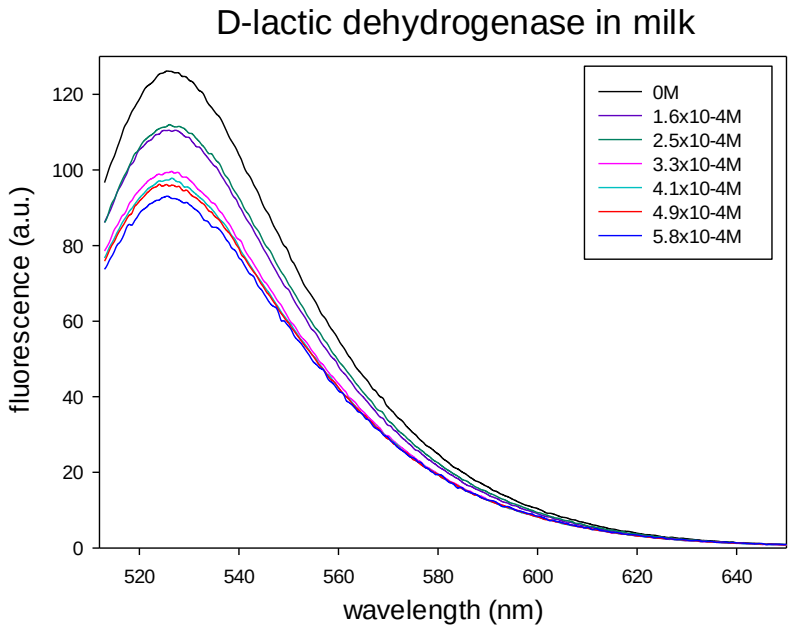

Figure 33. Comparison of the fluorescence curves at various concentrations of lactate in milk. Fluorimetric parameters: Excitation 505nm; emission 513nm; excitation and emission bandwidth 5nm. Maximum fluorescence value at 525nm.

Lactic acid concentrations (M)	Fluorescence emissions (a.u)
0	**84.3±0.06**
$1.6x10^{-4}$M	**81.4±0.1**
$2.5x10^{-4}$M	**79.3±0.19**
$3.3x10^{-4}$M	**77.6±0.04**
$4.1x10^{-4}$M	**76.3±0.01**
$4.9x10^{-4}$M	**75.5±0.04**
$5.8x10^{-4}$M	**73.8±0.01**

Table 17. Averages of fluorescence emissions at the maximum peak in presence of various D-lactic acid concentrations after 15min from the analyte addition. Fluorimetric parameters: excitation 505nm; emission 513nm; excitation and emission bandwidth 5nm. Maximum fluorescence value at 525nm.

Biosensor set-up

After the analysis performed with the spectrofuorimeter shown above, the experiments performed in milk were replicated using the biosensor Multilight based on fluorescence. Results shown in this part are preliminary and other tests are in progress.

In **Table 18** the data obtained in acetylcholinesterase experiments are shown. Range of analyte used is between $2x10^{-9}$ and $1x10^{-7}$M.

chlorpyrifos concentrations (M)	Fluorescence emissions (a.u)
0	**260.0±4.1**
$2.0x10^{-9}$	**299.0±0.5**
$4.0x10^{-9}$	**305.0±2.6**
$1.0x10^{-8}$	**359.0±2.6**
$1.4x10^{-8}$	**369.0±2.6**
$5.4x10^{-8}$	**430.0±34.8**
$1.0x10^{-7}$	**510.0±4.7**

Table 18. Averages of fluorescence emissions at the maximum peak in presence of various chlorpyrifos concentrations. The data derived from the automatic baseline correction. Measurements were performed after 15 min of dark, 11sec of light at light intensity of 1 (arbitrary units of the instrument).

As reported in the table, using this instrument it is possible to obtained a response of fluorescence emission in presence of various analyte concentrations with the same progress obtained in the experiment with the spectrofluorimeter.

Below, in **Table 19** the results obtained with tyrosinase enzyme are summarized.

Catechol concentrations (M)	Fluorescence emissions (a.u)
0	**282.0±7.9**
$2.0x10^{-10}$	**206.0±7.2**
$2.0x10^{-9}$	**63.0±5.8**
$3.0x10^{-9}$	**11.0±3.6**
$5.0x10^{-9}$	**-47±4.7**
$1.0x10^{-9}$	**-111.0±32.5**

Table 19. Averages of fluorescence emissions at the maximum peak in presence of various catechol concentrations. The data derived from the automatic baseline correction. Measurements were performed after 15 min of dark, 11sec of light at light intensity of 1 (arbitrary units of the instrument).

The data show that increasing catechol concentration decreases fluorescence emission. Also in this case, the data obtained show the same reaction progress observed in the experiments previously mentioned.

Urea concentrations used in this experiment are between 10 and 40mg/dl. As shown in **Table 20** the increase of urea determines an increase of fluorescence emission.

Urea concentrations (M)	Fluorescence emissions (a.u)
0	**2257.0±11.0**
10	**2300.0±12.0**
15	**2319.0±11.2**
20	**2327.0±2.7**
25	**2328.0±5.1**
30	**2330.0±0.58**
35	**2432.0±2.3**
40	**2458.0±8.14**

Table 20. Average of fluorescence emissions at the maximum peak in presence of various urea concentrations. The data derived from the automatic baseline correction. Measurements were performed after 15 min of dark, 11sec of light at light intensity of 1 (arbitrary units of the instrument).

Experiments performed with β-galactosidase were performed using the range of lactose concentrations between 10 and 90g/l. The data obtained with Multilight are shown in **Table 21**.

Lactose concentrations (g/l)	Fluorescence emissions (a.u.)
0	**552.0±2.6**
10	**552.0.0±6.4**
20	**519.0±8.6**
40	**584.0±3.2**
50	**522.0±1.6**
70	**464.0±3.5**
90	**541.0±6.6**

Table 21. Averages of fluorescence emissions at the maximum peak in presence of various lactose concentrations. The data derived from the automatic baseline correction. Measurements were performed after 15 min of dark, 11sec of light at light intensity of 1 (arbitrary units of the instrument).

Unfortunately, in this case, the results have not good and other repetitions are in progress.

For experiments with the last biomediator, concentrations of lactic acid used are between $1x10^{-4}$ and $8x10^{-4}$M. The data obtained are reported in **Table 22**.

Lactic acid concentrations (M)	Fluorescence emissions (a.u.)
0	**1162.0±39.7**
$1.0x10^{-4}$M	**1158.0±6.1**
$2.0x10^{-4}$M	**1117.0±12.3**
$3.0x10^{-4}$M	**718.0±13.0**
$4.0x10^{-4}$M	**330±12.1**
$5.0x10^{-4}$M	**323.0±1.1**
$6.0x10^{-4}$M	**241±13.0**
$7.0x10^{-4}$M	**22±5.13**
$8.0x10^{-4}$M	**-723±80.4**

Table 22. Average of fluorescence emissions at the maximum peak in presence of various lactic acid concentrations. The data derived from the automatic baseline correction. Measurements were performed after 15 min of dark, 11sec of light at light intensity of 1 (arbitrary units of the instrument).

The data show that there is a decrease of fluorescence emission in presence of increasing analyte concentration.

DISCUSSION

In this work using as biomediators algal cells and enzymes, an optical biosensor was realized. The device was developed in order to obtain a configuration which enables a parallel monitoring in real time of various analytes, important for the assessment of milk safety and quality. This instrument allowing reduction of time, cost and sample volume needed for milk analysis, will be used directly in cowshed for analyses of the raw milk before its distribution.

It is known that milk is a complete food being a source of essential nutrients like carbohydrates, proteins, fats, vitamins and minerals. Being required for promoting growth and maintenance of health its consumption spread all over the world.

Milk contamination can be due to several factors that are often correlated with the health of the producing animals. Generally, animals can be exposed to various chemical or biological contaminants that can lead to diseases with consequent milk alteration. Pesticides are influent chemicals since dairy cows can be exposed to pesticides through contaminated water and forage. Chemicals that are soluble in water are metabolized in the liver and mostly eliminated with urine and feces, but fat soluble chemicals are eliminated through milk (Bertand, 2010). Cows can also be exposed to pathogenic microorganisms that determine the onset of various diseases, such as mastitis, affecting the health and quality of milk. Animals with mastitis produce milk with various negative characteristics given by unusual quantities of metabolites such as great quantity of urea and lactic acid and low amount of lactose.

For milk safety assessment, photosynthetic herbicides, organophosforus pesticides and phenolic compounds were tested. These compounds are common pollutants in environment and in agrifood products, repeatedly reported in European Legislations since inhibitors of human endocrine and

nervous systems. Their limits according to EU are present in the four regulations Reg. 852/853/854/882/2004.

In this work, in order to test the presence of chemicals and milk metabolites, we have developed a multiarray biosensor conceived as an alarm system for revealing the concentrations of the reported analytes out of the limits indicated by European legislations. The limits were used to identify a range of concentrations under biosensor's analysis that sometimes are very narrow as for urea and lactic acid concentrations. In **Table 23** the biomediators considered with the tested ranges are summarized.

Biomediators	Analytes	Limits according to EU legislations	Range tested in milk (M)
algae	**photosynthetic herbicides: triazines, uree, diammines**	**0.05-0.1mg/kg**	**10^{-10}-10^{-6}**
acetylcholinesterase	**carbamates and organophosphates**	**1mg/l**	**1.4- 8.5x10^{-9}**
tyrosinase	**phenolic compounds**	**0.02-0.05mg/kg**	**2.0x10^{-9}- 1.8x10^{-8}**
urease	**urea**	**23-35mg/dl**	**2.0-6.5x10^{-3}**
β-galactosidase	**lactose**	**45-50g/l**	**2.6x10^{-7}-1.5x10^{-6}**
D-lactic dehydrogenase	**D-lactic acid**	**30ppm**	**1.6-5.5x10^{-4}**

Table 23. List of biomediators and relative analytes analyzed in this study. In the third column, the limits indicated by UE legislation are reported.

For all biomediators used, we have carried out experiments to determine the optimal working conditions. First experiments were performed in buffer, in order to determine the progress of the enzymatic reactions. The first difficulty encountered in this part of the work was to find the optimal conditions that would allow to detect the fluorescence signal in milk. In fact, in the literature there are many papers in which the milk is used in fluorescence experiments however, it is reported that it can give several problems: first of all its white color can reflect light, secondly being a complete food, it constitutes a complex matrix that can interact with enzymes or with the fluorophores. Thus, many experiments were performed as reported in the result section in order to obtain the best

conditions of reaction and further experiments performed in milk have required adjustments of the protocols, compared to the tests in buffer (reported in the result section).

For experiments with algae, fluorescence is guaranteed by its autofluorescence while the enzymes do not have an intrinsic fluorescence. For this reason, in order to monitor enzymatic reactions by the optical biosensor, the enzymes were coupled with special molecules defined as fluorophores. Fluorophores are fluorescent chemical compounds that typically contain several combined aromatic groups, or plane or cyclic molecules with several π bonds. The fluorophore absorbs light energy of a specific wavelength and re-emits light at a longer wavelength. The absorbed wavelengths, energy transfer efficiency and time before emission depend on both the fluorophore structure and its chemical environment, as the molecule in its excited state interacts with surrounding molecules. In the following table (**Table 24**), the fluorophores used in this work are listed.

Biomediators	Action mechanism	Fluorophores	λEx (nm) and λEm (nm)
algae	Q_A/Q_B electron flow inhibition	Autofluorescent	645- 730
acetylcholinesterase	Acetylcholine+H_2O → acetic acid+choline	Fluorescein 5-(6)-isothiocyanate	495- 503
tyrosinase	Catechol+1/2 O_2 benzoquinone + H_2O	Fluorescein 5-(6)-isothiocyanate	495-505
urease	Urea+3 H_2O → acetic acid +2ammonia	5-(6)-Carboxynaphthofluorescein	598- 620
β-galactosidase	lactose+ H_2O galactose+glucose	Fluorescein 5-(6)-isothiocyanate	495- 500
D-lactic dehydrogenase	D-lactic acid+NAD^+ → pyruvate+ $NADH+H^+$	5-(6)-Carboxynaphthofluorescein	505- 513

Table 24. List of selected biomediators and relative fluorophores.

Fluorescein 5-(6)-isothiocyanate (FITC) is a probe that physically binds to the protein being reactive towards nucleophiles including amine and sulfhydryl groups of proteins. When the substrate is added, the FITC-labeled enzyme shows an increase in the fluorescence emission since the binding of the substrate to the enzyme determines a conformational change. Instead, the fluorescent probe 5-(6)-Carboxynaphthofluorescein is a fluorophore pH sensitive with excitation wavelength at 512nm and emission at 567nm in an acidic or neutral environment, while in a basic environment excitation wavelength is at 598nm and emission at 668nm.

In the following, we report the best conditions obtained in our studies.

Algae for detection of photosynthetic herbicides

Whole cells of the green alga *Chlamydomonas reinhardtii* were employed for the detection of photosynthetic herbicides. Photosynthetic herbicides are able to target and inhibit the photosystem II at the reducing site, competing with the native plastoquinone at the Q_B-site with a higher affinity than plastoquinone itself. Consequently, linear electron transport from plastoquinone to the cytochrome b6/f-complex is fully or partially blocked. Since the reoxidation of Q_A^- in presence of herbicides is inhibited, there are changes in the fluorescence emission (Kautsky curve) and in the relative parameters in a way proportional to herbicide concentrations. Herbicides that inhibit photosystem II determine changes in different parameters of the curve. From this curve it is possible to extrapolate various parameters, in relation to photosynthetic efficiency. In our case, the parameter 1-Vj was used: Vj corresponds to $(Fj-F_0)/(Fm-F_0)$, where Fj is the fluorescence at step J, that corresponds to a variation of the slop correlated to the degree of oxidation of the electron acceptor Q_A. F_0 is the basal fluorescence and the Fm is the maximum fluorescence. For a detailed explanation of the Kautsky curve for *Chlamydomonas reinhardtii* (see introduction part II and Buonasera et al., 2011).

Measurements with a range of diuron concentrations between 10^{-10} and 10^{-6}M were performed both in buffer and milk. In buffer, in our conditions it is possible to detect modification of fluorescence emission starting from a diuron concentration of 10^{-9}M.

In **Figure 34** the data obtained in experiments with *Chlamydomonas* with and without milk are shown.

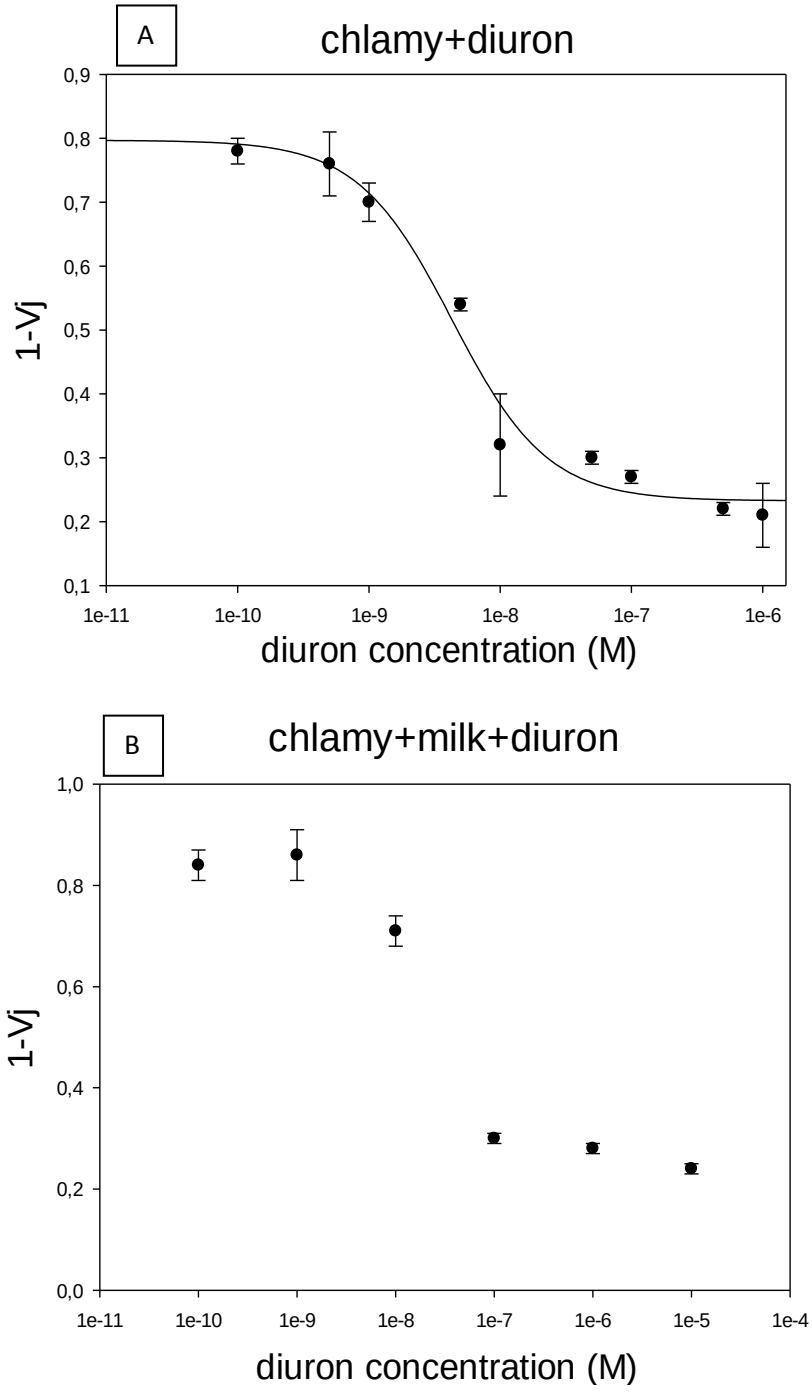

Figue 34. Data obtained in experiments with diuron. Measurements were performed using Multilight fluorimeter. Samples with diuron before measurements were incubated for 10min at light in constant stirring. The points represent the average of 1-Vj parameter calculate for each wall of the instrument and for each pesticide concentration. 1-Vj = 1-(Fj-F0)/(Fm-F0).

A) Results obtained in buffer. Instrument setting used: 10min of dark; 11sec of light and light intensity 127 arbitrary units. Diuron concentrations were between 10^{-10} and 10^{-6}M.

B) Results obtained in buffer. Instrument setting used: 10min of dark; 11sec of light and light intensity 127 arbitrary units. Diuron concentrations were between 10^{-10} and 10^{-5}M.

These experiments show that the presence of diuron in the range of tested concentrations in both buffer and milk determines a decrease of 1-Vj value.

Acetylcholinesterase for detection of organosphosphorus and carbamates

For the detection of organophosphorus pesticides, the enzyme acetylcholinesterase from *Electric eel* was employed as biomediator. Acetylcholinesterase hydrolyzes acetylcholine into acetic acid and choline and oganophosphorus pesticides act by blocking irreversibly this enzymatic reaction determining acetylcholine accumulation. The accumulation of acetylcholine has been shown to be harmful for children that are more sensitive to these substances in respect to adults in fact, the exposure to organophosphorus pesticides can interfere with normal growth and can cause irreversible diseases on nervous and endocrine systems (Rodriguez et al., 2013). Chlorpyrifos is a broad-spectrum insecticide and if taken individually by man has a moderate toxic effect, but if taken with other organophosphorus it can determine high toxicity on nervous system for cumulating effect. It also acts on cardiocirculatory and respiratory systems leading to chronic disorders in continuously exposed people.

Experiments with acetylcholinesterase using FITC as fluorophore were performed. When pesticide is added, the FITC-labeled acetylcholinesterase shows an increase in fluorescence emission since the binding of pesticide to the enzyme determines a conformational change. Increase of pesticide concentration determines a proportional increase in the fluorescence emission.

In these experiments, we used as analyte chlorpyrifos, one of the organophosphorus most commonly used in agriculture. As stated before, the safe limit for organophosphorus compounds in water and foods is set to 1mg/l that for chlorpyrifos corresponds to $2.8x10^{-9}$M. Thus, in these experiments we used a range of chlorpyrifos concentrations between 1.4 and $8.5x10^{-9}$M. Experiments under the same conditions both in buffer and milk were performed. In milk, fluorescence variation is lower compared to the experiments performed in buffer probable due to the shield effect of milk. Thus, in order to amplify fluorescence signal, we selected an emission bandwidth greater than that used in buffer, obtaining the satisfying results reported in **Figure 35 B**.

In **Figure 35** results obtained in these experiments show that the presence of chlorpyrifos in the range of the tested concentrations determines the increase of fluorescence.

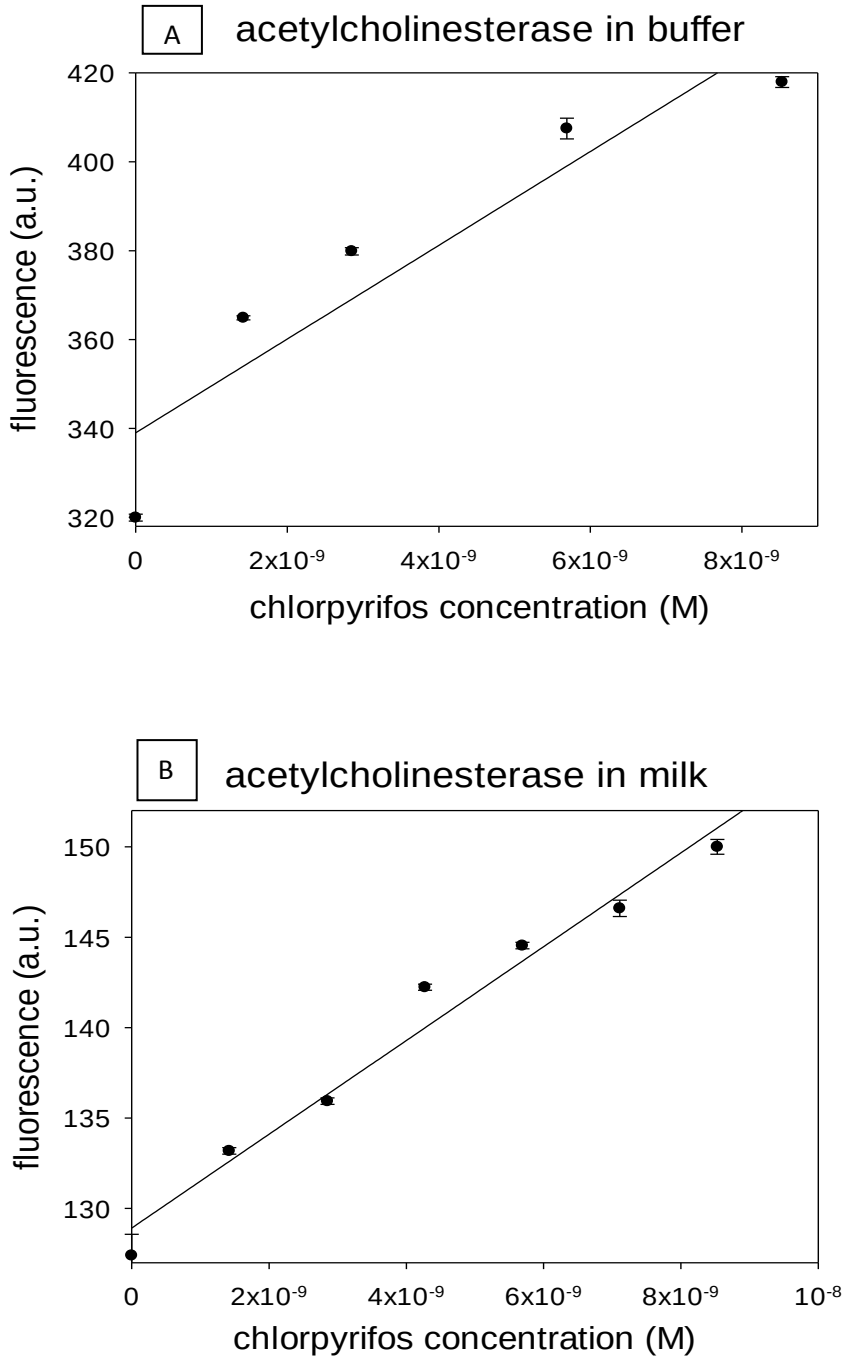

Figure 35. Data obtained in experiments with chlorpyrifos. Measurements were performed after 15min from the addition of chlorpyrifos. In order to ensure the repeatability the experiments were performed three times for each analyte concentration. The points represent the averages of the maximum fluorescence values for each pesticide concentration. Standard error bars are shown for all values.

A) Results obtained in buffer. Fluorimetric parameters: excitation 495nm; emission 500nm; excitation and emission bandwidth 2.5nm. Maximum fluorescence values are obtained at 518nm. Data are represented as a dose response curve.

B) Results obtained in test performed in milk. Milk is diluted to 50% with buffer. Fluorimetric parameters: excitation 495nm; emission 503nm; excitation bandwidth 2.5nm and emission 5nm. Maximum fluorescence values are obtained at 518nm. Data are represented as a linear curve.

Tyrosinase for the detection of phenolic contaminants

To detect phenolic compounds tyrosinase from mushroom was used. Tyrosinase is a cuproproteic complex most common in animal and vegetal kingdoms that catalyzes the oxidation of mono and bi-hydrophenols to ortochinones. Phenolic compounds were largely used in the past in various fields, such as insecticides, sunscreens, surfactants and as pharmacology compounds. Phenolic compounds include very harmful substances, like bisphenol A [4,4'-(propane-2,2-diyl)diphenol] and 4-nonylphenol [4-(2,4-dimethylheptan-3-yl)phenol] and others. Their residues are present in massive concentration in the environment and their toxic effects on human health aare highly known. It has been shown that they act on the endocrine system in particular on the hormone balance and can be responsible of breast cancer in woman. In this study, we used as analyte catechol, a precursor of phenolic compounds with lower toxic activity.

European Legislation has established that the maximum concentration of phenolic compounds in food should not exceed the limit value of 0.02-0.05mg/kg that for catechol corresponds to $1.8x10^{-8}$M. Thus, concentrations in the range between 10^{-9}M and 10^{-8}M were used for experiments in buffer. Fluorescence signal was determined by FITC with the same method indicated for acetylcholinesterase. In milk, we used a range of catechol concentrations between $2x10^{-9}$ and $1.8x10^{-8}$M.

The data obtained in these experiments are shown in **Figure 36**.

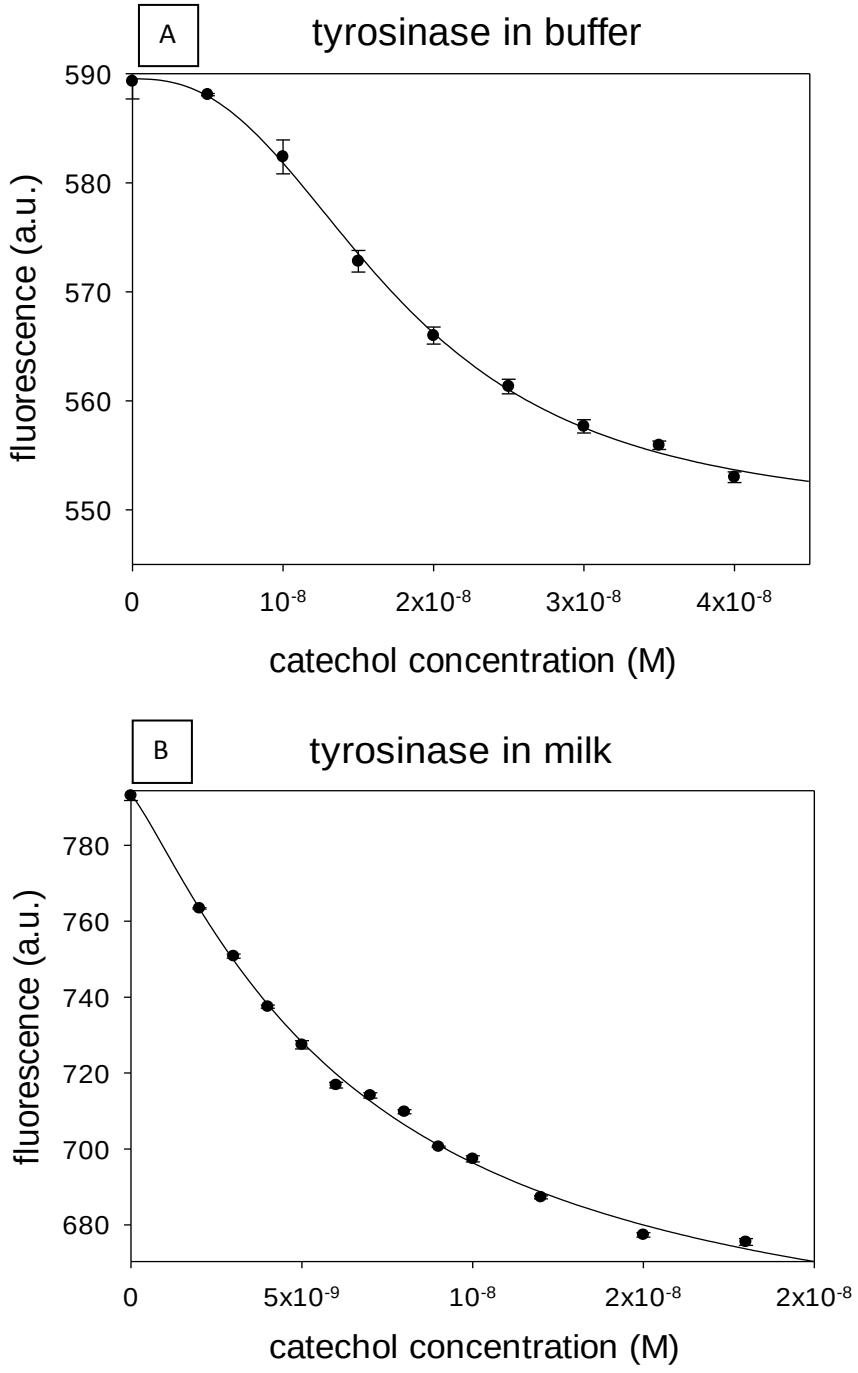

Figure 36. Graphic representation of results obtained in tyrosinase experiments. Measurements were performed after 15 min from the addition of catechol. In order to ensure the repeatability, the experiments were performed three times for each concentration. The points represent the averages of the maximum fluorescence values for each measure and for each catechol concentration. Standard error bars are shown for all values.

A) Representation of buffer test results. Fluorimetric parameters: excitation 495nm; emission 520nm; excitation and emission bandwidth 5nm. Maximum fluorescence values are obtained at 520nm. Data are represented as a dose response curve.
B) Results obtained in test performed in milk. Milk is 50% diluted with buffer. Fluorimetric parameters: excitation 495nm; emission 505nm; excitation and emission bandwidth 5nm. Maximum fluorescence values are obtained at 525nm. Data are represented as a dose response curve.

These data indicate that, after 15min after catechol addition, the FITC-labeled tyrosinase shows a decrease of fluorescence emission. In this case, milk does not interfere with the fluorescence measurements, so the same range of fluorimetric parameters were used.

Quality of milk determined as content of urea, lactose and lactic acid

As previously mentioned, the safety and quality of milk are correlated with cow health. In particular, an important disease that determines variations in milk is mastitis. Mastitis, a major endemic disease of dairy cattle, is an inflammation of the mammary gland and of udder tissue. It usually occurs as an immune response to bacterial invasion of the teat canal by a variety of bacterial sources and can also occurs as a result of chemical, mechanical, or thermal injury to cow's udder. This problem is caused by microorganisms such as *Escherichia coli*, *Streptococcus uberis* and *Staphylococcus aureus*, but also a wide variety of other microorganisms have been identified as potential mastitis pathogens. It is known that milk produced by mastitic cows has significant changes in protein amount and composition and in general, a higher urea concentration and lower lactose concentration of that produced by healthy cows.

Urease for analyses of urea content

Urea is a metabolite produced in liver and kidneys from ammonia, deriving from the degradation of crude proteins in the rumen. It's the main nitrogen non protein compound in milk and its concentration in milk of healthy cows is between 23 and 35mg/dl. Outliers of urea in milk can be due to errors rationing or diseases. A high content of urea in milk (more than 35mg/dl) is indicative of a reduced uptake of ammoniac nitrogen caused by an excess of protein degradable and/or deficiency of fermentable energy in the ration. High concentrations of urea in milk generally accompany typical pathologies of hyperammonaemia (metabolic alkalosis, reduced fertility,

lameness, etc) determining negative quality characteristics. Low levels of urea in milk (less than 20 mg/dl) are generally the result of insufficient protein intake in the diet.

In order to detect urea concentration in milk, experiments with urease from *Canavalia ensiformis* were performed.

Urease hydrolyzes urea to ammonia and carbon dioxide. In this case, the optical mechanism was developed by the use of fluorescent probe 5-(6)-Carboxynaphthofluorescein with urease in order to sense the pH variation of the solution due to urea hydrolysis. We monitored fluorescence variation in a range of urea concentrations between 12 and 36mg/dl, chosen according to the optimal range for EU regulatory as previously reported (**Table 23**).

In the experiments with milk we used a similar range of urea concentrations to obtain a significant change of fluorescence signal. To overcome the problems due to milk interference, buffer concentration used to dissolve the enzyme and the fluorophore was modified from a concentration of 0.1M to 0.14M.

In order to improve fluorescence signal, milk experiments were performed increasing excitation bandwidth, so that a good fluorescence response to urea addition was obtained.

In **Figure 37**, the data obtained in these experiments are shown.

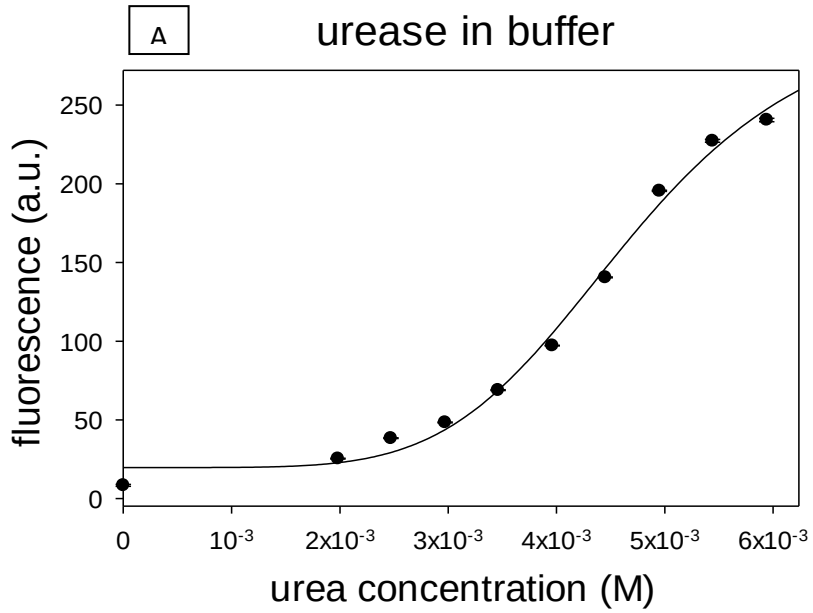

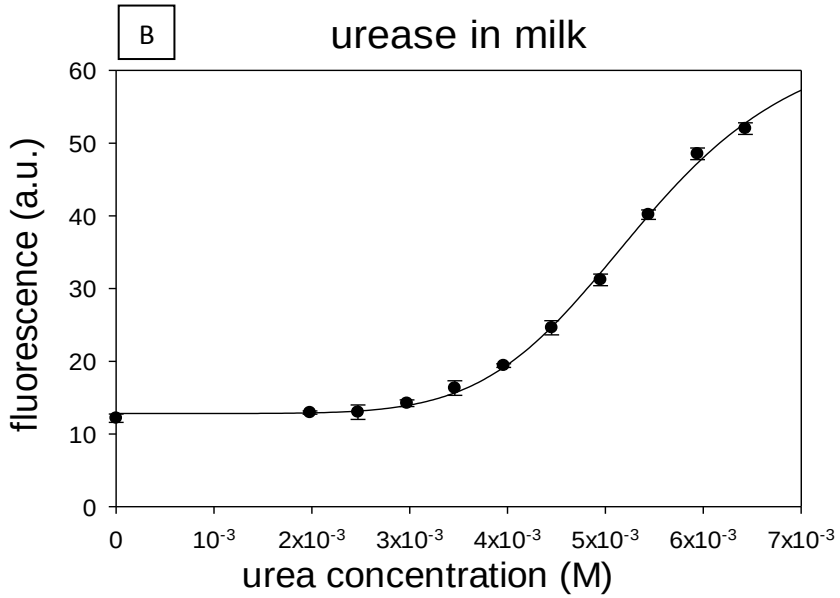

Figure 37. Graphic representation of results obtained in urease experiments. Measurements were performed after 15 min from the addition of urea. In order to ensure the repeatability, the experiments were performed three times for each concentration. The points represent the averages of the maximum fluorescence values for each measure and for each urea concentration. Standard error bars are shown for all values. Urea concentrations are reported as molarity.

A) Representation of buffer test results. Fluorimetric parameters: excitation 598nm; emission 610nm; excitation and emission bandwidth 5nm. Maximum fluorescence values are obtained at 650nm. Data are represented as a dose response curve.
B) Results in test performed in milk. Milk is 50% diluted with buffer. Fluorimetric parameters: excitation 598nm; emission 610nm; excitation and emission bandwidth 5nm. Maximum fluorescence values are obtained at 660nm. Data are represented as a dose response curve.

Using these urea concentrations, it is possible to obtain small but significant variations in fluorescence, in particular signals from a fluorescence value of 10 to 240 arbitrary units in buffer and from 12 to 51arbitrary units in milk were obtained.

Both in buffer and milk, the relationship between urea concentration and fluorescence describes a sigmoidal dose response curve. From the **Figure 37** it is possible to verify that the consequence of the increase of the substrate concentration is the increase of the fluorescence signal.

β-galactosidase for analyses of lactose

Lactose represents the 98% of total carbohydrates present in milk. It is a disaccharide composed by glucose and galactose linked by a β-1,4 bond. It is a hygroscopic sugar and has a strong tendency to absorb flavors and odors and causes many defects in refrigerated products such as crystallization in dairy foods, development of sandy or gritty texture and deposit formation (Panesar et al., 2006). Cow milk has a lactose concentration between 45 and 50g/l and this parameter is conserved for all cow types. Drastic reduction of lactose occurs in milk only in case of mastitis.

In our study, we used the enzyme β-galactosidase from *Aspergillus oryzae* that is able to break lactose in its two monomers. For optical detection, the β-galactosidase was coupled with FITC probe.

The data obtained in this experiment are summarized in **Figure 38**.

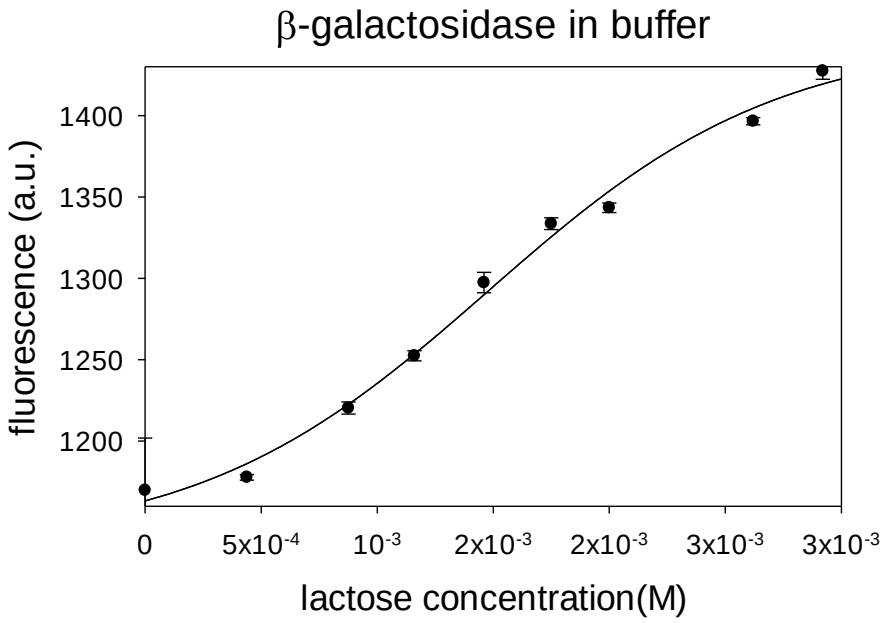

Figure 38. Results obtained in the experiment with lactose. Measurements were performed after 15 min from the addition of lactose. Experiments were performed three times for each analyte concentration. The points represent the average of the maximum fluorescence values for each lactose concentration. Standard error bars are shown for all values. Substrate concentrations are reported as molarity. Fluorimetric parameters: excitation 495nm and emission 510nm; excitation and emission bandwidth 2.5nm. Maximum fluorescence values are obtained at 518nm. Data are represented as a dose response curve.

The experiments in buffer were performed using lactose concentrations between 0.1 and 1g/l (from $4.3x10^{-4}$ to $2.9x10^{-3}$M). Lactose concentrations used are lower than the optimal values given by EU legislation, because to metabolize 50g/l of lactose a great amount of enzyme is necessary.

Experiments with milk were performed differently than those in buffer because adding exogenous lactose no results were obtained. For this reason, new experiments adding whole milk in the reaction buffer were performed. In this case, fluorescence decrease was obtained when milk was added as analyte.

Other tests were performed using skimmed and semi-skimmed milk. Using a double enzyme concentration an adding semi-skimmed milk to the reaction mix, reduction of fluorescence was obtained; on the contrary, adding skimmed milk a fluorescence increase was obtained. This result indicates that the fat component interferes with the enzyme.

Experiments with skimmed milk were performed in order to determine the best reaction conditions. The results are shown in **Figure 39**.

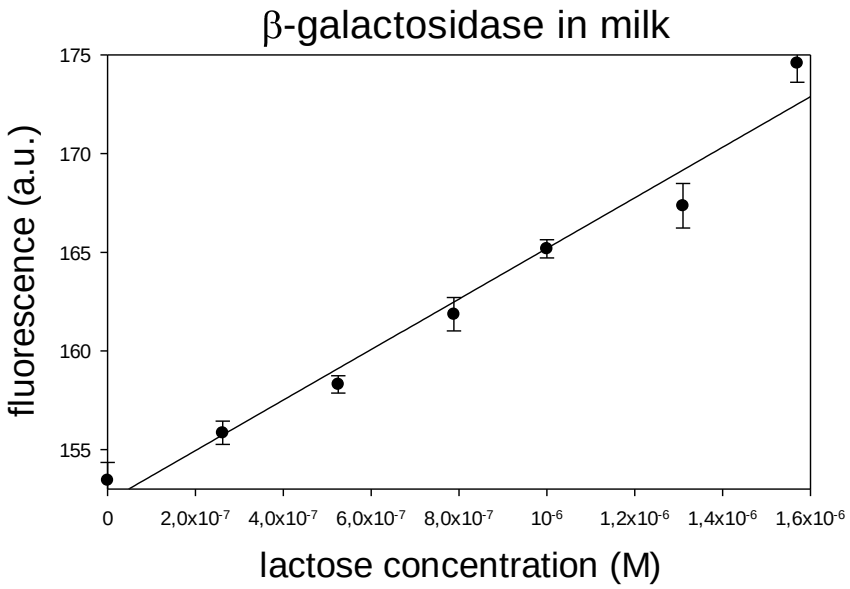

Figure 39. Results obtained in experiments used milk as lactose. Measurements were performed after 15 min from milk addition. Experiments were performed three times for each analyte concentration. The points represent the averages of the maximum fluorescence values for each measure. Standard error bars are shown for all values. Substrate concentrations are reported as molarity. Fluorimetric parameters: excitation 495nm; emission 500nm; excitation and emission bandwidth 10nm. Maximum fluorescence values are obtained at about 518nm. Data are represented as a linear dose response.

It is possible to see that the increase of the amount of milk determines a significant increase of fluorescence signal though these differences are not marked.

D-lactic dehydrogenase for analyses of D-lactic acid

Last analyte employed as biomediator was lactic acid. It is an important parameter indicating the quality and freshness of milk and its derivatives. Lactate concentration limit imposed by European legislation is 30ppm ($3.3x10^{-4}$M). A milk with a lactate concentration higher than this value can indicate presence of pathogen bacteria. In this work, D-lactic dehydrogenase from *Lactobacillus leichmannii* was used as biomediator in order to detect lactate concentration. This NAD^+-dependent enzyme catalyzes the conversion of D-lactic acid into pyruvate with production of NADH and H^+. This reaction determines a pH change in the environment allowing the use of 5-(6)-Carboxynaphthofluorescein as fluorophore. Using as reference the legislation limit, we tested a range of concentrations of lactic acid between 1.6 and $5.8x10^{-4}$M.

Figure 40 shows the results obtained in this test. It is possible to see that an increase of lactate concentration corresponds to a decrease of fluorescence signal.

Experiments with D-lactic dehydrogenase were performed also in milk and the progress of the reaction was found to be similar to that obtained in experiments in buffer where the increase of D-lactate concentration determines a decrease in the fluorescence signal.

In **Figure 40**, the results of tests performed with lactic acid are shown.

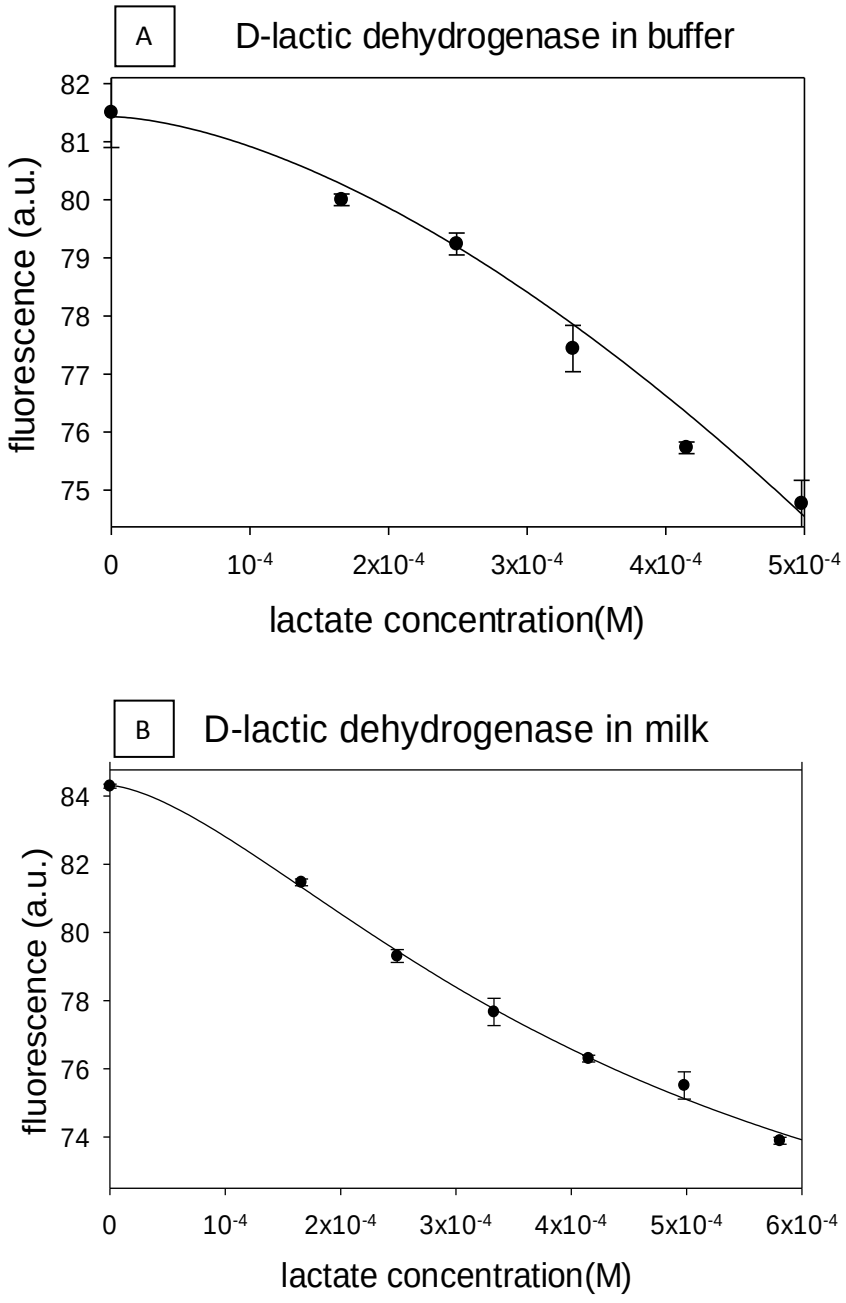

Figure 40. Graphic representation of results obtained in D-lactic dehydrogenase experiments. Measurements were performed after 15 min from the addition of lactic acid. In order to ensure the repeatability, the experiments were performed three times for each concentration. The points represent the averages of the maximum fluorescence values for each measure and for each lactate concentration. Standard error bars are shown for all values.

A) Representation of buffer test results. Fluorimetric parameters: excitation 505nm; emission 513nm; excitation and emission bandwidth 5nm. Maximum fluorescence values are obtained at 538nm. Data are represented as a dose response curve.

B) Results obtained in test performed in milk. Milk is 50% diluted with buffer. Fluorimetric parameters: excitation 505nm; emission 513nm; excitation and emission bandwidth 5nm. Maximum fluorescence values are obtained at 530nm. Data are represented as a dose response curve.

Multiarray biosensor

The device developed in collaboration with Biosensor s.r.l. is a multiarray fluorimeter able to recognize different biological elements at the same time because it is constituted by six static chambers hosting the excitation light sources. The static chambers are made of an inert material that not interact with the sample. In each well there is a set of optic fibers with appropriate excitation wavelengths and a set of other ones with the appropriate emission wavelengths, in order to provide a flexible excitation and fluorescence emission measurement for the different biological compounds used. Each photodiode is coupled with a high-pass filter that will capture only the spectral range where the fluorescence signal will be emitted. The device is made with an electronic control, LED drivers, a pre-processing signal conditioning module, a timer a flash memory card for data storage in field application and it has a USB connection in order to permit data storage and transmission to the computer.

In **Figure 41** the tridimentional scheme of Multilight biosensor is shown.

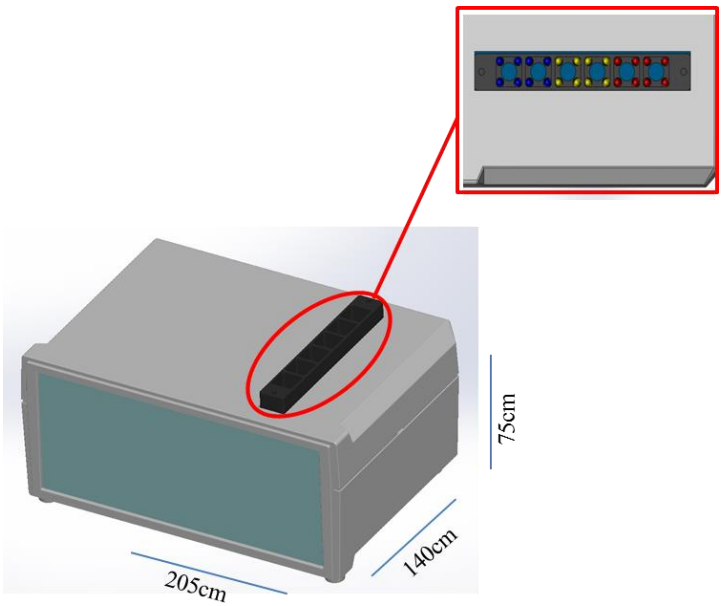

Figure 41. Multilight biosenosor scheme, with a detail of well array. Device dimensions are 205x140x75cm. Wells are shown with specific color LEDs.

As shown in the scheme, Multilight is small and portable. **Table 25** reports the LED colors, the wavelengths and the biomediators relating to each pair of cells

Cells	Led colors	Wavelength (nm)		Biomediators
		Ex	Em	
0-1	red	630	730	Algae
2-3	yellow	595	655	Urease; D-lactic dehydrogenase
4-5	blue	470	510	Acetylcholinesterase; Tyrosinase; β-galactosidase

Table 25. Specific annotations of Multilight wells.

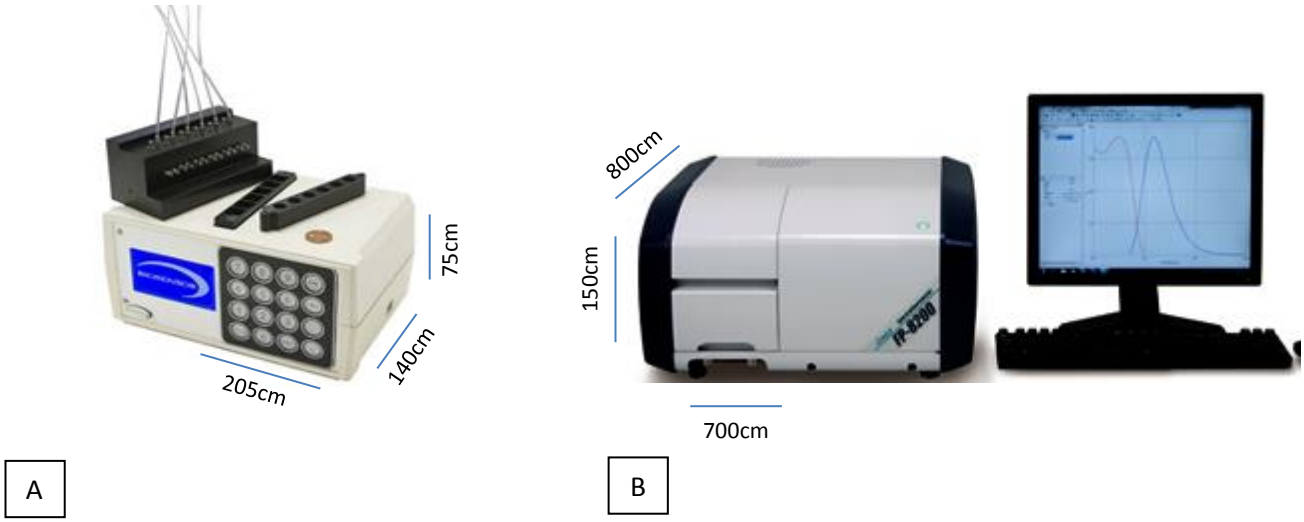

Figure 42. Multilight biosensor compared to the spectrophotometer Jasco PF-8200.

The **Figure 42** shows the comparison between Multilight (A) and spectrophotometer Jasco PF-8200 (B) in order to demonstrate the small size of our biosensor compared to the instrument used for the first laboratory analyses and the possibility of on line measurements with the enclosed flow system.

Up to now, we performed preliminary experiments with this instrument and the results are shown.

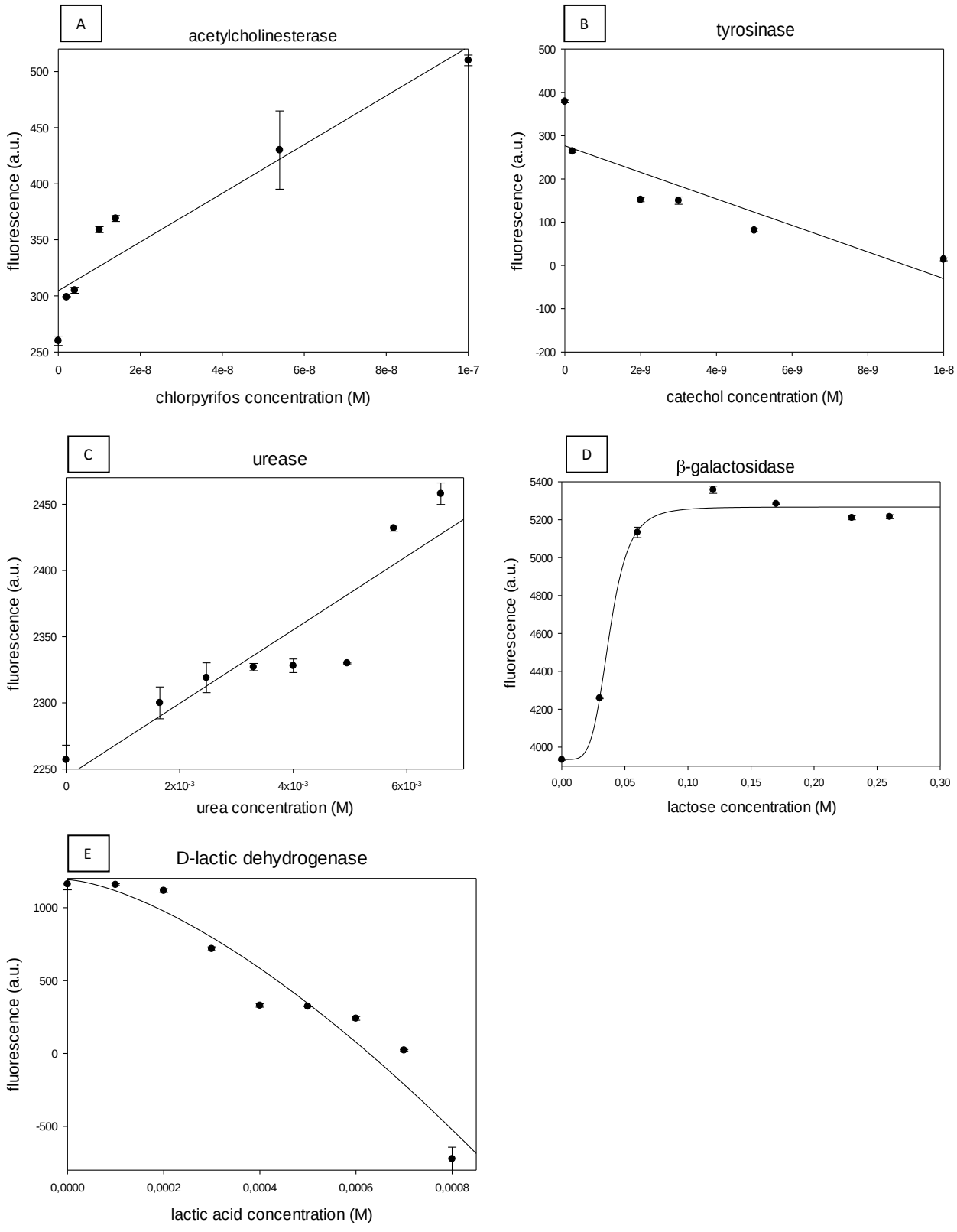

Figure 43. Graphic representations of the preliminary results obtained in experiments performed in milk using the multiarray fluorimeter. A) Acetylcholinesterase experiments. B) Tyrosinase experiments. C) Urease experiments. D) β-galactosidase experiments. E) D-lactic dehydrogenase experiments.

All the data obtained using the miniaturized portable biosensor instrument are on line with those obtained using the laboratory spectrofluorimeter, but other experiments must be carried out for better results.

CONCLUSIONS

In conclusion, using a commercial fluorometer we studied optimal biomediators in order to perform analyses for quality and safety assessment of milk. The presence of various analytes such as toxic compounds and metabolites at the low concentrations required by EU legislations was determined.

A new optical device was realized in collaboration with Biosensor srl to analyze cow milk directly in cowshed. This instrument is equipped with six wells with three different LEDs (red, yellow and blue) in order to analyze the parameters of 6 biological materials at the same time. The experimental protocols on this device were carried out but other experiments are actually ongoing in order to select optimal measurements conditions.

Other toxic analytes, like aflatoxines, dioxins and organic persistent compounds need to be studied to find the biomediators/conditions for their detection in milk by biosensors.

REFERENCES

Ackerman F. (2007) The Economics of Atrazine. *Intl. J. Occup. Environ. Health***. 13**, 441-449.

Andrews, R.K., Blakeley, R.L. & Zerner, B. (1984). Urea and urease. *Adv. Inorg. Biochem.* **6**, 245-283.

Balasubramanian, A. & Ponnuraj, K. (2010). Crystal structure of the first plant urease from Jack bean: 83 years of journey from its first crystal to mulecular structure. *J. Mol. Biol.* **400;** 274-283.

Belluzo, M.S., Ribone, M.É. & Lagier, C.M. (2008). Assembling amperometric biosensors for clinical diagnostics. *Sensors*. **8**, 1366-1399.

Bennett , J. W. & Klich, M. (2003). Mycotoxins. *Clin Microbiol Rev*.**16**(3), 497–516.

Bergveld, P. (1970). Development of an ionsensitive solid state device for neurophysiological measurements, IEEE *Trans. Biomed. Eng*. BME- **17**, 70-71.

Bergveld, P. (2003). Thirty years of isfetology what happened in the past 30 years and what may happen in the next 30 years. *Sens. Actuators B.* **88**, 1-20.

Blum, L.J. & Coulet, P.R. (1991). Eds Biosensor Principles and Applications (Biotechnology and Bioprocessing) Marcel Dekker Inc.

Borisov, S.M. & Wolfbeis, O.S. (2008). Optical biosensors. *Chem. Rev*. **108**, 423-461.

Brayner, R., Couté, A., Livage, J., Perrette, C. & Sicard, C. (2011). Microalgal biosensors. *Anal. Bioanal. Chem*. **401**, 581-597.

Brown, J.A. & Nielsen, P.J. (1974). Transfer of photosynthetically produced carbohydrate from endosymbiotic Chlorellae to *Paramecium bursaria*. *The journal of protozoology*. **21**(4), 569–570.

Buchinger, S. & Reifferscheid, G. (2012). Whole cell biosensors: applications to environmental health, in: V.R. Preedy, V. Patel (Eds.), Biosensors and Environmental Health. CRC Press and Taylor & Francis Group, London, UK. 107–126.

Buerk, D.G. (1993). Biosensors. Theory and Applications. *Technomic Publ. Co.,* Lancaster, Pennsylvania. 54.

Buonasera, K., Pezzotti, G., Scognamiglio, V., Tibuzzi, A. & Giardi, M.T. (2010). New platform for prescreening of pesticides residues to support laboratory analyses. *J. Agric. Food Chem*. **58**, 5982–5990.

Caron, D. A. & Swanberg, N. R. (1990). The ecology of planktonic sarcodines. *Rev. Aquat. Sci.* **3**,147–80.

Cavalcanti, A., Shirinzadeh, B., Zhang, M. & Kretly, L.C. (2008). Nanorobot hardware architecture for medical defense. *Sensors*. **8**(5), 2932–2958.

Cosnier, S. & Innocent, C. (1993). A new strategy for the construction of a tyrosinase-based amperometric phenol and o-diphenol sensor. *Bioelectrochemistry and Bioenergetics* **31**(2), 147-160.

De Faria, R.O., Moure, V.R., Amazonas, M.A., Krieger, N. & Mitchell, D.A. (2007). The biotechnological potential of mushroom Tyrosinase. *Food technol. Biotechnol.* **45** (3), 287-294.

Dixon, N. E.; Gazzola, C.; Blakeley, R. L. & Zerner, B. (1975). Jack bean urease (EC 3.5.1.5). A metalloenzyme. A simple biological role for nickel? *J. Am. Chem. Soc.* **97**, 4131-4133.

Eggins, B.R. (2002). Chemical sensors and biosensors. (Analytical Techniques in the Sciences (AnTs)) Willey-VCH.

Emerson, R. & Arnold, W. (1932). The photochemical reaction in photosynthesis. *The Journal of general physiology*. 191-206.

for the evaluation of water toxicity. *Analytica Chimica Acta*. **530,** 191–197.

Gasser, F. & Gasser, S. (1971). Immunological relationships among lactic dehydrogenases in the genera *Lactobacillus* and *Leuconostoc*. *Journal of Bacteriology*. **106**, 113-125.

Giardi, M.T. & Piletska, E.V.(2006). Biotechnological Applications of Photosynthetic Proteins: Biochips, Biosensors and Biodevices.

Giardi, M.T., Rea, G., Lambreva, M.D., Antonacci, A., Pastorelli, S., Bertalan, I., Johanningmeier, U. & Mattoo, A.K. (2013). Mutations of Photosystem II D1 Protein That Empower Efficient Phenotypes of Chlamydomonas reinhardtii under Extreme Environment in Space. PloS one. 8(5), e64352.

Gormant, D.S. & Levine R.P. (1965). *Cytochrome ƒ and plastocyanin: their sequence in the photosynthetic electron transport chain of Chlamydomonas reinhardtii. PNAS **54***(6), 1665-1669.

Grosova, Z., Rosenberg, M. & Rebros, M. (2008). Perspectives and applications of immobilized β galactosidase in food industry: a review. *Czech J .Food Sci.* **26**, 1–14.

Guibault, G.G. (1976). Analysis of Substrates. In Handbook of Enzymatic Methods of Analysis; Schwartz, M.K., Ed.; Clinical and Biochemical Analysis; Marcel Dekker, Inc.: New York, 189–344.

Haghbeen, K. & Tan, E.W. (2003). Direct spectrophotometric assay for monooxygenase and oxidase activities of mushroom tyrosinase in the presence of synthetic and natural substrates. *Anal. Biochem.* **312**, 23-32.

Harris, E.H. (2009). The genus Chlamydomonas, in: E.H. Harris (Ed.), The Chlamydomonas Sourcebook, 2nd ed., *Elsevier*, Oxford, UK. 1–24.

Harvey, R.B., Phillips, T.D., Ellis, J.A., Kubena, L.F., Huff, W.E & Petersen, H.D. (1991). Effects on aflatoxin M1 residues in milk by addition of hydrated sodium calcium aluminosilicate to aflatoxin-contaminated diets of dairy cows. *American Journal of Veterinary Research*. **52**(9):1556 1559.

Hemschemeier, A., Fouchard, S., Cournac, L., Peltier, G. & Happe, T. (2008). Hydrogen production by *Chlamydomonas reinhardtii*: an elaborate interplay of electron sources and sinks. *Planta*. **227**(2), 397-407.

Hermanson, G.T. (1996). Bioconjugute Techniques. *Academic Press: San Diego*.

Heyman, M.B.; Committee on Nutrition. (2006). Lactose intolerance in infants, children, and adolescents. *Pediatrics*. **118**, 1279–1286.

Hoef-Emden, K. (2005). Multiple independent losses of photosynthesis and differing evolutionary rates in the genus *Cryptomonas* (Chryptophyceae): combined phylogenetic analyses of DNA sequences of the nuclear and the nucleomorph ribosomal operons. *J. Mol. Evo.* **60**, 183-195.

Hofstadler, S.A., Sampath, R., Blyn, L.B., Eshoo, M.W., Hall, T.A., Jiang, Y., Drader, J.J., Hannis, J.C., Sannes-Lowery, K.A., Cummins, L.L., Libby, B., Walcott, D.J., Schink, A., Massire, C., Ranken, R., Gutierrez, J., Manalili, S., Ivy,C., Melton, R., Levene, H., Barrett-Wilt, G., Li, F., Zapp V., White, N., Samant, V., McNeil, J.A., Knize, D., Robbins D., Rudnick, K., Desai, A., Moradi, E. & Ecker, D.J. (2005). TIGER: the universal biosensor. *International Journal of Mass Spectrometry*. **242**(1), 23-41.

Hollenstein, M., Hipolito, C., Lam, C., Dietrich, D. Perrin, D. & Angew, M. (2008). *Chem. Int.* Ed. 47, 4346-4350.

Hsu, C.A., Yu, R.C. & Chou, C.C. (2005). Production of beta-galactosidase by Bifidobacteria as influenced by various culture conditions. *Int. J. Food Microbiol.* **104**, 197–206.

Husain, Q. (2010). B-Galactosidases and their potential applications: a review. *Critical Reviews in Biotechnology*. **30**(1), 41–62.

Husu, I., Rodio, G., Touloupakis, E., Lambreva, M.D., Buonasera, K., Litescu, S.C., Giardi, M.T. & Rea, G. (2013). Insights into photo-electrochemical sensing of herbicides driven by *Chlamydomonas reinhardtii* cells. *Sensors and Actuators B: Chemical.* **185**, 321-330.

Johanneke, L.H., Busch, C., Hrncirik, K., Bulukin, E., Boucon, C. & Mascini, M. (2006). Biosensor measurements of polar phenolics for the assessment of the bitterness and pungency of virgin olive oil. *J. Agric. Food Chem.* **54**(12), 4371–4377.

Johanningmeier U. & Heiss S. (1993). Construction of a *Chlamydomonas reinhardtii* mutant with an intronless *psbA* gene. *Plant Mol. Biol.* **22**, 91-99.

Jose´, I., De Corcuera, R. & Cavalieri, R.P. (2003). Biosensors. *Encyclopedia of Agricultural, Food, and Biological Engineering*. 119-123.

Jurado, E., Camacho, F., Luzon, G.& Vicaria, J.M. (2002). A new kinetic model proposed for enzymatic hydrolysis of lactose by a β galactosidase from *Kluyveromyces fragilis*. *Enzy. Microb. Technol.* **31**, 300–309.

Karakashian, S.J., Karakashian, M.W. & Rudzinska, M.A. (1968). Electron microscopic observations on the symbiosis of *paramecium bursaria* and its intracellular algae. *The jurnal of protozoology*. 15(1), 113–128.

Karube, I. (1987). Micro-organism Based Biosensors. In Biosensors Fundamentals and Applications; Turner, A.P.F., Karube, I., Wilson, G.S., Eds.; Oxford Science Publications: Oxford, 13–29.

Karube, I., Sode, K. (1991). Microbial Sensors for Process and Environmental Control. In Bioinstrumentation and Biosensors; Wise, D.L., Ed.; Marcel Dekker, Inc.: New York, 1–18.

Kautsky, H. & Hirsch, A. (1931). Neue Versuche zur Kohlensaureassimilation *Naturwissenschaften*. **19**, 964.

Kissinger, P.T., Heineman, W.R. (1983). Cyclic voltammetry. *J. Chem. Educ*. **60**, 702.

Kitajima, M. & Butler, W.L. (1975). Quenching of chlorophyll fluorescence and primary photochemistry in chloroplasts by dibromothymoquinone. *Biochim. Biophys. Acta.* **376**,105-115.

Kobayashi, H., Minshull, J., Ford, C., Golsteyn, R., Poon, R., & Hunt, T. (1991). On the synthesis and destruction of A- and B-cycling during oogenesis in meiotic maturation in *Xenopus laevis*. *J. Cell Biol.* **114**, 755–765.

Kodama, Y. & Fujishima M. (2011). Four important cytological events needed to establish endosymbiosis of symbiotic *Chlorella sp*. to the alga- free *Paramecium bursaria*. *Jpn. J. Protozool.* **44**.

Ladero, M., Santos, A. & García-Ochoa, F. (2000). Kinetic modeling of lactose hydrolysis with an immobilized beta-galactosidase from *Kluyveromyces fragilis*. *Enzyme Microb. Technol.* **27**, 583–592.

Ladero, M., Santos, A., Garcia, J.L. & Garcia-Ochoa, F. (2001). Activity over lactose and ONPG of a genetically engineered β galactosidase from Escherichia coli in solution and immobilized kinetic modeling. *Enzy. Microb. Technol.* **29**, 181–193.

Landis, W.G., (1988). Ecology. In Görtz H-D (ed) *Paramcium*. Springer, Berlin, pp419-436.

Lavecchia, T., Rea, G., Antonacci, A. & Giardi, M.T. (2013). Healthy and adverse effects of plant-derived functional metabolites: the need of revealing their content and bioactivity in a complex food matrix. *Critical Review in Food Science and Nutrition*. **53**, 198–213.

Liu, K-S. (1994). Preparation of fatty acid methyl esters for gas-chromatographic analysis of lipids in biological materials. *Jurnal of the American oil chemists' society*. 17(11), 1179-1187.

Mahler, G.J., Esch, M.B., Glahn, R.P., and Shuler, M.L. (2009). Characterization of a gastrointestinal tract microscale cell culture analog used to predict drug toxicity, *Biotechnol Bioeng*, **104**, 193-205.

Mahler, G.J., Shuler, M.L., and Glahn, R.P. (2009a) Characterization of Caco-2 and HT29-MTX cocultures in an in vitro digestion/cell culture model used to predict iron bioavailability, *J Nutr Biochem*, **20**, 494-502.

Margulis, L. & Fester, R. (1992). Symbiosis as a Source of Evolutionary Innovation: Speciation and

Morphogenesis. *MIT Press*, Cambridge, Massachusetts, 454.

Mascini M., (2005). A brief story of biosensor technology in technological applications of photosynthetic proteins, Eds M.T. Giardi and E. Piletska. Landes Bioscience/eurekah.com, Georgetown, Texas, U.S.A.

Massouli, J. & Bon, S. (1982). The Molecular forms of cholinesterase and acetylcholinesterase in vertebrates. *Annu. Rev. Neurosci*. **5**, 57-106.

Maxwell, K. & Johnson, G.N. (2000). Chlorophyll fluorescence – a practical guide. *Journal of Experimental Botany*. **51**(345), 659-668.

Mehta, J. & Rouah-Martin, E. (2011). *Anal. Chem*. **84**, 1669-1676.

Merchant, S.S., Prochnik, S.E., Vallon, O., Harris, E.H., Karpowicz, S.J. et al., (2007). The Chlamydomonas genome reveals the evolution of key animal and plant functions. *Science*. **318**, 245–250.

Mozas, S.R, Marco, M-P, Lopez de Alda, M.J. & Barcelo, D. (2004). Biosensor for environmental application: future development trends-Review. *Pure Appl. Chem*. **76**(4), 723-752.

Mucibabic, S. (1957). The growth of mixed populations of *Chilomonas paramecium* and *Tetrahymena pyriformis. J. gen.microbiol.***16**, 561-571.

Nagyvary J., Bechert J., (1999). Biochem. Edu. **27**, 193.

Neri, D.F.M., Balcao, V.M., Carneiro-da-Cunha, M.G., Carvalho, Jr. L.B. & Teixeira, J.A. (2008). Immobilization of β galactosidase from *Kluyveromyces lactis* onto a polysiloxane-polyvinyl alcohol magnetic (mPOS-PVA) composite for lactose hydrolysis. *Catal. Comm.* **4**, 234–239.

Newman, J.D. & Setford, S.J. (2006). Enzymatic biosensors. *Mol. Biotechnol*. **32**,249–268.

Newman, J.D. & Turner, A.P.F., (2005). Home Blood Glucose Biosensors: A Commercial Perspective. *Biosensors and Bioelectronics*. **20**, 2435-2453.

Ngeh-Ngwainbi, J., Suleiman, A.A. & Guilbault, G.G. (1990). Piezoelectric crystal biosensors. *Biosensor and Bioelectronics.* **5**(1), 13-26.

Nickelsen, J. (2005). Cell Biology: The Green Alga *Chlamydomonas reinhardtii* - A Genetic Model Organism. *Progress in Botany*. **66**, 68-89.

Nunes, G. S. & Marty, J. L. (2006). Immobilization of enzymes on electrodes immobilization of enzymes and cells (methods in biotechnology). J. M. Guisan. Totowa, NJ, Humana Press Inc., 239.

Oettmeier, W., Hilp, U., Draber, W. , Fedtke, C. & Schmidt, R.R. (1991). Structure–activity relationships of triazinone herbicides on resistant weeds and resistant Chlamydomonas reinhardtii. *Pest. Science*. **33**, 399–409.

Patel, P. N., Mishra, V. & Mandloi A.S. (2010). Optical biosensors fundamentals and trends. *JERS* **1**(I), 2010/15-34.

Patel, P.D. (2002). (Bio)sensors for measurement of analytes implicated in food safety: a review. *Trends in Analytical Chemistry*. **21**(2), 96-115.

Pinalysa, C. Longobardi, F. & Agostiniano A. (2005). Signal transduction techniques for photosynthetic proteins. Eds. M.T. Giardi and E. Piletska. Landes Bioscience/ eurekah.com, Georgetown, Texas, U.S.A.

Pohanka, M. & Skládal, P. (2008). Electrochemical biosensors – principles and applications. Review. *J. Appl. Biomed*. **6**, 57-64.

Pohanka, M., Skladal, P. & Kroca, M. (2007). Biosensors for biological warfare agent detection. *Def. Sci. J.* **57**(3),185-93.

Prodromidis, M.I. & Karayannis, M.I. (2002). Enzyme based amperometric biosensors for food analysis-Review. *Electroanalysis.* **14**(4), 241-261.

Rajinder, S.S (1994). Transducer Aspect of Biosensors Biosensor and Bioelectronics. 243-264.

Ravindra, N.M., Prodan, C., Fnu, S., Padronl, I. & Sikha, S.K. (2007). Advances in the manufacturing, types, and applications of biosensors. *JOM Journal of the Minerals, Metals and Materials Society.* **59**, 37-43.

Rawn. D., 1988 "The photosynthesis" in Biochemistry, **1**(18), 489, McGraw-Hill.

Rawson, D.M., Willmer, A.J. & Cardosi, M.F. (1987). The development of whole cell biosensors for on-line screening of herbicide pollution of surface waters. Toxicity essment. Wiley Online Library.

Rea, G., Lambreva, M., Polticelli, F., Bertalan, I., Antonacci, A., Pastorelli, S., Damasso, M., Johanningmeier, U. & Giardi M.T. (2011). Directed evolution and in silico analysis of reaction centre proteins reveal molecular signatures of photosynthesis adaptation to radiation pressure. *PLoS ONE* **6**(1).

Rea, G., Polticelli, F., Antonacci, A., Scognamiglio, V., Katiyar, P., Kulkarni, S.A., Johanningmeier, U. & Giardi, M.T. (2009). Structure-based design of novel *Chlamydomonas reinhardtii* D1–D2 photosynthetic proteins for herbicide monitoring. *Protein Science.* **18**, 2139–2151.

Richmond, M.L., Gray, J.I. & Stine, C.M. (1981). β galactosidase: review of recent research related to technological application, nutritional concerns, and immobilization. *J. Dairy Sci.* **64**, 1759–1771.

Rodriguez-Mozaz, S., Lopez de Alda, M. J. A. & Barcelo, D. (2006). Biosensors as useful tools for environmental analysis and monitoring. *Anal. Bioanal. Chem*. **386**(4), 1025–1041.

Ronkainen, N.J., Halsall, H.B. & Heineman, W.R. Electrochemical biosensors. (2010). *Chem. Soc. Rev*. 39,1747-1763.

Rouillon, R., Piletsky, S.A., Piletska, E.V., Euzet, P. & Carpentier R. (2005). Comparison of the immobilization techniques for photsystem ii, in technological applications of photosynthetic proteins. Eds M.T. Giardi and E. Piletska. Landes Bioscience/ eurekah.com, Georgetown, Texas, U.S.A.

Salminen, S., von Wright, A., Ouwehand, A.C. & Lahtinen, S. (2004). Microbiological and Functional Aspects, Third Edition.

Sanchez-Ferandin, S., Leroy, F., Bouget, F.Y., & Joux, F. (2013). A new, Sensitive marine microalgal recombinant biosensor using luminescence monitoring for toxicity testing of antifouling biocides. *Applied and Environmental Microbiology*. **79**, 631–638.

Sanchez-Ferrer, A., Bur, R. & García-Carmona, F. (1990). Partial purification of a thylakoid-bound enzyme using temperature-induced phase partitioning. *Anal. Biochem.* **184**, 279-282.

Sanchez-Ferrer, A., Villalba, J. & García-Carmona, F. (1989). Triton X-114 as a tool of purifying spinach polyphenol oxidase. *Phytochemistry* **28**, 1321-1325.

Scognamiglio V., Stano, P., Polticelli, F., Antonacci, A., Lambreva, M. D., Pochetti, G., Giardi, M. T. & Rea, G. (2013). Design and biophysical characterization of atrazine-sensing peptides mimicking the Chlamydomonas reinhardtii plastoquinone binding nichel. Physical Chemistry Chemical Physics 15(31), 13108-13115.

Scognamiglio, V., Pezzotti, G., Cano, J., Manfredonia, I., Buonasera, K., Arduini, F., Moscone, D., Palleschi, G. & Giardi, M.T. (2012). Towards an integrated biosensor array for simultaneous and rapid multi-analysis of endocrine disrupting chemicals. *Analytical Chim Acta*. **751**, 161– 170.

Scognamiglio, V., Pezzotti, I., Pezzotti, G., Cano, J. B., Manfredonia, I., Buonasera K., Rodio, G. & Giardi, M.T. (2013). A new embedded biosensor platform based on micro-electrodes array (MEA) technology. *Sensors and Actuators B.* **176**, 275– 283.

Sener, N., Apar, D.K. & Ozbek, B. (2006). A modeling study on lactose hydrolysis and β galactosidase stability under sonication. *Proc. Biochem*. **41**, 1493–1500.

Seo, S.Y.; Sharma, V.K.; Sharma, N. (2003). Mushroom tyrosinase: recent prospects. *J. Agric. Food Chem.* **51**, 2837-2853.

Shitanda, I., Takada, K., Sakai, Y. & Tatsuma, T. (2005). Compact amperometric algal biosensors.

Sommaruga, M., Sonntag, B. and Sommaruga, R., (2008). Ciliate-symbiont specificity of freshwater endosymbiotic *Chlorella* (Trebouxiophyceae, Chlorophyta). *J. Phycol.* **44,** 77-84.

Sommaruga, R. & Sonntag, B. (2009). Photobiological aspects of the mutualistic association between *Paramecium bursaria* and *Chlorella. M. Fujishima (ed.9, Endosymbionts in paramecium, Microbiology Monographs).*

State of the Art in Biosensors - *Environmental and Medical Applications, Edited by Toonika Rinken p. cm.*

Strothkemp, K.G., Jolley, R.L. & Mason, H. (1976). Quaternary structure of mushroom tyrosinase. *Biochem. Biophys. Res. Commun.* **70**, 519-524.

Stryer L, (1995). "The photosynthesis" in *Biochemistry*, chapt. 26, 4th ed., W . H. Freeman and Company, New York and Basingstoke.

Takeda, H., Sekiguchi, T., Nunokawa, S. & Usuki, I. (2011). Species-specificity of Chlorella for establishment of symbiotic association with Paramecium bursaria — Does infectivity depend upon sugar components of the cell wall? *European Journal of Protistology.* **34**(2), 133-137.

Tao, N. J., Boussaad, S., Huang, W. L., Arechabaleta, R. A. & D'Agnese, J. (1999). High resolution surface plasmon resonance spectroscopy. *Review of scientific instruments*. **(70)**12, 4656-4660.

Thevenot, D.R., Tòth, K., Durst, R.A. & Wilson, G.S, (1999) Electrochemical biosensors: recommended definitions and classification. *Pure Appl. Chem.* **71**, 2333.

Tibuzzi, A., Rea, G., Pezzotti, G., Esposito, D., Johanningmeier, U. & Giardi, M.T. (2007). A new

miniaturized multiarray biosensor system for fluorescence detection. *J. Phys*.: Condens. Matter 19-395006.

Tougu, V. (2001). Acetylcholinesterase: Mechanism of Catalysis and Inhibition. Current Medicinal Chemistry Central Nervous System Agents. 1(2), 155–170.

Touloupakis, E., Giannoudi, L., Piletsky, S.A., Guzzella, L., Pozzoni, F. & Giardi, M.T. (2005). A multi-biosensor based on immobilized Photosystem II on screen-printed electrodes for the detection of herbicides in river water. *Biosensors and Bioelectronics*. **20**, 1984–199.

Van Benschoten, J.J., Lewis, J.Y., Heineman, W.R., Rosten, D.A. & Kissinger, P.T. J. (1983**)**. Cyclic voltammetry experiment. *Chem. Educ.* **60**, 772.

Vedrine, C., Leclerc, J.C., Durrieu, C. & Tran-Minh, C. (2003). Optical whole-cell biosensor using *Chlorella vulgaris* designed for monitoring herbicides. *Biosensors and Bioelectronics*. **18**, 457–463.

Vo-Dinh, T. & Cullum, B. (2000). Biosensors and biochips: advances in biological and medical diagnostics. *Fresenius Journal of Analytical Chemistry* **366**, 6-7.

Watanabe, E. & Tanaka, M. (1991). Determination of Fish Freshness with a Biosensor System. *In Bioinstrumentation and Biosensors*; Wise, D.L., Ed.; Marcel Dekker, Inc.: New York, 39–73.

Watson, L.D., Maynard, P., Cullen, D.C., Sethi, R.S., Brettle, J. & Lowe, C.R. (1987/88). A microelectronic conductimetric biosensor. *Biosensors*. **3**, 101-115.

Wilski, S., Johanningmeier, U., Hertel, S. & Oettmeier, W. (2006). Herbicide binding in various mutants of the photosystem II D1 protein of *Chlamydomonas reinhardtii*, *Pesticide Biochemistry and Physiology*. **84**, 157–164.

Witzemann, V. & Boustead, C. (1983). Structural differences in the catalytic subunits of acetylcholinesterase forms from the electric organ of *Torpedo marmorata*. *The EMBO Journal*. **2**(6), 873-878.

Zhang, C.Y., Yeh, H.C., Kuroki, M.T. & Wang, T.H. (2005). Single-quantum-dot-based DNA nanosensor. Nat. Mat. 4, 826-831.

Zhang, X.B., Kong, R.M., Lu, Y. (2011). *Annu. Rev. Anal. Chem*. **4**, 105-128.

THANKS TO

Grazie alla dott.ssa Maria Teresa Giardi per avermi incessantemente seguita in questo percorso per la professionalità e affetto dimostrati.

Alla prof. ssa Stefania Masci per la disponibilità e la gentilezza.

A miei preziosi e fondamentali colleghi, ma soprattutto amici: Silvia, Ivano, Giuseppe, Gianni, Juan e Memhet che mi hanno sostenuta, aiutata e spesso sopportata.

Alla mia famiglia sempre vicina, porto sicuro della mia vita.

A Giuseppe amore della mia vita e prezioso per la sua costante presenza.